



IntechOpen

Immunohistochemistry

The Ageless Biotechnology

Edited by Charles F. Streckfus



Immunohistochemistry - The Ageless Biotechnology

Edited by Charles F. Streckfus

Published in London, United Kingdom



IntechOpen





Supporting open minds since 2005



Immunohistochemistry - The Ageless Biotechnology
<http://dx.doi.org/10.5772/intechopen.73770>
Edited by Charles F. Streckfus

Contributors

Shuji Yamashita, Edwin Roger Parra, Amir Hassan Zarnani, Yutaka Tsutsumi, Mireia Martín-Satué, Carla Trapero, Aitor Rodríguez-Martínez

© The Editor(s) and the Author(s) 2020

The rights of the editor(s) and the author(s) have been asserted in accordance with the Copyright, Designs and Patents Act 1988. All rights to the book as a whole are reserved by INTECHOPEN LIMITED. The book as a whole (compilation) cannot be reproduced, distributed or used for commercial or non-commercial purposes without INTECHOPEN LIMITED's written permission. Enquiries concerning the use of the book should be directed to INTECHOPEN LIMITED rights and permissions department (permissions@intechopen.com).

Violations are liable to prosecution under the governing Copyright Law.



Individual chapters of this publication are distributed under the terms of the Creative Commons Attribution 3.0 Unported License which permits commercial use, distribution and reproduction of the individual chapters, provided the original author(s) and source publication are appropriately acknowledged. If so indicated, certain images may not be included under the Creative Commons license. In such cases users will need to obtain permission from the license holder to reproduce the material. More details and guidelines concerning content reuse and adaptation can be found at <http://www.intechopen.com/copyright-policy.html>.

Notice

Statements and opinions expressed in the chapters are these of the individual contributors and not necessarily those of the editors or publisher. No responsibility is accepted for the accuracy of information contained in the published chapters. The publisher assumes no responsibility for any damage or injury to persons or property arising out of the use of any materials, instructions, methods or ideas contained in the book.

First published in London, United Kingdom, 2020 by IntechOpen
IntechOpen is the global imprint of INTECHOPEN LIMITED, registered in England and Wales,
registration number: 11086078, 7th floor, 10 Lower Thames Street, London,
EC3R 6AF, United Kingdom
Printed in Croatia

British Library Cataloguing-in-Publication Data
A catalogue record for this book is available from the British Library

Additional hard and PDF copies can be obtained from orders@intechopen.com

Immunohistochemistry - The Ageless Biotechnology
Edited by Charles F. Streckfus
p. cm.
Print ISBN 978-1-83880-820-4
Online ISBN 978-1-83880-821-1
eBook (PDF) ISBN 978-1-83880-822-8

We are IntechOpen, the world's leading publisher of Open Access books Built by scientists, for scientists

4,600+

Open access books available

120,000+

International authors and editors

135M+

Downloads

151

Countries delivered to

Our authors are among the
Top 1%

most cited scientists

12.2%

Contributors from top 500 universities



WEB OF SCIENCE™

Selection of our books indexed in the Book Citation Index
in Web of Science™ Core Collection (BKCI)

Interested in publishing with us?
Contact book.department@intechopen.com

Numbers displayed above are based on latest data collected.
For more information visit www.intechopen.com



Meet the editor



Dr. Charles F. Streckfus is Professor of Biomedical and Diagnostic Sciences at the University of Texas Dental Branch at Houston. Prior to this appointment, he was Assistant Dean of Research and Graduate Programs, University of Mississippi Medical Center. Dr. Streckfus has published over 100 peer-reviewed journal articles. His honors and awards include the prestigious President's Award for Scientific Excellence, presented by the International Society for Preventive Oncology, 6th International Symposium Predictive Oncology Intervention Strategies, Pasteur Institute, Paris, France, February 12, 2002 for his discovery of salivary Her2/neu as a biomarker for breast cancer. He also received the NIH Award of Merit in 1992.

Contents

Preface	XIII
Section 1 Technical Aspects of Immunohistochemistry	1
Chapter 1 Detection Systems in Immunohistochemistry <i>by Sorour Shojaeian, Nasim Maslehat Lay and Amir-Hassan Zarnani</i>	3
Chapter 2 Antigen Retrieval for Light and Electron Microscopy <i>by Shuji Yamashita</i>	29
Section 2 Use of Immunohistochemistry in Disease Detection	53
Chapter 3 Immune Cell Profiling in Cancer Using Multiplex Immunofluorescence and Digital Analysis Approaches <i>by Edwin Roger Parra</i>	55
Chapter 4 Low-Specificity and High-Sensitivity Immunostaining for Demonstrating Pathogens in Formalin-Fixed, Paraffin-Embedded Sections <i>by Yutaka Tsutsumi</i>	69
Chapter 5 In Situ Identification of Ectoenzymes Involved in the Hydrolysis of Extracellular Nucleotides <i>by Mireia Martín-Satué, Aitor Rodríguez-Martínez and Carla Trapero</i>	115

Preface

Immunohistochemistry (IHC) is a technology that has been part of the scientific and medical community since the 1930s. It was officially reported in the scientific literature by Dr. Albert Coons and his colleagues in 1942 [1]. IHC combines immunological and biochemical techniques to create discrete images of the components within tissues by using appropriately labeled antibodies. By utilizing this technique, IHC makes it possible to visualize and document specific cellular components within cells. Fortunately, IHC continues to incorporate new technology and still remains widely accepted by scientists and physicians 70 years later.

It is the purpose of this book to introduce the reader to some of the most recent uses and developments in the field of IHC. Chapter 1 discusses the history and development of IHC over the decades. Additionally, the chapter offers a reconsideration of the concept of applying heat-induced antigen retrieval for immunological studies using a variety of tissue specimens to determine the effects of antibody diluents on IHC. Chapter 2 provides a review of IHC detection systems with an emphasis on their principles, history, advantages, and limitations, and delineates factors that need to be considered for choosing an appropriate detection system for IHC applications. The aim of the third chapter is to highlight the tyramide signal amplification methodology to multiplex immunofluorescence and image analysis to identify several proteins at the same time in one single tissue. This type of methodology associated with image analysis can be performed using high-quality throughput assay for translational research studies to apply to cancer prevention and treatments. In Chapter 4 the authors explain how low-specificity but high-sensitivity immunostaining can be used for visualizing pathogens in paraffin-embedded sections. Chapter 5 describes how IHC can be employed for in situ identification of ectoenzymes involved in the hydrolysis of extracellular nucleotides.

The above is only a brief description of the contents of this book. As the reader will observe, the book provides new and useful information concerning the rapidly advancing field of IHC.

Charles F. Streckfus, DDS, MA, FAAOM, FAGD
University of Texas School of Dentistry at Houston,
Department of Diagnostic and Biomedical Sciences,
Behavioral and Biomedical Sciences Bldg.,
Houston, TX, USA

Reference

[1] Coons AH, Creech HJ, Jones RN, Berliner E. The demonstration of pneumococcal antigen in tissues by the use of fluorescent antibody. *Journal of Immunology*. 1942;**45**:159-170

Section 1

Technical Aspects of
Immunohistochemistry

Detection Systems in Immunohistochemistry

*Sorour Shojaeian, Nasim Maslehat Lay
and Amir-Hassan Zarnani*

Abstract

Immunohistochemistry (IHC) is a process of selectively imaging antigens in cells or tissue sections by exploiting antibody specificity. This technique is widely used in diagnostic pathology and research experiments for tracking specific molecular markers characteristic of a particular cell type or cellular events such as cancerous cell development, cell proliferation, or apoptosis. Visualizing the target antigen following an antibody-antigen interaction is accomplished by different detection systems. In the simplest instance, primary antibody directly conjugated to an enzyme is responsible for both specifically binding to the antigen and catalyzing a color-producing reaction. Alternatively, complex detection systems could be designed to profoundly improve minimal detection level of the antigen. During the past years, there has been a considerable improvement in designing and introduction of new and highly sensitive detection systems. The choice of an IHC detection system is a compromise of a variety of variables including desired sensitivity, cost, and the time needed for an IHC staining to be performed. This chapter covers the immunohistochemistry detection systems with emphasis on their principle, history, advantages, and limitations and delineates factors needed to be considered for choosing an appropriate detection system for IHC applications.

Keywords: immunohistochemistry, antibody, detection systems, sensitivity, background

1. Introduction

Immunohistochemistry (IHC) represents a way to build a picture of particular distribution and localization of molecular markers within cells and in the proper tissue context and is a powerful tool that provides important diagnostic, prognostic, and predictive information supplemental to the morphological assessment of the tissues. Although less sensitive quantitatively than such immunoassays as western blotting or ELISA, IHC enables observation of molecular signature in the context of intact tissue. In its very simplified method, IHC visualizes target antigens by using target-specific antibodies tagged with appropriate labels. However, lack of need for labeling of molecular marker-specific primary antibodies and higher sensitivity made indirect staining methods as the preferred staining method. The need for more sensitive detection systems in case of minimally expressed markers was a provocative factor that eventually led to the emergence of next generations of IHC detection methods with the hope to amplify staining signal. IHC

methods based on avidin-biotin interaction and polymer- and tyramide-based signal amplification are among IHC signal amplification methods that have greatly enhanced the sensitivity of IHC staining. However, when more sensitive methods are used, background signal tends to increase along with the target signal and so highly sensitive detection systems are not always desirable. Therefore, the optimal IHC method is planned as a compromise between sensitivity that allows proper and reliable visualization of a given molecular marker and at the same time avoiding background signals that impair staining index and specificity of the staining method. In an optimal IHC detection system, tissue type, level of expression of the marker of interest, localization of the marker, and cost are among important factors that should be taken into consideration. As a general rule of thumb, there is no a *bona fide* IHC detection method that is universally accepted. Although it does not rely on chemical reactions that take place in IHC, immunofluorescence (IF) staining follows almost the same rules as with IHC and so concerns on detection systems that are also applicable to IF staining methods. In this chapter, we will focus on detection methods in immunohistochemistry and immunofluorescence stainings and highlight in detail potential application, advantages, and disadvantages of each method.

2. Direct method

Direct detection methods are known as a one-step process applying a primary antibody, which is directly labeled with reporter molecules, such as biotin, colloidal gold, fluorochromes, or enzymes [1, 2]. The conjugated antibody makes a direct contact with cognate antigen in histological or cytological preparations (**Figure 1**). Direct detection methods are widely used for detecting highly expressed antigens. Furthermore, when the use of the secondary antibodies causes nonspecific and unwanted reactions, owing to the histological nature of the tissue and/or host species of the primary antibody, direct detection could be the technique of choice. For instance, in case of mouse lymph node immunostaining, labeled primary mouse monoclonal antibodies are preferred because antimouse secondary antibodies are not only bound to mouse primary antibodies bound to the tissue antigens of interest but will also react with endogenous immunoglobulins vastly found in lymph nodes. This would lead to a strong nonspecific staining. Hence, direct detection methods using mouse primary antibodies conjugated to a fluorophore or enzyme would be a better option [3]. If this approach is not practically feasible, for example, due to the low expression level of the target antigen or technical problems in primary antibody labeling, indirect methods using primary antibodies from species other than that of target tissue would be desirable.

One of the advantages of direct detection is that the incubation step with a secondary reagent is eliminated. Hence, this method is time saving and easy to



Figure 1.
Direct immunostaining method.

perform. In addition, due to the wide range of fluorochromes that are commercially available, direct detection is vastly used in multicolor experimental designs [4, 5].

It is important to note that insufficient sensitivity to detect most of the antigens found in routinely processed tissues is one of the drawbacks of using direct detection method. Furthermore, each primary antibody needs to be individually conjugated with fluorophores or enzymes, which increases considerably the cost of the whole process. Another concern with direct staining methods is the possibility of functional impairment of the antibody affinity if the process of antibody labeling is nonoptimal. This is especially case for monoclonal antibodies in which all antibody molecules in a given preparation have almost the same affinity and so are most likely to be affected all together by improper labeling. This issue is less problematic for polyclonal antibodies in which antibodies with diverse physicochemical properties are produced against an antigen [5–7].

Needless to say, direct detection methods are the method of choice in such high-sensitive protein detection systems as flow cytometry. Although this system is the simplest and the most convenient method for detection of a given marker expression, it is not routinely employed in clinical and research applications due to the limitations mentioned above.

3. Indirect method

The need for more sensitive detection systems for antigens with low expression pattern was a provoking factor that prompted Coons et al. in 1941 to develop two-step detection methods [8]. This system employs an unlabeled primary antibody as the first layer and the secondary antibody, which is raised against the primary antibody and is labeled with different fluorophores or enzymes (**Figure 2**) [6, 9–11]. In indirect methods, primary antibodies retain full avidity because they remain unlabeled. Indeed, higher number of labels per molecule of primary antibody is achieved in indirect compared to direct detection methods. The later stems from the fact that at least two labeled secondary antibodies can bind to each primary antibody molecule. These factors result in increased reaction intensity and the higher sensitivity in indirect staining methods. Accordingly, indirect methods are able to detect fewer number of antigens with less primary antibody. Moreover, indirect methods are more practical than direct methods since the same secondary antibody can be applied for detection of different sets of primary antibodies if they have been raised in the same species [12]. Another benefit of indirect method in IF stainings is possibility to select secondary antibodies with fluorophores of different colors. For example, if the tissue shows strong endogenous red autofluorescence, the secondary antibody labeled with green

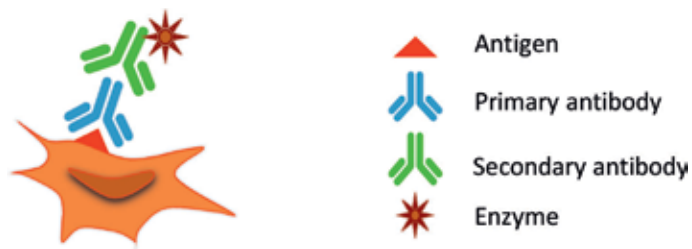


Figure 2.
Indirect immunostaining method.

fluorophore could be a right choice [3]. Previously mentioned advantages of indirect detection systems eventually led to its widespread applications in research and clinical settings.

Despite advantages mentioned above, indirect immunostaining methods suffer from some shortcomings. First, additional controls and blocking steps are inevitable when using secondary antibodies. Indeed, there is possibility of nonspecific staining that happens when the secondary antibody interacts with unwanted tissue targets. If nonspecific staining is noticed, blocking reagents have to be used to treat the tissue sections that could be time-consuming and cause additional costs to IHC experiment [6, 13]. The blocking agent should contain nonimmune antibody fraction from the same species in which secondary antibody has been produced. This results in competitive blocking of the nonspecific binding sites for secondary antibody in the target tissue by the unlabeled antibodies from the same species. The addition of further layers beyond their use in the two-step indirect method for increasing the sensitivity of detection can be problematic as addition of every new species of antibody considerably increases the risk of nonspecific interactions and background staining [14]. Desire for more sensitive detection systems triggered researchers to develop next-generation detection systems, especially for those antigenic markers, which are not expressed in physiological condition, and any level of their upregulation would be interpreted as a pathological condition.

4. Bridge methods

Early conjugation protocols were not efficient and did not label all antibodies leaving a fraction of antibodies unlabeled. These unlabeled antibodies were able to compete with labeled antibodies for binding to the cognate antigen and reduced the efficiency of detection. To overcome this problem, new approaches were invented that eliminated the need for chemical conjugation of antibodies. In these approaches, antigen specificity of antibodies is employed to couple antibodies to the enzymes. Taking advantage of antigen specificity of antibodies, antiperoxidase or antialkaline phosphatase antibodies are easily coupled with peroxidase or alkaline phosphatase after incubation with these enzymes without need for any chemical modifications of the antibody. These preformed soluble enzyme-antienzyme immune complexes are then used as the third layer reporter antibody for detection of the antigen-bound primary antibody in tissue section. Taking advantage of the bivalent properties of IgG binding, a second-step antibody with binding specificity to primary antibody and tertiary antienzyme antibody complexed with the enzyme bridges two layers (**Figure 3a**). The bridge antibody is usually used in excess, so that one of its two identical binding sites interacts with enzyme-coupled tertiary antibody, while the other site interacts with primary antibody. The tertiary antienzyme antibody has the same animal species of origin as the primary antibody. The bridge methods are collectively called as soluble enzyme-antienzyme methods [5, 8, 15–17].

The classical immunoenzyme bridge method [18] was rapidly replaced with an improved version in which peroxidase-antiperoxidase complex (PAP, MW: 400–430 KDa) contained three peroxidase molecules and two antiperoxidase antibodies (**Figure 3b**) [15]. In this system, antibodies against alkaline phosphatase can also be employed to form alkaline phosphatase-antialkaline phosphatase complexes (APAAP, MW: approximately 560 KDa) [17]. In contrast to PAP complexes, APAAP complexes include two molecules of alkaline phosphatase and only one antibody. The APAAP method is usually used as an alternative to PAP technique when high levels of endogenous peroxidase in such tissues as bone marrow aspirate specimens, spleen and peripheral blood, interfere with the staining or when double labeling approaches are desired [19].

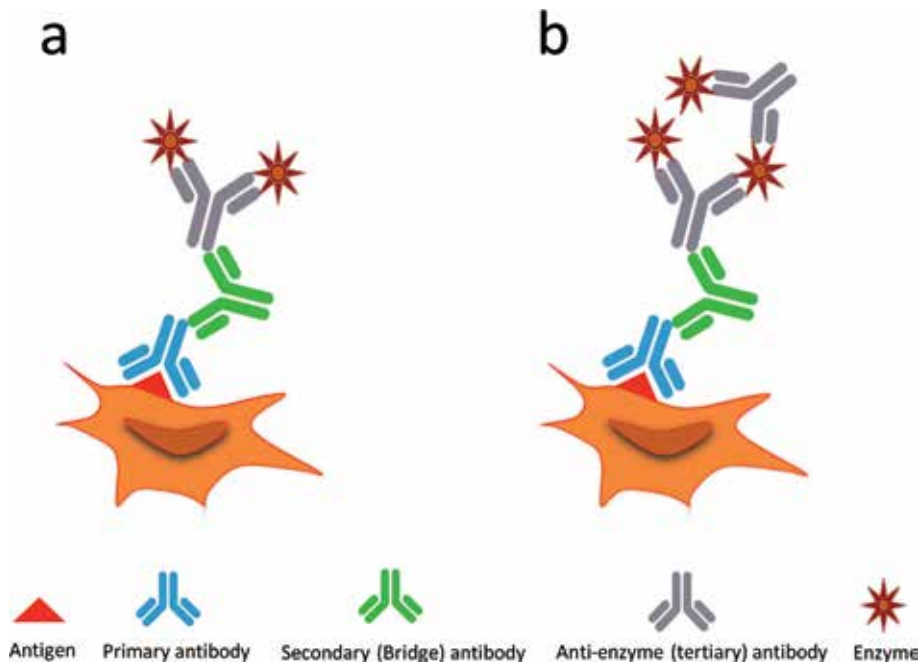


Figure 3.
Two- (a) and three-step (b) bridge immunostaining methods.

Soluble enzyme-antienzyme methods offer several advantages over direct and indirect detection methods. The drawback of chemical conjugation process, which could potentially lead to impairment of antibody activity, is entirely avoided in enzyme-antienzyme methods. Due to a greater number of enzyme molecules localized per antigenic site, enzyme-antienzyme process shows the higher sensitivity compared to previously described methods. It is reported that PAP method exhibits nearly 100- to 1000-fold higher sensitivity than two-step indirect method [7]. Although multilayering of detection antibodies could potentially increase the risk for nonspecific interaction with the tissue antigens, PAP and APAAP methods that offer triple level detection are among the exceptions. These methods are suitable for cell and cryosection IHC [14].

In comparison to two-step indirect methods, PAP and APAAP are more time-consuming. Indeed, these methods may not have sensitivity enough required for use in formalin-fixed paraffin-embedded (FFPE) preparations, especially when used in combination with monoclonal antibodies [14]. Although PAP and APAAP methods have been known as the highly sensitive, reliable, and popular techniques in pathology laboratories for a long time, they have gradually been replaced by more improved methods such as streptavidin-biotin- and polymer-based systems.

5. Biotin-avidin/streptavidin-based methods

5.1 Labeled avidin/streptavidin-biotin (LAB/LSAB)

Labeled avidin/streptavidin-biotin (LAB/LSAB) are among very sensitive IHC detection methods, which take advantage of high-affinity binding of avidin/streptavidin to a water-soluble vitamin, biotin (vitamin H or B₇) [5, 20–22]. The affinity constant of avidin binding to biotin (10^{15} M^{-1}) is nearly 10^3 – 10^6 times more than the binding affinity of antibody-antigen interaction [22].

The potential of avidin-biotin system to be used in immunoassays was inspired for the first time from a study in 1972 in which it has been shown that avidin could inactivate the biotinylated bacteriophages [23]. Avidin-biotin-based system was used for the first time in an immunological experiment in 1976 when an erythrocyte surface antigen was localized by using biotin-labeled antibody and ferritin-avidin conjugate [24]. In 1979, Guesdon et al. showed that avidin-biotin complex could be effectively used for immunoassays. Using avidin-biotin system, they suggested different related methods for enhancing the specificity and sensitivity of solid-phase immunoassays. They also used avidin-biotin-based immunohistochemistry for localization of intracellular immunoglobulins [25].

The principle of labeled avidin-biotin (LAB) technique is based on sequential interaction of biotin-labeled antibody with tissue antigen and enzyme-labeled avidin with biotinylated primary antibody (**Figure 4a**). In the bridged avidin-biotin (BRAB) technique, however, avidin bridges biotin-labeled primary antibody and biotin-labeled enzyme (**Figure 4b**). BRAB is particularly suitable in cases where intracellular penetration and/or sensitivity of the staining reaction are the major concerns. An indirect approach of BRAB technique (IBRAB) can also be applied for identification of antigens in formalin-fixed paraffin-embedded tissues in which avidin and biotin-labeled peroxidase are added sequentially to the system after primary antibody and biotin-labeled secondary antibody. The superiority of BRAB over LAB method is that there is no need to prepare protein-protein conjugate [20, 25].

Avidin extracted from egg white is a large tetrameric glycoprotein with molecular weight of about 66 KDa. Each subunit (MW 16,400 Da) contains one high-affinity binding site for biotin [26] and one oligosaccharide modification (Asn-linked). Tryptophan and lysine residues in each subunit are believed to be involved in forming the binding pocket with high affinity for biotin molecule [27–29]. Biotin with molecular weight of about 244.31 Da is a small molecule, which has only one binding site specific for avidin. Biotin can be easily conjugated with an antibody or other macromolecules such as fluorochrome and enzymes through other sites [6, 22].

Due to some limitations mentioned below, avidin has been mostly substituted by streptavidin in IHC applications. In this regard, labeled streptavidin-biotin methods (LSAB) are now more popular than LAB methods in both diagnostic and research IHC laboratories [30–34]. The sequence of streptavidin from *Streptomyces avidinii* shows only 30% similarity to avidin, while it has nearly identical secondary, tertiary, and quaternary structure [35]. It is a nonglycosylated protein with a molecular weight of 60 KDa [36]. Avidin is a basic glycoprotein (pI ~ 10.5) that contains nearly 7% carbohydrates, which gives avidin a natural tendency to nonspecifically bind to lectin-like substances found in kidney, liver, brain, and mast cells [7, 36–38]. Avidin can also bind electrostatically to negatively charged tissue elements at physiological pH. Streptavidin (pI ~ 6.5), however, remains uncharged at neutral pH and does not contain carbohydrate in its structure eliminating its nonspecific binding to tissue lectins. In addition, streptavidin shows less propensity for aggregation [7, 39–41]. Although avidin shows higher binding affinity to free, unconjugated biotin, streptavidin has more tendency to bind biotin-protein conjugates [42]. Indeed, lot to lot variations in binding affinity of biotin and avidin have been reported, which negatively affect sensitivity and reproducibility of the procedure [7].

LAB/LSAB methods offer several advantages for IHC applications. Biological activities of macromolecules (e.g., enzymatic catalysis or antibody binding) are not affected when they are conjugated with biotin. On the other hand, the affinity of avidin/streptavidin to biotin is quite high enough that ensures the biotin-avidin/

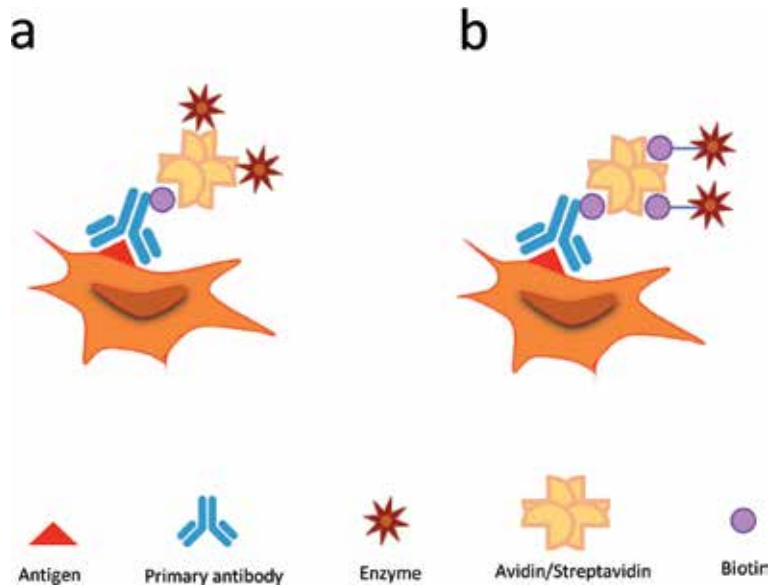


Figure 4.
LAB/LSAB (a) and BRAB (b) immunostaining methods.

streptavidin complex is not disrupted by manipulations like multiple washing when the complex is immobilized in the tissue sections or by changes in pH and presence of chaotropes [22]. LAB/LSAB techniques considerably improve the sensitivity and efficiency of the immunohistochemical detections and allow researchers to use even more diluted primary antibodies. An immunohistochemical staining that employs a single layer of biotin-labeled monoclonal antibody provides sensitivity equivalent or much greater than PAP methods [43]. The increased sensitivity of avidin-biotin methods stems from larger numbers of biotin molecules that is conjugated to a primary antibody [20, 25, 44]. Due to very high sensitivity, IHC stainings using LAB/LSAB techniques are rapid [45, 46]. LAB and LSAB technique can also be applied in an indirect manner, where biotinylated secondary antibodies are used in conjunction with unlabeled primary antibody [47].

The main challenge of LAB/LSAB techniques is the nonspecific (false-positive) staining, which occurs when the tissue of target contains endogenous biotin [6, 7]. Endogenous avidin biotin activity (EABA) or tissue affinity for avidin/streptavidin is especially common in tissues and cells that contain high amount of biotin, such as placenta, mammary glands, kidney, adrenal cortex, brain, liver, fat, and mast cells [3, 6, 48]. EABA is much highlighted by heat-induced epitope retrieval (HIER) but also develops in tissues subjected to other types of antigen retrieval [49–51]. The level of endogenous biotin activity is especially higher in frozen compared to FFPE tissue sections, which leads to unwanted nonspecific reaction [52, 53]. EABA is typically found in cytoplasm, but it has been reported in the nucleus as well [51, 54–56]. Although paraffin embedding and formalin fixation have been found to significantly decrease the level of endogenous biotin, it is highly recommended to use a biotin blocking step when using avidin/streptavidin-biotin-based detection systems to decrease endogenous biotin activity. Since the commercially available EABA blocking reagents (pure avidin and biotin solutions) are very expensive, many researchers prefer to use homemade blocking reagent containing egg white and 5% powdered milk as sources of avidin and biotin, respectively [57–60].

5.2 Avidin-biotin complex (ABC) method

For signal amplification, another biotin-based IHC detection method was developed, namely avidin-biotin complex (ABC) method, in which a preformed avidin-biotin-peroxidase complex is used as the detection layer [20, 61]. This technique induces three different layers; an unconjugated primary antibody, a biotinylated secondary antibody, and finally a large complex of enzyme-labeled biotin and avidin, which is attached to the biotin molecules conjugated to the secondary antibodies (**Figure 5**). Two biotins from adjacent biotinylated enzyme molecules can be joined via an avidin molecule [62]. Four biotin binding site of avidin molecule could result in formation of lattice complexes in which avidins are attached together by biotinylated enzyme molecules creating a large complex, which is attached to the biotinylated secondary antibody [20, 63]. In normal circumstances, not all the four avidin's capacity for biotin are taken up by biotinylated enzyme. This allows the complexes to attach to biotin of primary or secondary antibodies [64].

Before the advent of biotin-avidin-based methods, the PAP method was considered the most sensitive detection technique. The ABC method was then found to be nearly 40 times more sensitive compared to PAP method [65, 66].

By applying biotinylated primary antibodies, the ABC protocol can be shortened to a two-step method [3]. It is reported that application of biotin-labeled primary antibody in the two-step ABC method creates an equal sensitivity to the unconjugated antibody in the three-step ABC method. This finding proposes that biotinylation does not impair antibody activity and that application of a secondary antibody to intensify the reaction would not be necessary, if a suitable biotin-labeled primary antibody is used [43].

Although formation of lattice complexes of avidin and biotinylated enzyme seems to increase the sensitivity of ABC method compared to LAB/LSAB, it was found that

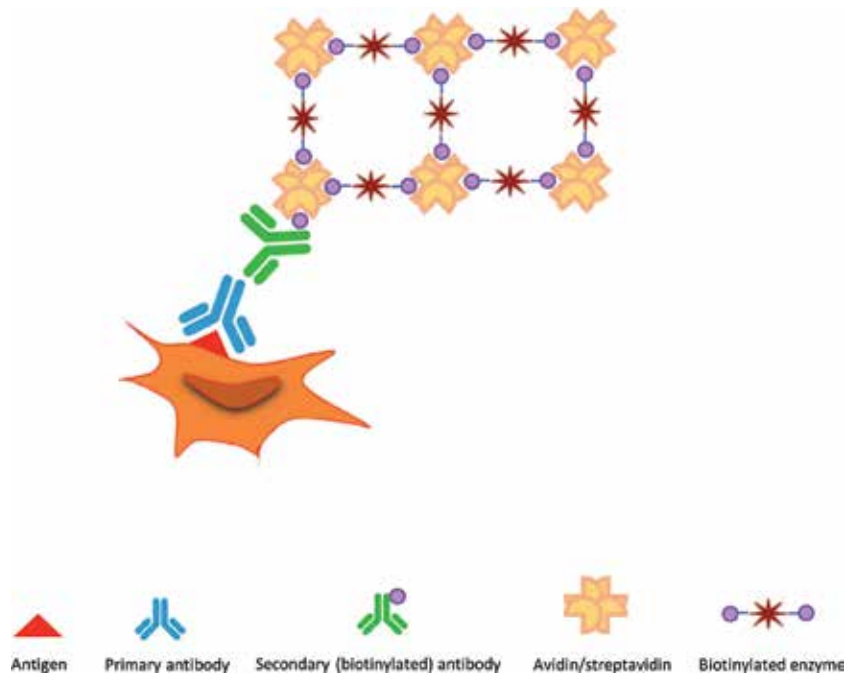


Figure 5.
Avidin/streptavidin immunostaining method.

the sensitivity of ABC method is 5–10 times less than the LSAB method [67]. This disadvantage of ABC method is due to the large size of lattice complexes that hinder their penetration into the cells. Indeed, as with LAB/LSAB methods, the background in ABC method cannot be removed due to the irreversibility of the avidin-biotin reaction [21, 68]. As with LAB/LSAB methods, tissue endogenous biotin is one of the concerns in ABC-based IHC staining methods that results in nonspecific staining.

6. Polymer-based immunohistochemistry

Desire for IHC detection systems with improved sensitivity led to the development of chain polymer-conjugate technology in the last decade of the former century [69, 70]. Improved sensitivity of this technology is based on using synthetic or natural polymers that increase the capacity for incorporating ligands or enzymes to be coupled to linker antibodies [71–78]. Using this technology, much higher antigen detectability could be obtained in comparison to standard ABC and LSAB methods or in enzyme-antienzyme immune complex techniques (PAP and APAAP) [69, 70]. The chain polymer-conjugate technology normally utilizes a backbone of an inert polymer molecule of dextran [71–73], polypeptides [74], dendrimers [75, 77], or DNA branches [78]. The backbone is able to carry both antibodies and multiple enzymes. Hence, nearly 11 antibodies and up to 40 HRP molecules could be anchor to one 500 KDa dextran molecule [79].

In 1993, a one-step direct polymer immunohistochemical staining method, namely enhanced polymer one-step staining (EPOS) system, was introduced by Bisgaard and Pluzed [80]. In this method, up to 10 monoclonal primary antibodies and 70 enzyme molecules are attached to a dextran backbone with a high molecular weight. This would enable the whole immunohistochemical staining process (from primary antibody to enzyme) to be completed in a single step (**Figure 6a**) [81]. The whole process can be performed in nearly 7 min for frozen sections and to less than 3 h for regularly processed, paraffin-embedded specimens. Hence, when a quick and reproducible IHC-based diagnostic approach is demanded in emergency circumstances, for example, during surgeries, this method should be taken into consideration [82]. However, applicability of this method is restricted to primary antibodies provided by the manufacturer and was not suitable for user supplied primary antibodies.

To overcome this limitation, a polymer-enhanced two-step IHC detection system (EnVision, EV) was introduced in 1995. EV system contains secondary anti-mouse and antirabbit Ig antibodies and could be applied to localize tissue-bound primary antibodies of mouse and rabbit origins (**Figure 6b**) [83–85]. The EnVision complex is composed of up to 20 secondary antibodies and nearly 100 molecules of peroxidase molecules, which all are directly attached to an activated dextran polymer backbone [86].

EnVision is a user-friendly technique and provides the users a rapid visualization in only 45 min. This method offers a very high sensitivity and does not lead to false-positive reaction due to the endogenous biotin [87]. Although the EV system is a very expensive method, it can be applied with higher dilutions of primary antibodies. Indeed, because endogenous biotin is not a problem anymore, EV permits more efficient heat-induced epitope retrieval (HIER) [69, 88]. The detection systems based on polymers could also be a choice for quick immunostaining of frozen sections when tumor margin and micrometastasis is to be identified. Furthermore, polymer-based detection systems are sensitive enough to be applied as an alternative detection system in western blotting [89] and in chromogenic *in situ* hybridization (CISH) [90].

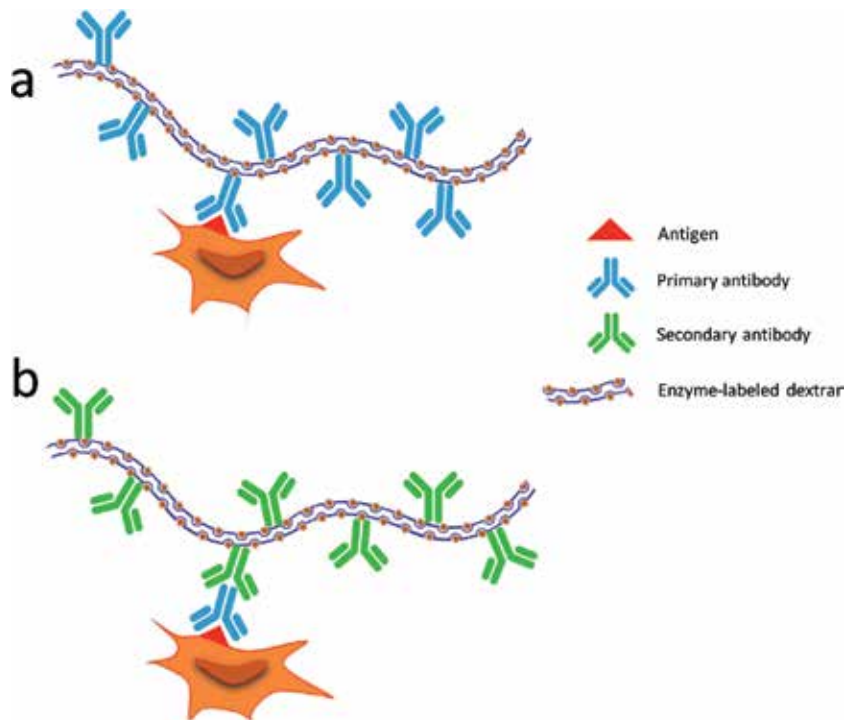


Figure 6.
Polymer-based immunostaining method: (a) EPOS and (b) EnVision.

Dextran carriers with a high molecular weight, however, appear to compromise the penetrative ability of the detection reagent due to spatial hindrance. Accordingly, the sensitivity of polymer-enhanced systems is profoundly affected by antigen localization. For instance, remarkably low sensitivity has been noticed in nuclear antigens [88, 91]. Indeed, in thick tissue sections, where the antigens are located beneath the surface area, only a part of antigens are amplified. This happens because of the large size of dextran-enzyme complex, which could not disperse into the deeper layers making quantitative results unreliable [87]. Subsequently, EnVision+ was developed, which was a modified version of EV system with higher sensitivity. EnVision+ contains a mixture of dextran polymers with two different secondary antibodies (goat antirabbit and goat antimouse IgG) anchored to it [86, 88, 92]. Nonetheless, EnVision systems were reported to give less sensitivity in case of some antibodies especially those that require proteolytic digestion, which was believed to stem from problems of tissue penetration of the labeled polymer.

Although the application of polymer gives a chance of increasing the number of enzymes coupled to the carrier backbone, it also profoundly increases the size of complex. Therefore, enzyme density per unit surface may not be increased to the degree that would be expected. Hence, it would be a desirable approach to design a compact polymer-enzyme-linker antibody conjugates with optimal number of enzyme molecules. Based on this goal, Shi et al. [91] suggested to use small linear molecules that have a capacity to polymerize with enzymes and linker antibodies in a tightly packed size. The IHC results with this newly designed detection system (Power Vision) showed that it possesses compact size and, compared to conjugates containing polymer linkers, shows higher detection efficiency for antigens located on the cell surface or in the nucleus [91]. Compared to EnVision+, this “second-generation” polymer-based conjugate was found to

be less expensive and fast and showed better reproducibility and capacity to be standardized [93, 94]. From clinical point of view, these methods are extremely useful when emergency results (for example, assessing the intraoperatively surgical margins of tumor specimens) are needed [95].

7. Tyramide-based signal amplification

7.1 Biotinylated tyramide signal amplification

In 1989, a novel signal amplification method for immunoassays was introduced by Bobrow et al. called catalyzed reporter deposition (CARD). The CARD was first used in western blots and immunodots [96–98] and was then adapted for IHC by Adams [99].

The signal amplification in this system is based on an analyte-dependent reporter enzyme (ADRE), which catalyzes the deposition of additional reporter molecules. The first step of this system relies on the same principle as LAB/LSAB detection system. Accordingly, primary antibody is first added to the tissue section followed by biotinylated secondary antibody and either HRP-labeled streptavidin (in tyramine signal amplification (TSA)) or streptavidin-biotin-HRP complex (in catalyzed signal amplification (CSA)). The amplification process happens when the peroxidase enzyme (ADRE) oxidizes the phenolic components to produce extremely unstable and reactive intermediate radicals, which are then bound to a tissue section [96, 100]. Tyramine, a biogen amine derived from aromatic amino acid tyrosine, is a substrate commonly used in this technique. It contains an amine at one end and a phenol at another end, which is used by peroxidase enzyme. The amine group is employed to conjugate the molecule with biotin or any other target molecules via an amide bond [101]. In the presence of HRP and H_2O_2 , biotinylated tyramine is oxidized and resulting highly reactive radicals will react with electron-rich aromatic components, such as tyrosine-rich moieties of proteins in the vicinity of the HRP binding sites in tissues. This binding occurs very rapidly within 10 min. Due to a very short half-life of tyramide radicals, they are deposited at the same location where they are generated [102]. This reaction is then followed by incubation of the tissues with streptavidin-peroxidase complex. This complex is attached to the biotin sites of the tyramine, which are remained free. This reaction is restricted to the sites of primary antibody binding site where HRP had previously accumulated (**Figure 7**).

Because of the high sensitivity of this method, biotinylated tyramide amplification enabled many antigens to be traced, which had previously been unreactive in formalin-fixed paraffin-embedded tissues [101]. In comparison to the avidin-biotin-based methods, biotinylated tyramide signal amplification exhibits 5- to 10-fold more sensitivity. Some researchers believed in even more sensitivity [103]. It was reported by Sanno et al. that staining of pituitary hormones with CSA showed nearly 100-fold higher sensitivity compared to standard ABC method [104]. It is recommended to use this method when (1) antigen expression in target tissue is extremely low or the amount of antibody available is limited and (2) primary antibodies possess low affinity or are not compatible with paraffin-embedded tissue sections [104, 105]. Repeating the biotinyl-tyramide reaction can further increase the signal intensity. However, this circuit is restricted to only two or three rounds before the background noise becomes an issue [106]. CSA and/or TSA methods are found to be cheaper than EnVision system but with the same effectiveness [86].

These methods, however, are laborious because they involve an initial avidin-biotin procedure followed by the tyramine reaction. Background can also be considered a serious problem, particularly with HIER. In this case, more prolonged

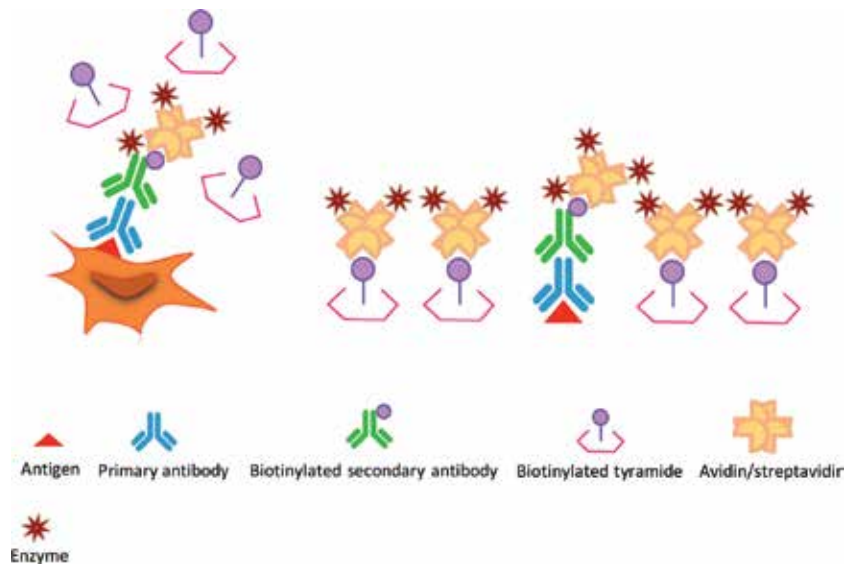


Figure 7.
Tyramide-based immunostaining method.

treatment of tissues to quench endogenous peroxidase or endogenous avidin-biotin activities (EABA) is usually necessary [105, 107–109]. Although TSA/CSA detection methods have resulted in satisfactory results in terms of significantly increased sensitivity in IHC and *in situ* hybridization (ISH), they are not widely employed in diagnostic pathology. The reasons include: additional steps that make the method more time-consuming, nonspecific background staining, and that optimal AR treatment with existing methods may achieve equivalent results and that second-generation polymer-based methods are simpler and equally sensitive [14, 110, 111].

7.2 Biotin-free TSA/CSA

In an attempt to reduce the problems associated with endogenous biotin in conventional tyramide signal amplification, a biotin-free system, fluorescyl-tyramide amplification system (FT-CSA or CSAII), was introduced. Rather than biotinyl-tyramide, this system uses fluorescyl-tyramide and does not contain avidin/biotin reagents avoiding the problem associated with endogenous biotin. In this method, addition of primary antibody is followed by a peroxidase-labeled secondary antibody. Peroxidase enzyme is responsible to catalyze the transformation and deposition of fluorescyl-tyramide in the tissue section. When the reaction terminates, it could be inspected by fluorescence microscopy. The produced signals could even be converted to a colorimetric reaction by using peroxidase-conjugated antifluorescein antibody and a diaminobenzidine-hydrogen peroxide substrate.

This method is highly sensitive enabling researchers to detect and localize antigens with low expression level and to use primary antibodies with very low affinities [105, 106]. Alternative reporter includes dinitrophenol, which also results in marked reduction of background from endogenous biotin. Absence of nonspecific staining is due to no endogenous tissue distribution of dinitrophenol [14].

In the latest improvement of the biotin-free CSA method, fluorescein is conserved in the substrate, while the tyramine is substituted with ferulic acid, which is a much better peroxidase substrate and increases signal-to-noise ratio. In this system, the incubation time in each step can be significantly reduced, making it possible to stain a tissue in less than 1 h [112].

8. Rolling circle amplification

Rolling circle amplification (RCA) reaction was first developed for the purpose of nucleic acid detection [106], but it was then adapted for amplification of signals from antibodies bound to antigens [113–118]. RCA is an enzymatic process in which a short DNA or RNA primer is amplified using a circular DNA template and special DNA or RNA polymerases to form a long single-stranded DNA or RNA [119, 120]. The end product of RCA is a long continuous sequence of DNA containing several tandem repeats complementary to the circular template. Unlike PCR, RCA could be performed at a constant temperature (room temperature to 37°C). A RCA reaction contains five different components: (i) a short DNA or RNA primer, (ii) a polymerase enzyme (e.g., Phi29 DNA polymerase for DNA, and T7 RNA polymerase for RNA), (iii) a suitable buffer compatible with polymerase enzyme, (iv) a circular DNA template, and (v) deoxy nucleotide triphosphates (dNTPs) [121].

RCA reaction has three different steps: (1) the circular DNA template with typically ~15–200 nt in length is synthesized through the intramolecular ligation of phosphate and hydroxyl end groups of a linear probe with the use of the target DNA or RNA as a ligation template [121–123], (2) the polymerase enzyme continuously adds dNTPs to a circular template-annealed primer to form a long ssDNA with tens to hundreds of tandem repeats, and (3) the RCA end products could be detected and even monitored by different signal readout methods (Figure 8) [121]. Different methods are available to visualize and also analyze the RCA process including (a) labeling the RCA products directly during the amplification process by using

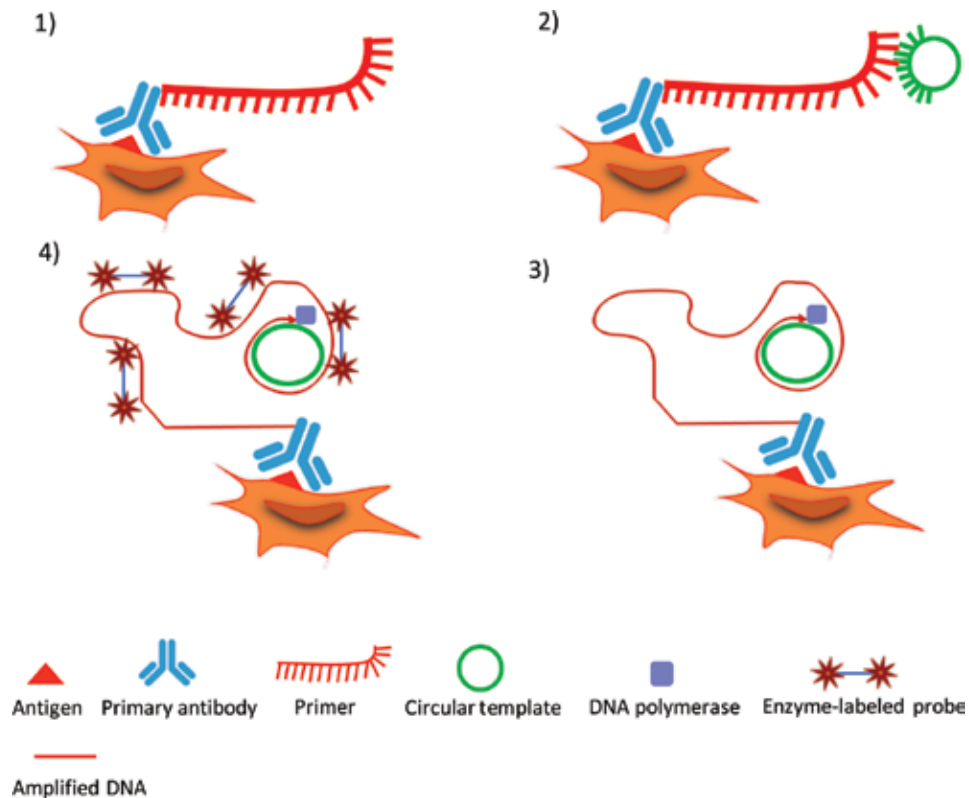


Figure 8. Rolling circle amplification immunostaining method. (1) Immunoconjugate bound to target antigen. (2) RCA primer hybridized to circle template (3) Synthesis of new DNA strand by DNA polymerase (4) Detection of amplified DNA by enzyme-labeled probe at the site of bound antibody.

fluorescent dyes-conjugated dNTPs; (b) detecting the RCA product with hybridization of fluorophore-tethered complementary strands; quantum dots or gold nanoparticles can be attached to RCA products via a complementary strand to visualize RCA product; (c) using molecular beacon for fluorescent detection of RCA products; (d) using DNA binding dyes such as SYBR green; (e) using biotinylated decorator and streptavidin-HRP conjugate or by DNA-peptide nucleic acid (PNA) intercalating dye for colorimetric detection of RCA product; and (f) using luciferase to generate light for bioluminescence detection of RCA products [121].

One of the important advantages of RCA is that circular templates can be customized so that the signals of a single binding event are amplified in an exponential manner (e.g., multiprimed RCA) [124–126]. In this approach, signal amplification more than 10^9 -fold is feasible, while a linear mode of RCA has a capacity to amplify signals to nearly 10^5 -fold [127]. RCA reactions could be accomplished on a solid surface and also in a solution environment. In solid-phase RCA, reaction is conducted on a solid surface such as glass, microwell plates, microbead or nanobead particles, paper strips, or microfluidic devices. This system gives researchers an advantage of high-throughput analysis and potential for easy detection of target from complex sample matrices [121].

RCA is appeared to be a powerful method in immunoassays. The combination of RCA method with ELISA is found to grant more sensitivity and decrease the lower detection limit. In this regard, there is an approach called immuno-RCA in which, a RCA primer-conjugated antibody is applied on a target antigen that has been coated on a solid surface followed by a RCA reaction. The first immuno-RCA test was introduced by Schweitzer B et al. (2000) on a glass slide for IgE quantification [128]. From that time, solid-phase RCA has become popular as signal amplification method in antibody microarray analysis of multiplexed proteins [129–132]. A sandwich immuno-RCA has been adapted to detect the target with high sensitivity. In this technique, the target antigen in biological media is first captured on a solid surface using coated antibody. In the next step, a RCA primer-conjugated secondary antibody is applied to conduct the RCA reaction [133–135].

Konry et al. [136], by combining the capacity of RCA reaction to detect a single-molecule and microfluidic technology, demonstrated the feasibility of identification of specific protein markers on tumor cell surfaces in miniaturized nanoliter reaction droplets. This approach of signal amplification in a microfluidic format could improve the applicability of existing methods by reducing consumption of sample and reagent and increasing the specificity and sensitivity for various applications such as early diagnosis of cancer [136]. Specific immunocytochemical and immunohistochemical identification of a wide range of intracellular molecules (prostate-specific antigen and vimentin) and cell surface antigens (epithelial membrane antigen, CD3 and CD20) in a variety of tissues (tonsil and breast) and cell lines (U266, Jurkat) has successfully been accomplished using RCA-mediated signal amplification. Indeed, immuno-RCA was reported to give more uniform staining pattern compared to the conventional methods [129]. *In situ* proximity ligation assays (*in situ* PLA) are an important adaptation of the RCA method in which primary antibodies against two distinct antigens are applied. Having two antigens in close proximity to each other, RCA reaction will occur and the proximity of two distinct antigens can be visualized [137].

It has been shown that attachment of a RCA primer to primary or secondary antibody does not impair affinity or avidity of the conjugate. Nonetheless, RCA reaction adds 60–90 min to the conventional IHC protocol. Although RCA is able to generate amplification of DNA up to 10^9 -fold, immuno-RCA in LSAB-based IHC applications is able to increase the signal to only about fourfold [129]. Simultaneous evaluation of TSA and RCA detection techniques by Warford et al. revealed that both methods are capable to produce results with a high signal-to-noise ratio. However, they found TSA detection system to be more sensitive than the RCA method [14].

9. Choice of detection system and concluding remarks

The sensitivity of an IHC staining is a function of detection method for signal amplification [138].

The choice of a detection system is mainly determined by laboratories based on the nature of the specimen, expression level of the antigen, cost, desired sensitivity, and possible automation [53]. Choosing an appropriate detection system enables maximum sensitivity and optimum visibility of the immune reaction with the fewest steps and in the shortest time [139]. As a general rule, the more complex an IHC method, the more sensitive it is. One- or two-step IHC procedures are usually less sensitive than more complex, multistep procedures. In addition, the detection system must be accurate, reproducible, and results in a high signal-to-noise ratio [140]. When choosing a desirable detection system, several factors are needed to be taken into consideration: (1) the expertise/experience of the technician; (2) type of the antigen to be identified; for example, some antigens are widely expressed and do not need a sensitive method to be visualized; (3) number of tests and the amount of antibody that is available; (4) the affinity of the antibody: each antibody has its own affinity that requires a specific detection system, antibodies with less affinity usually need more sensitive detection systems; (5) species idiosyncrasies (does the tissue contain endogenous biotin), (6) budget; (7) localization of the antigen of interest (some detection systems do not have high cell penetration capacity due to the large size and regardless of having high sensitivity for detection of surface antigens, do not yield a high sensitivity for intracellular or nuclear antigens), (8) the need for or type of antigen retrieval; typically, a non-biotin-labeled detection system is recommended if HIER is used to avoid background from endogenous avidin-biotin activity (EABA) [141].

A detection system should be compatible with animal species as well. A detection system with an outstanding performance in human is not always suitable for animal models [6, 142]. The sensitivity of commercially available detection kits, some optimized for particular animal species, should be validated in-house before use. The secondary and tertiary reagents of some kits may contain antibodies or other compounds that potentially nonspecifically react with tissue antigens, leading to a background or staining. This is one justification for negative controls in IHC [141].

As a further general rule, one should always try to use the simplest detection method with sensitivity enough for detection of the antigen. The multilayering of detection antibodies beyond this threshold can be problematic as with the addition of every new step, the risk of nonspecific interaction with the preparation increases. There are some exceptions to this rule. For example, in tumor-specific antigens, which are not expressed in normal condition, the use of more sensitive methods might decrease detection level cutoff and increase the likelihood for early detection of cancer [143, 144].

In emergency conditions when results are needed in a short amount of time (such as evaluating intraoperatively surgical margins of tumor specimens), applying a detection method with high sensitivity will definitely improve accuracy of the procedure and help surgeon to obtain wider surgical margins if needed.

Acknowledgements

The authors dedicate this book chapter to all mice, which generously made substantial contribution for improving authors' knowledge of immunohistochemical staining during experimental researches.

Conflict of interest

The authors declare no conflict of interest.

Author details

Sorour Shojaeian^{1,2}, Nasim Maslehat Lay² and Amir-Hassan Zarnani^{2,3,4*}

1 Department of Clinical Biochemistry, Alborz University of Medical Sciences, Karaj, Iran


2 Reproductive Immunology Research Center, Avicenna Research Institute (ACECR), Tehran, Iran

3 Department of Immunology, School of Public Health, Tehran University of Medical Sciences, Tehran, Iran

4 Immunology Research Center (IRC), Iran University of Medical Sciences, Tehran, Iran

*Address all correspondence to: zarnania@sina.tums.ac.ir

IntechOpen

© 2018 The Author(s). Licensee IntechOpen. This chapter is distributed under the terms of the Creative Commons Attribution License (<http://creativecommons.org/licenses/by/3.0>), which permits unrestricted use, distribution, and reproduction in any medium, provided the original work is properly cited. 

References

- [1] Coons AH, Kaplan MH. Localization of antigen in tissue cells: II. Improvements in a method for the detection of antigen by means of fluorescent antibody. *Journal of Experimental Medicine*. 1950;**91**(1):1-13
- [2] Bunea M, Zarnescu O. New current aspects on the immunohistochemical techniques. *Romanian Biotechnological Letters*. 2001;**6**:177-206
- [3] Kalyuzhny AE. *Immunohistochemistry: Essential Elements and Beyond*. 1st ed. Switzerland: Springer; 2016. p. 49-61
- [4] Ramos-Vara J. Technical aspects of immunohistochemistry. *Veterinary Pathology*. 2005;**42**(4):405-426
- [5] Childs G. History of Immunohistochemistry. In: McManus LM, Mitchell RN, editors. *Pathobiology of Human Disease. A Dynamic Encyclopedia of Disease Mechanisms*. Amsterdam: Academic Press; 2014. p.3775-3796
- [6] Ramos-Vara J, Miller M. When tissue antigens and antibodies get along: Revisiting the technical aspects of immunohistochemistry—The red, brown, and blue technique. *Veterinary Pathology*. 2014;**51**(1):42-87
- [7] Taylor CR et al. Techniques of immunohistochemistry: Principles, pitfalls, and standardization. *Diagnostic Immunohistochemistry*. 2013;**2**:1-42
- [8] Coons AH, Leduc EH, Connolly JM. Studies on antibody production: I. A method for the histochemical demonstration of specific antibody and its application to a study of the hyperimmune rabbit. *Journal of Experimental Medicine*. 1955;**102**(1):49-60
- [9] Moravej A et al. Evaluation of thyroglobulin expression in murine reproductive organs during pregnancy. *American Journal of Reproductive Immunology*. 2010;**64**(2):97-103
- [10] Shojaeian S et al. Heterologous immunization, a way out of the problem of monoclonal antibody production against carcinoma antigen 125. *Iranian Journal of Immunology*. 2009;**6**(4):174-185
- [11] Rasoulzadeh Z et al. Placental kisspeptins differentially modulate vital parameters of estrogen receptor-positive and-negative breast cancer cells. *PLoS One*. 2016;**11**(4):e0153684
- [12] Ramos-Vara J. Book Review: *Introduction to Immunocytochemistry*. Los Angeles, CA: SAGE Publications; 2004
- [13] Renshaw S. Immunohistochemical staining techniques. In: *Immunohistochemistry Methods Express*. Oxfordshire: Scion Publishing Group; 2007
- [14] Warford A, Akbar H, Riberio D. Antigen retrieval, blocking, detection and visualisation systems in immunohistochemistry: A review and practical evaluation of tyramide and rolling circle amplification systems. *Methods*. 2014;**70**(1):28-33
- [15] Sternberger LA et al. The unlabeled antibody enzyme method of immunohistochemistry preparation and properties of soluble antigen-antibody complex (horseradish peroxidase-antihorseradish peroxidase) and its use in identification of spirochetes. *Journal of Histochemistry and Cytochemistry*. 1970;**18**(5):315-333
- [16] Kroese FG. *Immunohistochemical Detection of Tissue and Cellular Antigens*. eLS. 2001

- [17] Cordell JL et al. Immunoenzymatic labeling of monoclonal antibodies using immune complexes of alkaline phosphatase and monoclonal anti-alkaline phosphatase (APAAP complexes). *Journal of Histochemistry and Cytochemistry*. 1984;**32**(2):219-229
- [18] Mason T et al. An immunoglobulin-enzyme bridge method for localizing tissue antigens. *Journal of Histochemistry and Cytochemistry*. 1969;**17**(9):563-569
- [19] Mason D, Sammons R. Alkaline phosphatase and peroxidase for double immunoenzymatic labelling of cellular constituents. *Journal of Clinical Pathology*. 1978;**31**(5):454-460
- [20] Hsu S-M, Raine L, Fanger H. Use of avidin-biotin-peroxidase complex (ABC) in immunoperoxidase techniques: A comparison between ABC and unlabeled antibody (PAP) procedures. *Journal of Histochemistry and Cytochemistry*. 1981;**29**(4):577-580
- [21] Hsu S-M, Raine L, Fanger H. A comparative study of the peroxidase-antiperoxidase method and an avidin-biotin complex method for studying polypeptide hormones with radioimmunoassay antibodies. *American Journal of Clinical Pathology*. 1981;**75**(5):734-738
- [22] Diamandis EP, Christopoulos TK. The biotin-(strept) avidin system: Principles and applications in biotechnology. *Clinical Chemistry*. 1991;**37**(5):625-636
- [23] Becker JM, Wilchek M. Inactivation by avidin of biotin-modified bacteriophage. *Biochimica et Biophysica Acta (BBA)—General Subjects*. 1972;**264**(1):165-170
- [24] Bayer EA, Wilchek M, Skutelsky E. Affinity cytochemistry: The localization of lectin and antibody receptors on erythrocytes via the avidin-biotin complex. *FEBS Letters*. 1976;**68**(2):240-244
- [25] Guesdon J-L, Ternynck T, Avrameas S. The use of avidin-biotin interaction in immunoenzymatic techniques. *Journal of Histochemistry and Cytochemistry*. 1979;**27**(8):1131-1139
- [26] Green NM. Avidin. In: Anfinsen CB, Edsall JT, Richards FM, editors. *Advances in Protein Chemistry*. New York; London: Academic Press; 1975. p. 85-133
- [27] Green N. Avidin. 1. The use of [¹⁴C] biotin for kinetic studies and for assay. *Biochemical Journal*. 1963;**89**(3):585
- [28] Gitlin G, Bayer EA, Wilchek M. Studies on the biotin-binding site of avidin. Lysine residues involved in the active site. *Biochemical Journal*. 1987;**242**(3):923-926
- [29] Gitlin G, Bayer EA, Wilchek M. Studies on the biotin-binding site of avidin. Tryptophan residues involved in the active site. *Biochemical Journal*. 1988;**250**(1):291-294
- [30] Mahmoudi AR et al. Distribution of vitamin D receptor and 1 α -hydroxylase in male mouse reproductive tract. *Reproductive Sciences*. 2013;**20**(4):426-436
- [31] Tavakoli M et al. Effects of 1, 25 (OH) 2 vitamin D3 on cytokine production by endometrial cells of women with recurrent spontaneous abortion. *Fertility and Sterility*. 2011;**96**(3):751-757
- [32] Shahbazi M et al. Expression profiling of vitamin D receptor in placenta, decidua and ovary of pregnant mice. *Placenta*. 2011;**32**(9):657-664
- [33] Shojaeian S et al. Production and characterization of monoclonal antibodies against the extracellular

domain of CA 125. Immunological Investigations. 2010;**39**(2):114-131

[34] Jeddi-Tehrani M et al. Indoleamine 2, 3-dioxygenase is expressed in the endometrium of cycling mice throughout the oestrous cycle. *Journal of Reproductive Immunology*. 2009;**80**(1-2):41-48

[35] Livnah O et al. Three-dimensional structures of avidin and the avidin-biotin complex. *Proceedings of the National Academy of Sciences*. 1993;**90**(11):5076-5080

[36] Bayer EA et al. Postsecretory modifications of streptavidin. *Biochemical Journal*. 1989;**259**(2):369-376

[37] Chalet L, Wolf FJ. The properties of streptavidin, a biotin-binding protein produced by *Streptomyces*. *Archives of Biochemistry and Biophysics*. 1964;**106**:1-5

[38] Regnier FE, Cho W. Affinity targeting schemes for biomarker research. In: Haleem J, Issaq and Timothy D. Veenstra, editors. *Proteomic and Metabolomic Approaches to Biomarker Discovery*. Amsterdam; Boston: Academic Press; 2013. p. 197-224

[39] Hama Y et al. In vivo spectral fluorescence imaging of submillimeter peritoneal cancer implants using a lectin-targeted optical agent. *Neoplasia*. 2006;**8**(7):IN1-IN2

[40] Sano T et al. Recombinant core streptavidins a minimum-sized core streptavidin has enhanced structural stability and higher accessibility to biotinylated macromolecules. *Journal of Biological Chemistry*. 1995;**270**(47):28204-28209

[41] Buckland R. Strong signals from streptavidin-biotin. *Nature*. 1986;**320**:557-558

[42] Pazy Y et al. Ligand exchange between proteins. Exchange of biotin and biotin derivatives between avidin and streptavidin. *Journal of Biological Chemistry*. 2002;**277**(34):30892-30900

[43] Hsu S-M, Cossman J, Jaffe ES. A comparison of ABC, unlabeled antibody and conjugated immunohistochemical methods with monoclonal and polyclonal antibodies—An examination of germinal center of tonsils. *American Journal of Clinical Pathology*. 1983;**80**(4):429-435

[44] Hsu S-M, Raine L. Protein A, avidin, and biotin in immunohistochemistry. *The Journal of Histochemistry and Cytochemistry*. 1981;**29**(11):1349-1353

[45] Zarnani A et al. Morphological and cytochemical characteristics of purified murine splenic dendritic cells. *Iranian Journal of Allergy, Asthma, and Immunology*. 2003;**2**(3):139-144

[46] Zarnani AH et al. The efficient isolation of murine splenic dendritic cells and their cytochemical features. *Histochemistry and Cell Biology*. 2006;**126**(2):275-282

[47] Elias JM, Margiotta M, Gaborc D. Sensitivity and detection efficiency of the peroxidase antiperoxidase (PAP), avidin-biotin peroxidase complex (ABC), and peroxidase-labeled avidin-biotin (LAB) methods. *American Journal of Clinical Pathology*. 1989;**92**(1):62-67

[48] Harley R, Gruffydd-Jones T, Day M. Non-specific labelling of mast cells in feline oral mucosa—A potential problem in immunohistochemical studies. *Journal of Comparative Pathology*. 2002;**127**(2-3):228-231

[49] Bussolati G et al. Retrieved endogenous biotin: A novel marker and a potential pitfall in diagnostic immunohistochemistry. *Histopathology*. 1997;**31**(5):400-407

- [50] Kim SH et al. The enhanced reactivity of endogenous biotin-like molecules by antigen retrieval procedures and signal amplification with tyramine. *The Histochemical Journal*. 2002;**34**(3-4):97-103
- [51] Nikiel B et al. Endogenous avidin biotin activity (EABA) in thyroid pathology: Immunohistochemical study. *Thyroid Research*. 2009;**2**(1):5
- [52] Zhou X et al. The influence of heat-induced epitope retrieval on endogenous avidin-binding activity (EABA) and blocking of EABA in immunohistochemistry. *Zhonghua bing li xue za zhi = Chinese Journal of Pathology*. 2002;**31**(6):491-496
- [53] Hecke DV. Routine immunohistochemical staining today: Choices to make, challenges to take. *Journal of Histotechnology*. 2002;**25**(1):45-54
- [54] Mount S, Cooper K. Beware of biotin: A source of false-positive immunohistochemistry. *Current Diagnostic Pathology*. 2001;**7**(3):161-167
- [55] Sickel JZ. Anomalous immunostaining of 'optically clear' nuclei in gestational endometrium. A potential pitfall in the diagnosis of pregnancy-related herpesvirus infection. *Archives of Pathology & Laboratory Medicine*. 1994;**118**(8):831-833
- [56] Yokoyama S et al. Biotin-containing intranuclear inclusions in endometrial glands during gestation and puerperium. *American Journal of Clinical Pathology*. 1993;**99**(1):13-17
- [57] Johnson DA et al. Improved technique utilizing nonfat dry milk for analysis of proteins and nucleic acids transferred to nitrocellulose. *Gene Analysis Techniques*. 1984;**1**(1):3-8
- [58] Wood GS, Warnke R. Suppression of endogenous avidin-binding activity in tissues and its relevance to biotin-avidin detection systems. *Journal of Histochemistry and Cytochemistry*. 1981;**29**(10):1196-1204
- [59] Duhamel RC, Johnson DDA. Use of nonfat dry milk to block nonspecific nuclear and membrane staining by avidin conjugates. *Journal of Histochemistry and Cytochemistry*. 1985;**33**(7):711-714
- [60] Banerjee D, Pettit S. Endogenous avidin-binding activity in human lymphoid tissue. *Journal of Clinical Pathology*. 1984;**37**(2):223-225
- [61] Zarnani A-H et al. Kinetics of murine decidual dendritic cells. *Reproduction*. 2007;**133**(1):275-283
- [62] Bratthauer GL. The avidin-biotin complex (ABC) method and other avidin-biotin binding methods. In: C Oliver, MC Jamur, editors. *Immunocytochemical Methods and Protocols*. 3rd ed. New York: Human Press; 2010. p. 257-270
- [63] Stemberger L, Stemberger N. The unlabeled antibody method: Comparison of peroxidase-antiperoxidase with avidin-biotin complex by a new method of quantification. *The Journal of Histochemistry and Cytochemistry*. 1986;**34**:599-605
- [64] Vyberg M, Nielsen S. Immunohistochemical detection of tissue and cellular antigens. In: Els. 2001. pp. 1-9
- [65] Hsu S, Raine L, Fanger H. The use of antiavidin antibody and avidin-biotin-peroxidase complex in immunoperoxidase technics. *American Journal of Clinical Pathology*. 1981;**75**(6):816
- [66] Elias J, Johnsen T. The utilization of radioimmunoassay antibodies for

the immunohistologic staining of polypeptide hormones on paraffin-embedded tissue. *American Journal of Clinical Pathology*. 1979;**71**(5):489-491

[67] Shi Z-R, Itzkowitz SH, Kim YS. A comparison of three immunoperoxidase techniques for antigen detection in colorectal carcinoma tissues. *Journal of Histochemistry and Cytochemistry*. 1988;**36**(3):317-322

[68] Childs GV, Unabia G. Application of a rapid avidin-biotin-peroxidase complex (ABC) technique to the localization of pituitary hormones at the electron microscopic level. *Journal of Histochemistry and Cytochemistry*. 1982;**30**(12):1320-1324

[69] Bisgaard K, Lihme A, Rolsted H. Polymeric conjugates for enhanced signal generation in enzyme immunoassays. In: *Scandinavian Society for Immunology XXIVth Annual Meeting*. University of Aarhus; 1993

[70] Van der Loos CM, Naruko T, Becker AE. The use of enhanced polymer one-step staining reagents for immunoenzyme double-labelling. *The Histochemical Journal*. 1996;**28**(10):709-714

[71] Manabe Y et al. Production of a monoclonal antibody-bleomycin conjugate utilizing dextran T-40 and the antigen-targeting cytotoxicity of the conjugate. *Biochemical and Biophysical Research Communications*. 1983;**115**(3):1009-1014

[72] Hurwitz E et al. The covalent linking of two nucleotide analogs to antibodies. *Journal of Medicinal Chemistry*. 1985;**28**(1):137-140

[73] Böcher M, Giersch T, Schmid RD. Dextran, a hapten carrier in immunoassays for s-triazines a comparison with ELISAs based on hapten-protein conjugates. *Journal of Immunological Methods*. 1992;**151**(1-2):1-8

[74] Slinkin M et al. Site-specific conjugation of chain-terminal chelating polymers to Fab'fragments of anti-CEA mAb: Effect of linkage type and polymer size on conjugate biodistribution in nude mice bearing human colorectal carcinoma. *Bioconjugate Chemistry*. 1992;**3**(6):477-483

[75] Roberts JC et al. Using starburst dendrimers as linker molecules to radiolabel antibodies. *Bioconjugate Chemistry*. 1990;**1**(5):305-308

[76] Barth RF et al. Boronated starburst dendrimer-monoclonal antibody immunoconjugates: Evaluation as a potential delivery system for neutron capture therapy. *Bioconjugate Chemistry*. 1994;**5**(1):58-66

[77] Singh P et al. Starburst dendrimers: Enhanced performance and flexibility for immunoassays. *Clinical Chemistry*. 1994;**40**(9):1845-1849

[78] Boeckh M, Boivin G. Quantitation of cytomegalovirus: Methodologic aspects and clinical applications. *Clinical Microbiology Reviews*. 1998;**11**(3):533-554

[79] Buchwalow I et al. Signal amplification in immunohistochemistry: Loose-jointed deformable heteropolymeric HRP conjugates vs. linear polymer backbone HRP conjugates. *Acta Histochemica*. 2013;**115**(6):587-594

[80] Bisgaard K, Pluzed K. Use of polymer conjugates in immunohistochemistry: A comparative study of a traditional staining method to a staining method utilizing polymer conjugates. In: *Abstract XXI Intl Cong Intl Acad Pathol and 12th World Cong Acad Environ Pathol*. Budapest, Hungary. 1996

[81] Chilosi M et al. A rapid immunostaining method for frozen sections. *Biotechnic & Histochemistry*. 1994;**69**(4):235-239

- [82] Tsutsumi Y, Serizawa A, Kawal K. Enhanced polymer one-step staining (EPOS) for proliferating cell nuclear antigen (PCNA) and Ki-67 antigen: Application to intra-operative frozen diagnosis. *Pathology International*. 1995;**45**(2):108-115
- [83] Madjd Z et al. Expression of EMSY, a novel BRCA2-link protein, is associated with lymph node metastasis and increased tumor size in breast carcinomas. *Asian Pacific Journal of Cancer Prevention*. 2014;**15**(4):1783-1789
- [84] Ghods R et al. Immunohistochemical characterization of novel murine monoclonal antibodies against human placenta-specific 1. *Biotechnology and Applied Biochemistry*. 2014;**61**(3): 363-369
- [85] Ghods R et al. High placenta-specific 1/low prostate-specific antigen expression pattern in high-grade prostate adenocarcinoma. *Cancer Immunology, Immunotherapy*. 2014;**63**(12):1319-1327
- [86] Sabattini E et al. The EnVision++ system: A new immunohistochemical method for diagnostics and research. Critical comparison with the APAAP, ChemMate, CSA, LABC, and SABC techniques. *Journal of Clinical Pathology*. 1998;**51**(7):506-511
- [87] Schmitt O, Preuße S, Haas SJ-P. Comparison of contrast, sensitivity and efficiency of signal amplified and nonamplified immunohistochemical reactions suitable for videomicroscopy-based quantification and neuroimaging. *Brain Research Protocols*. 2004;**12**(3):157-171
- [88] Vyberg M, Nielsen S. Dextran polymer conjugate two-step visualization system for immunohistochemistry: A comparison of EnVision+ with two three-step avidin-biotin techniques. *Applied Immunohistochemistry*. 1998;**6**(1):3-10
- [89] Banks RE et al. Use of a sensitive EnVision™+ -based detection system for Western blotting: Avoidance of streptavidin binding to endogenous biotin and biotin-containing proteins in kidney and other tissues. *Proteomics*. 2003;**3**(4):558-561
- [90] Wiedorn KH et al. EnVision+, a new dextran polymer-based signal enhancement technique for in situ hybridization (ISH). *Journal of Histochemistry and Cytochemistry*. 2001;**49**(9):1067-1071
- [91] Shi S-R et al. Sensitivity and detection efficiency of a novel two-step detection system (PowerVision) for immunohistochemistry. *Applied Immunohistochemistry & Molecular Morphology*. 1999;**7**(3):201
- [92] Heras A, Key M. Enhanced polymer detection system for immunohistochemistry: Infectious bronchitis virus as a model. In: *Western Poultry Disease Conference*. 1995
- [93] Petrosyan K, Tamayo R, Joseph D. Sensitivity of a novel biotin-free detection reagent (Powervision+™) for immunohistochemistry. *Journal of Histotechnology*. 2002;**25**(4):247-250
- [94] Hansen TP, Nielsen O, Fenger C. Optimization of antibodies for detection of the mismatch repair proteins MLH1, MSH2, MSH6, and PMS2 using a biotin-free visualization system. *Applied Immunohistochemistry & Molecular Morphology*. 2006;**14**(1):115-121
- [95] Bricca GM, Brodland DG, Zitelli JA. Immunostaining melanoma frozen sections: The 1-hour protocol. *Dermatologic Surgery*. 2004;**30**(3):403-408
- [96] Bobrow M et al. The use of catalyzed reporter deposition as a means of signal amplification

in a variety of formats. *Journal of Immunological Methods*. 1992;150(1-2):145-149

[97] Bobrow MN et al. Catalyzed reporter deposition, a novel method of signal amplification application to immunoassays. *Journal of Immunological Methods*. 1989;125(1-2):279-285

[98] Bobrow MN, Shaughnessy KJ, Litt GJ. Catalyzed reporter deposition, a novel method of signal amplification: II. Application to membrane immunoassays. *Journal of Immunological Methods*. 1991;137(1):103-112

[99] Adams J. Biotin amplification of biotin and horseradish peroxidase signals in histochemical stains. *Journal of Histochemistry and Cytochemistry*. 1992;40(10):1457-1463

[100] Gross AJ, Sizer IW. The oxidation of tyramine, tyrosine, and related compounds by peroxidase. *The Journal of Biological Chemistry*. 1959;234(6):1611-1614

[101] Jackson P, Blythe D. Immunohistochemical technique. In: Bancroft JD, Floyd AD, Suvarna SK, editors. *Bancroft's Theory and Practice of Histological Techniques*. 7th ed. Oxford: Churchill Livingstone. 2013. p. 381-426

[102] Hayat M. Factors Affecting Antigen Retrieval. *Microscopy, Immunohistochemistry, and Antigen Retrieval Methods: For Light and Electron Microscopy*. 1st ed. New York: Kluwer Academic/Plenum. 2002

[103] Speel EJ, Hopman AH, Komminoth P. Amplification methods to increase the sensitivity of in situ hybridization: Play card (s). *Journal of Histochemistry and Cytochemistry*. 1999;47(3):281-288

[104] Sanno N et al. Application of catalyzed signal amplification in immunodetection of gonadotropin subunits in clinically nonfunctioning pituitary adenomas. *American Journal of Clinical Pathology*. 1996;106(1):16-21

[105] Hasui K, Murata F. A new simplified catalyzed signal amplification system for minimizing non-specific staining in tissues with supersensitive immunohistochemistry. *Archives of Histology and Cytology*. 2005;68(1):1-17

[106] Key ME. Trends in immunohistochemistry: The integration of tissue-based analysis and molecular profiling. *Journal of Histochemistry*. 2002;25(4):243-245

[107] Okada H et al. Detection of disease-associated prion protein in the optic nerve and the adrenal gland of cattle with bovine spongiform encephalopathy by using highly sensitive immunolabeling procedures. *Journal of Histochemistry and Cytochemistry*. 2012;60(4):290-300

[108] van Gijlswijk RP et al. Fluorochrome-labeled tyramides: Use in immunocytochemistry and fluorescence in situ hybridization. *Journal of Histochemistry and Cytochemistry*. 1997;45(3):375-382

[109] Hasui K et al. Improvement of supersensitive immunohistochemistry with an autostainer: A simplified catalysed signal amplification system. *The Histochemical Journal*. 2002;34(5):215-222

[110] Mengel M, Werner M, von Wasielewski R. Concentration dependent and adverse effects in immunohistochemistry using the tyramine amplification technique. *The Histochemical Journal*. 1999;31(3):195-200

[111] Mayer G, Bendayan M. Amplification methods for the

immunolocalization of rare molecules in cells and tissues. *Progress in Histochemistry and Cytochemistry*. 2001;**36**(1):3-84

[112] Lohse J et al. Improved catalyzed reporter deposition, iCARD. *Bioconjugate Chemistry*. 2014;**25**(6):1036-1042

[113] Sano T, Smith CL, Cantor CR. Immuno-PCR: Very sensitive antigen detection by means of specific antibody-DNA conjugates. *Science*. 1992;**258**(5079):120-122

[114] Ruzicka V et al. Immuno-PCR with a commercially available avidin system. *Science*. 1993;**260**(5108):698-700

[115] Zhou H, Fisher RJ, Papas TS. Universal immuno-PCR for ultra-sensitive target protein detection. *Nucleic Acids Research*. 1993;**21**(25):6038

[116] Sano T, Smith CL, Cantor CR. Response. *Science*. 1993;**260**(5108):699-699

[117] Sano T, Cantor CR. A streptavidin-protein chimera that allows one-step production of a variety of specific antibody conjugates. *Nature Biotechnology*. 1991;**9**(12):1378

[118] Hendrickson ER et al. High sensitivity multianalyte immunoassay using covalent DNA-labeled antibodies and polymerase chain reaction. *Nucleic Acids Research*. 1995;**23**(3):522-529

[119] Fire A, Xu S-Q. Rolling replication of short DNA circles. *Proceedings of the National Academy of Sciences*. 1995;**92**(10):4641-4645

[120] Liu D et al. Rolling circle DNA synthesis: Small circular oligonucleotides as efficient templates for DNA polymerases. *Journal of*

the American Chemical Society. 1996;**118**(7):1587-1594

[121] Ali MM et al. Rolling circle amplification: A versatile tool for chemical biology, materials science and medicine. *Chemical Society Reviews*. 2014;**43**(10):3324-3341

[122] Yan L et al. Isothermal amplified detection of DNA and RNA. *Molecular BioSystems*. 2014;**10**(5):970-1003

[123] Nilsson M. Lock and roll: Single-molecule genotyping in situ using padlock probes and rolling-circle amplification. *Histochemistry and Cell Biology*. 2006;**126**(2):159-164

[124] Hutchison CA et al. Cell-free cloning using $\phi 29$ DNA polymerase. *Proceedings of the National Academy of Sciences*. 2005;**102**(48):17332-17336

[125] Dean FB et al. Rapid amplification of plasmid and phage DNA using $\phi 29$ DNA polymerase and multiply-primed rolling circle amplification. *Genome Research*. 2001;**11**(6):1095-1099

[126] Polidoros AN, Pasentsis K, Tsiftaris AS. Rolling circle amplification-RACE: A method for simultaneous isolation of 5' and 3' cDNA ends from amplified cDNA templates. *BioTechniques*. 2006;**41**(1):35-42

[127] Wiltshire S et al. Detection of multiple allergen-specific IgEs on microarrays by immunoassay with rolling circle amplification. *Clinical Chemistry*. 2000;**46**(12):1990-1993

[128] Schweitzer B et al. Immunoassays with rolling circle DNA amplification: A versatile platform for ultrasensitive antigen detection. *Proceedings of the National Academy of Sciences*. 2000;**97**(18):10113-10119

[129] Gusev Y et al. Rolling circle amplification: A new approach to increase sensitivity for

immunohistochemistry and flow cytometry. *The American Journal of Pathology*. 2001;**159**(1):63-69

[130] Kingsmore SF, Patel DD. Multiplexed protein profiling on antibody-based microarrays by rolling circle amplification. *Current Opinion in Biotechnology*. 2003;**14**(1):74-81

[131] Schweitzer B et al. Multiplexed protein profiling on microarrays by rolling-circle amplification. *Nature Biotechnology*. 2002;**20**(4):359

[132] Yan J et al. Nano rolling-circle amplification for enhanced SERS hot spots in protein microarray analysis. *Analytical Chemistry*. 2012;**84**(21):9139-9145

[133] Lee J et al. Diffractometric detection of proteins using microbead-based rolling circle amplification. *Analytical Chemistry*. 2009;**82**(1):197-202

[134] Akter F et al. Detection of antigens using a protein-DNA chimera developed by enzymatic covalent bonding with phiX gene a. *Analytical Chemistry*. 2012;**84**(11):5040-5046

[135] Zhou XJ, Gibson G. Cross-species comparison of genome-wide expression patterns. *Genome Biology*. 2004;**5**(7):232

[136] Konry T et al. Ultrasensitive detection of low-abundance surface-marker protein using isothermal rolling circle amplification in a microfluidic nanoliter platform. *Small*. 2011;**7**(3):395-400

[137] Söderberg O et al. Characterizing proteins and their interactions in cells and tissues using the in situ proximity ligation assay. *Methods*. 2008;**45**(3):227-232

[138] Hou L et al. Tyramine-based enzymatic conjugate repeats

for ultrasensitive immunoassay accompanying tyramine signal amplification with enzymatic biocatalytic precipitation. *Analytical Chemistry*. 2014;**86**(16):8352-8358

[139] Hewitt S M. Clinical, Institute LS. Quality Assurance for Design Control and Implementation of Immunohistochemistry Assays; Approved Guideline. 2nd ed CLSI document I/LA28-A2. Wayne, PA: Clinical and Laboratory Standards Institute; 2011

[140] Ramos-Vara JA, Miller MA. Comparison of two polymer-based immunohistochemical detection systems: ENVISION+™ and ImmPRESS™. *Journal of Microscopy*. 2006;**224**(2):135-139

[141] Burchette J, Zimmerman B. Antibody optimization and validation. *Histologic*. 2010;**43**(2):29-33

[142] Ramos-Vara JA et al. Suggested guidelines for immunohistochemical techniques in veterinary diagnostic laboratories. *Journal of Veterinary Diagnostic Investigation*. 2008;**20**(4):393-413

[143] Shojaeian S et al. Quantum dot-labeled tags improve minimal detection limit of CA125 in ovarian cancer cells and tissues. *Iranian Journal of Allergy, Asthma, and Immunology*. 2018;**17**(4):326-335

[144] Tabatabaei-Panah A-S et al. Accurate sensitivity of quantum dots for detection of HER2 expression in breast cancer cells and tissues. *Journal of Fluorescence*. 2013;**23**(2):293-302

Antigen Retrieval for Light and Electron Microscopy

Shuji Yamashita

Abstract

Heat-induced antigen retrieval (HIAR) method reported by Shi et al. in 1991 has greatly contributed not only to immunohistochemistry but also to studying gene expressions using archived formalin-fixed and paraffin-embedded (FFPE) specimens. Heating cleaves crosslinks (methylene bridges) in formaldehyde-fixed proteins and extends polypeptides to expose epitopes hidden in the inner portion of antigens or covered by adjacent macromolecules. In this chapter, the following topics are described to reconsider the concept of immunohistochemistry flexibly and to apply HIAR for further immunological studies using a variety of specimens: (1) antigen-antibody interactions in tissues; (2) mechanisms of chemical fixation with formaldehyde, glutaraldehyde, and osmium tetroxide; (3) unmasking of epitopes using HIAR for specimens fixed with chemical fixatives, including highly masked epitopes; (4) a standardized fixative for immunoelectron microscopy-based HIAR; (5) HIAR for conventionally processed electron microscopy specimens embedded in epoxy resins; and (6) effects of antibody diluents on immunohistochemistry.

Keywords: heat-induced antigen retrieval, antigen-antibody reaction, mechanism of chemical fixations, mechanisms of antigen retrieval, epitope exposure, immunoelectron microscopy, standardized fixative, osmicated specimens, antibody diluents

1. Introduction

Immunohistochemistry is used for identifying the localization of cellular or tissue constituents (antigens) based on antigen-antibody interactions using labeled antibodies that can be visualized under light and electron microscopes. Therefore, the use of specific primary antibodies and tissue preparation techniques that conserve fine structures, the immobilization of antigens, and antigen-antibody interaction is essential. Until the end of the 1980s, the conservation of protein conformation was thought to be important for the immunohistochemistry of protein antigens for the following reasons. (1) The production and specificity of antibodies were mainly confirmed by immunoprecipitation using Ouchterlony double diffusion test and immunoelectrophoresis, in which native purified antigen proteins or tissue extracts were reacted with antisera to form precipitation lines at the proper antigen/antibody ratio in agar or agarose gels. (2) Strong immunoreactions were observed in tissues and cells that were fixed using formaldehyde within a short time or using other physical fixatives, such as cold acetone. (3) Frozen sections provided stronger immunostaining than paraffin sections, which denatured protein conformations during dehydration and embedding.

On the other hand, monoclonal antibodies began to be prepared in many laboratories in the 1980s, and commercially available monoclonal antibodies that recognized special cell types were being applied for pathological diagnosis. Western blotting and enzyme-linked immunosorbent assays (ELISAs) were introduced as the main techniques for detecting antigen-antibody reactions. Since these techniques involve the immobilization of both native and denatured antigens on membranes or plastic plates and antigen-antibody reactions are visualized using enzyme-labeled antibodies, these techniques have a higher sensitivity than immunoprecipitation methods independent of the antigen/antibody ratio. These new antibody preparation techniques and assay systems have gradually changed the concept that it is important to expose epitopes for immunoreactions rather than preserving the conformation of whole antigen molecules.

Histopathologists have made great efforts to use formalin-fixed and paraffin-embedded (FFPE) specimens for immunohistochemistry, since such specimens have long been used as the standard for light microscopy and are archived in many biological and clinical laboratories. In the early 1970s, treatments with enzymes such as proteases, nucleases, and hyaluronidase and with protein denaturants were introduced to enable the partial recovery of immunostaining. The development of heat-induced antigen retrieval (HIAR), as reported by Shi et al. in 1991 for FFPE specimens, completely changed the concept of immunohistochemistry [1]. Although the mechanism of HIAR was originally a mystery, several studies have elucidated that heating cleaves chemical crosslinks (methylene bridges) formed by formaldehyde and exposes epitopes in tissues [2, 3]. HIAR is now applied not only to FFPE sections but also to frozen sections, cultured cells, physically fixed materials, and plastic embedded specimens for both light and electron microscopy [4]. It is also applied to other histochemical fields, such as in situ hybridization and lectin histochemistry. Furthermore, FFPE specimens are recognized as useful resources to study protein expression, DNA aberrations, and RNA expression in normal and diseased tissues [5, 6].

In this chapter, the following topics will be described, focusing on a flexible reconsideration of the concept of immunohistochemistry: (1) antigen-antibody interactions in tissues, (2) mechanisms of chemical fixation, (3) mechanisms of HIAR in formaldehyde-fixed specimens including exposure of highly masked epitopes, (4) HIAR in immunoelectron microscopy including the use of conventionally processed specimens embedded in epoxy resins, and (5) effects of antibody diluents on immunohistochemistry.

2. Antigen-antibody reactions

Antibodies recognize epitopes, which are small areas of antigen proteins but not the entire antigen molecule. When purified proteins from tissues or recombinant proteins are injected into animals, polyclonal antibodies that react with multiple epitopes and have different affinities and immunoglobulin classes for each epitope are generated. If a synthesized linear peptide is used for the immunogens, generated antibodies with different affinities and classes and subclasses of immunoglobulins may react with a single epitope. Therefore, we should notice that a commercially available polyclonal antibody may show different immunoreactions when we use the antibody with different lot numbers. On the other hand, a monoclonal antibody reacts with a single epitope with a monovalent affinity and a single immunoglobulin class and subclass. Antibodies prepared using the phage display technique have almost the same characteristics as monoclonal antibodies.

There are two types of epitopes, i.e., linear and conformational epitopes [4]. Linear epitopes are composed of a particular stretch of 5–20 consecutive amino

acids. Linear epitopes located on the surfaces of protein molecules can react with antibodies independent of whether the protein is in its native or denatured and extended states. Meanwhile, linear epitopes located on surfaces in contact with other proteins or the subunits and internal linear epitopes cannot bind to antibodies when the protein is in its native state and can only bind to antibodies when the polypeptides have been extended by heating or treatment with protein denaturants, such as sodium dodecyl sulfate (SDS) and urea. A few linear internal epitopes are rarely in contact with antibodies because the antigen proteins contain multiple disulfide bonds and the protein remains stable even after heating. The reduction of these disulfide bonds may be necessary for the exposure of such epitopes, as described later. Conformational epitopes are composed of amino acids that are located far apart in their linear sequence but become juxtaposed when the protein is folded into its native shape. Some conformational epitopes are stabilized by disulfide bonds and resistant to denaturation by heating and protein denaturants, but others associated with noncovalent forces may be sensitive to denaturation.

In immunohistochemistry, fixation is essential to conserve tissue structures and to prevent the diffusion of antigens. Chemical fixatives directly modify epitopes and crosslink proteins and nucleic acids to form gel-like structures that inhibit antigen-antibody interactions. The antigen-antibody reactions can be interfered with in special regions, such as cell organelles with intact membrane and secretory granules and deposits of protein fibrils that contain highly concentrated proteins, as well as in nuclei and extracellular matrices with highly negative electrostatic charges. Therefore, immunohistochemistry must be performed under conditions that promote the epitope-antibody association in the target tissues through the use of tissue-processing procedures, i.e., fixation, embedding, antigen retrieval, and the selection of suitable diluents for antibodies.

3. Mechanisms of chemical fixation

Chemical fixatives used for immunohistochemistry are limited to formaldehyde and glutaraldehyde. Formaldehyde is used for tissue fixation in both light and electron microscopy, while glutaraldehyde is used as a fixative only in electron microscopy. Although formaldehyde and glutaraldehyde are popular fixatives for histology and pathology, the characteristics and fixation mechanisms are assumed to be quite different. Since formalin is composed of about 35% formaldehyde aqueous solution containing about 10% methanol to prevent the polymerization of formaldehyde and is usually diluted 10-fold as 10% formalin, its fixation mechanisms should be the same as those for 4% formaldehyde.

3.1 Formaldehyde

The mechanism of fixation using formaldehyde is thought to be as follows. Formaldehyde forms an adduction of hydroxymethyl/methylol (CH_2OH) to functional groups of amino acids (such as lysine, arginine, and cysteine) (**Figure 1a, d, and f**), the N-terminus of polypeptides, and bases of RNA and single strand DNA [7, 8]. A part of the methylol group of lysine and arginine forms imines (Schiff base) through the removal of H_2O (**Figure 1a and d**), and the imines of lysine then combine with the side chains of amino acids, such as tyrosine (**Figure 1b**), tryptophan (**Figure 1c**), asparagine, glutamine, and histidine, and the imine of arginine (**Figure 1e**) to form approximately 0.25-nm methylene bridges ($-\text{CH}_2-$). Although lysines are reported to be major reactive residues for formaldehyde in native proteins, only lysines located on the surface area are modified by formaldehyde [9]. Methylols of cysteine form methylene

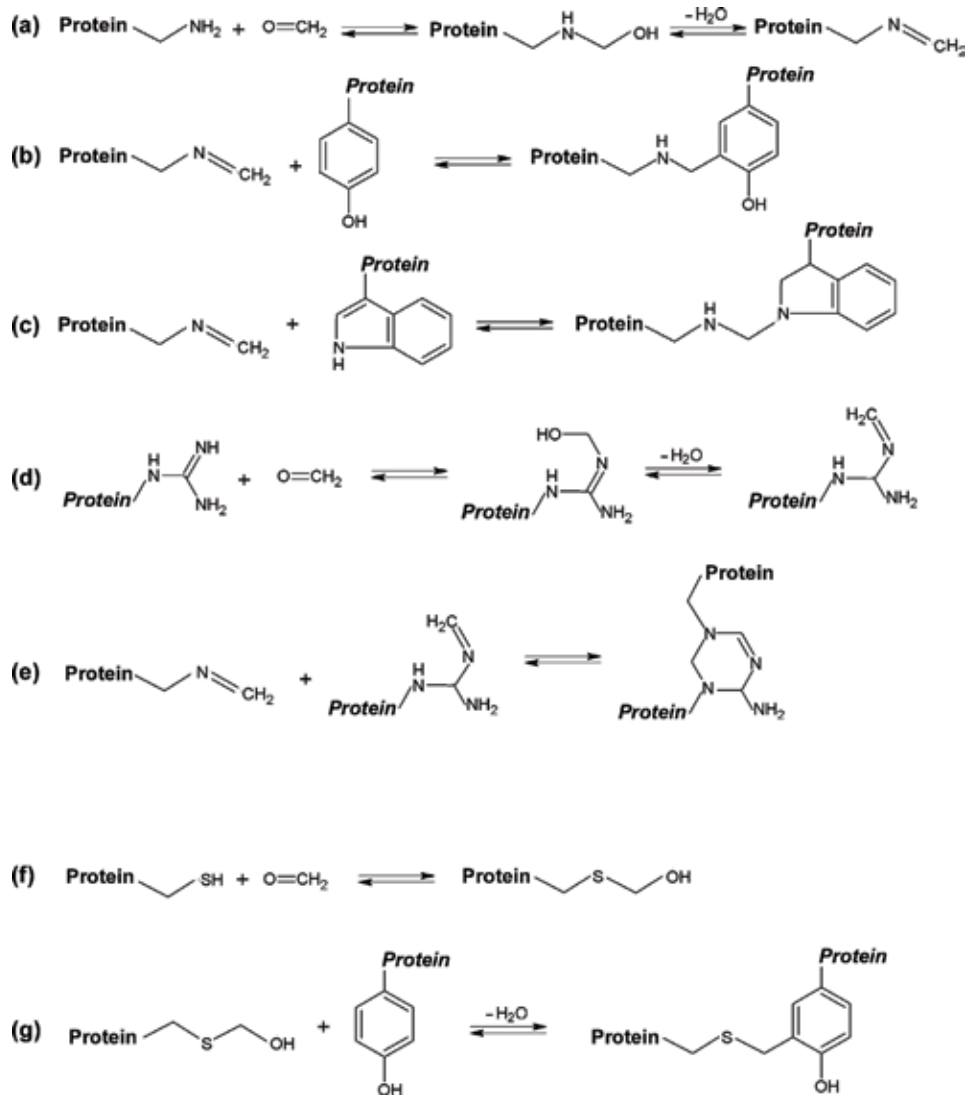


Figure 1.
Reaction of formaldehyde with proteins.

bridges with tyrosine (**Figure 1g**), arginine, and the N-terminus of peptides. These adductions, imine formations, and crosslinks progress in a time-dependent and temperature-dependent manner. Although formaldehyde is rapidly and freely permeable into cells and tissues blocks, the chemical reactions are relatively slow. Fox et al. reported that the binding of ^{14}C formaldehyde to 16 μm of fresh frozen sections only reached a plateau after 24 h at 25°C [10].

Although formaldehyde forms intra- and intermolecular crosslinks in proteins, the tertiary structures of the proteins are almost completely preserved [9, 11]. The methylene bridges between lysine and the phenyl residue of tyrosine are stable but most methylene bridges are unstable and reversible. Since basic residues of amino acids are modified with formaldehyde and the isoelectric point of proteins shifts to acidic, basic proteins should be precipitated at around the pH of the buffer (pH 7.2–7.4) used to dissolve the formaldehyde, based on the principle of isoelectric precipitation. Formaldehyde may first produce crosslinks among proteins in relatively stable core complexes, such as cell organelles, filament proteins in the cytoplasm

and extracellular matrix, and chromatin, and then soluble proteins attach to these complexes to form a gel-like structure. Thus, these crosslinks interfere with the access of antibodies to antigens even if the epitopes do not have functional groups of amino acids that are directly modified by formaldehyde, as demonstrated in the model system by Sompran et al. using peptide epitopes coupled to glass slides [12].

FFPE specimens are assumed to be highly cross-linked, compared with formalin-fixed frozen sections. Since ethanol accelerates the imine formation of methylol groups and causes the rearrangement of the β -sheet of polypeptides and the exposure of hydrophobic amino acids, which are hidden in aqueous solutions, both intra- and intermolecular crosslinking should advance during dehydration and clearing with ethanol and xylene [13], and immersion in paraffin at around 60°C facilitates further crosslinking. On the other hand, some antigens in cell organelles might come in contact with antibodies more easily than those in frozen sections because membrane lipids are extracted and barriers are destroyed during dehydration.

3.2 Glutaraldehyde

Glutaraldehyde has been widely used as the standard primary fixative for electron microscopy specimens since introduced by Sabatini et al. in 1963 [14]. A mixture of glutaraldehyde and formaldehyde is also a popular fixative for cytology, enzyme cytochemistry, and immunoelectron microscopy. Glutaraldehyde (**Figure 2a**) has two aldehydes that can directly crosslink with the ϵ -amino residues of lysine and the N-terminus of polypeptides by forming a Schiff base. However, most investigators think that the rapid and extremely stable crosslinks formed by glutaraldehyde are based on the oligomeric form of glutaraldehyde. Kawahara et al. demonstrated that protein crosslinkage by forming the Schiff base and the aldol condensation of glutaraldehyde monomers occur almost in parallel and result in the formation of a linear glutaraldehyde oligomer with several Schiff base linkages branching off forming $(-\text{CH}=\text{CH}-\text{CH}=\text{N}-\text{R})_n$ (**Figure 2b**), since glutaraldehyde solution showed no absorbance at 235 nm caused by α,β -unsaturated bonds in the absence of amines [15]. The resulting resonance structures are extremely stable to both heat and acid treatments [16].

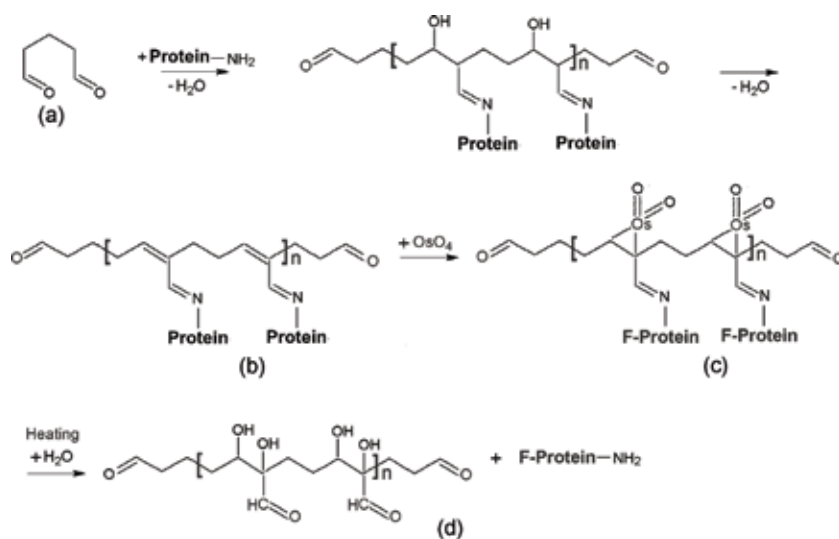


Figure 2. Reaction of glutaraldehyde and osmium tetroxide with proteins and effect of heating. F-protein, fragmented protein by osmium tetroxide post-fixation.

Since the cross-linked proteins rapidly form harder gel-like structures, compared with those created by formaldehyde, only thin layers of tissues can be fixed well using immersion fixation. Since aldehyde residues remain in the tissues fixed with glutaraldehyde, the aldehyde should be quenched using amides, such as glycine, ammonium chloride, and tris(hydroxymethyl) aminomethane, or reduced to alcohols using sodium borohydride prior to immunostaining.

3.3 Osmium tetroxide

Since osmium tetroxide binds to the unsaturated bonds of fatty acids and fixes membrane lipids, providing contrast by scattering electron beams, it is used as the post-fixing reagent after glutaraldehyde fixation in electron microscopy. Osmium tetroxide should also bind to the carbon-carbon double bonds formed by glutaraldehyde fixation (**Figure 2c**). However, since osmium tetroxide cleaves polypeptides in tryptophan residues and oxidizes methionine to methionine sulfone and cysteine to cysteic acid [17], osmium tetroxide significantly inhibits immunoreactions.

4. Mechanisms of HIAR

After the first report for HIAR by Shi et al. [1], investigators have tried to select the most suitable heating conditions (heating devices, temperatures, kinds of solutions, solution pH, and additives). However, the total amount of applied heat energy is now recognized as being more important than the type of heating devices. In this section, the effects of pH and the ionic strength of retrieval solutions for HIAR will be reviewed, and the mechanisms of HIAR will be described.

4.1 Effects of pH on proteins treated with formaldehyde

When purified proteins are treated with formaldehyde and analyzed using SDS-PAGE (polyacrylamide gel electrophoresis), protein oligomers formed by intermolecular crosslinks were recognized. Monomer and oligomers treated with formaldehyde showed smaller apparent molecular weight compared with those of unmodified native proteins, since intramolecular crosslinks prevented the complete unfolding of proteins in the SDS solution [2, 18, 19]. The cleaving efficiency of the crosslinks was almost the same when the formaldehyde-treated proteins were heated for 5 min at 100°C in 10 mM Tris-HCl at pH 3.0, pH 6.0, pH 7.5, or pH 9.0 while analyzed with SDS-PAGE. When the proteins were drastically heated by autoclaving for 10 min at 120°C at a pH close to their respective isoelectric points, the proteins tended to produce insoluble protein precipitates [2]. However, many investigators have demonstrated that the efficiency of HIAR for immunohistochemistry is highly dependent on the pH of the retrieval solution.

4.2 Effect of pH of HIAR solutions on immunohistochemistry

Shi et al. systematically studied the effects of the pH of antigen retrieval solution on HIAR [20]. They classified the pH-influenced HIAR immunostaining patterns as follows: type A, in which staining was almost the same at any pH, with a slight decrease in intensity between pH 3.0 and pH 6.0; type B, in which a dramatic increase in immunostaining was observed at acidic and basic pH; and type C, in which the immunostaining intensity increased at basic pH. We re-examined the pH dependency of HIAR using 17 different antibodies and observed two immunostaining patterns for the pH dependency of HIAR [3]. The majority of the antibodies produced the first immunostaining pattern; that is, they yielded a positive

immunoreaction when heated in buffers that had either an acidic pH or a basic pH. This HIAR pattern may correspond to the type-B pattern of the classification by Shi et al. If highly diluted antibodies had been used in the immunohistochemical studies, the type-A pattern described by Shi et al. might have become nearly equivalent to the type-B pattern. The second immunostaining pattern that we observed was a strong immunostaining reaction when heated in basic buffer, corresponding to the type-C pattern described by Shi et al. Pileri et al. and Kim et al. have also reported that a basic buffer is effective for HIAR for most antigens [21, 22]. On the other hand, Kajiya et al. reported that heating at an acidic pH (pH 3.0 or pH 6.0) frequently enabled excellent immunostaining for the detection of basic proteins or epitopes composed of basic amino acids [23].

4.3 pH-dependent reversibility of HIAR efficiency

Yamashita and Okada demonstrated that the intensities of the immunoreactions obtained by heating in a buffer are reversibly altered by successive heating in another buffer with a different pH [2]. For example, when the first heating in a buffer (pH 6.0) yielded a weak immunostaining in FFPE sections, a second heating at pH 9.0 significantly increased the immunostaining; however, the third heating in the acidic buffer weakened the immunostaining. These results indicate that the degradation or extraction of antigens is not a major factor in the pH dependency of HIAR and that the pH of the solution is a critical factor for the exposure of tissue epitopes in HIAR.

4.4 Effect of ionic strength of HIAR solution

We studied the effects of ionic strength on HIAR using 10 antibodies. Three buffer systems with different pH values were examined. When FFPE specimens were autoclaved for 10 min at 120°C in 20 mM Tris-HCl buffer (pH 9.0), 50 mM citraconic anhydride aqueous solution (pH 7.4), or 10 mM citrate buffer (pH 6.0) containing 0, 50, 100, or 200 mM NaCl, all the antibodies showed the strongest immunostaining while the sections were autoclaved in the NaCl-free solutions. The staining intensity decreased as the NaCl concentration increased in all antibodies examined [24]. These results demonstrated that the ionic strength of the solution is a critical factor for HIAR and that a high concentration of salt inhibits the exposure of epitopes.

4.5 Mechanisms of HIAR in FFPE sections

The results described above demonstrate that the fundamental mechanism of HIAR is based on the cleavage of protein-protein crosslinks and the exposure of epitopes. Heating destroys the gel-like structure formed by formaldehyde-fixation and partially extracts the macromolecules, enabling the antibodies to penetrate tissues easily; this process is similar to the effects of enzyme digestion. Western blot analyses have demonstrated that soluble, nuclear, and membrane proteins are extracted from FFPE specimens after heating but not from those without heat treatment [2]. Recent proteomics studies using a mass spectrum technique have also revealed that heating facilitates protein extraction from archived FFPE specimens [6]. Furthermore, heat-induced cleaving of the shortest crosslinks induced by formaldehyde can be applied to chromatin immunoprecipitation assays and to the crosslinks of adjacent proteins to investigate temporal interactions [8, 25, 26].

The second mechanism is assumed to be as follows based on the pH-dependent and ionic strength-dependent phenomena described above [3, 4]. When the methylene bridges are cleaved by heating, the higher order structure of the protein is destroyed and the polypeptide chains are extended, exposing both hydrophobic

and hydrophilic regions and epitopes. The polypeptide chains then rapidly refold during the cooling process. In tissues, many kinds of proteins with different isoelectric points and molecular weights are tightly packed, and neighboring polypeptides can come in contact with each other. Therefore, epitopes should be concealed during the refolding of the proteins at around a neutral pH because a strong hydrophobic attractive force would randomly entangle the neighboring polypeptides: an electrostatic force may act locally as either an attractive or a repulsive force. At basic or acidic pH values, however, the majority of the extended polypeptides would be charged negatively or positively, and the electrostatic repulsive force would act to prevent random aggregation and entanglement with neighboring polypeptides caused by the hydrophobic force, thereby maintaining a suitable extended conformation for antigen-antibody interactions. When salt is added to the retrieval solutions, the electrostatic force between neighboring polypeptides is canceled, and the hydrophobic attractive force may cause the antigen proteins and neighboring proteins to aggregate, masking the epitopes. Namimatsu et al. reported that heating in citraconic anhydride solution at a neutral pH was useful as a universal antigen retrieval method [27]. Since citraconic anhydride binds to the ϵ -amino groups of lysine residues re-exposed after heating and places numerous negative charges on proteins, an electric repulsive force may help to keep polypeptides in an unfolded state.

On the other hand, strong heating at around the isoelectric points of proteins induces their coagulation [2], and increasing the ionic strength also promotes isoelectric precipitation. Therefore, many proteins with neutral isoelectric points can be precipitated in a solution with a neutral pH. The finding that an acidic buffer is effective for some basic antigens probably indicates that these antigens are precipitated by heating in basic buffers [23, 28]. Since heating may destroy the protein conformation, most conformational epitopes associated with noncovalent forces should lose their reactivity to antibodies. On the other hand, HIAR may be effective for conformational epitopes that have been stabilized by disulfide bonds.

Basic or acidic solutions are effective for HIAR as described above, whereas citrate buffer (pH 6.0) is frequently used in pathological studies. Citrate buffer may be suitable for examining detailed nuclear structures, since heating in basic solutions cleaves and extracts RNAs and reduces the nuclear stainability with hematoxylin. In practice, at least three antigen retrieval solutions at pH 3.0, pH 6.0, and pH 9.0 should be examined when studying the localization of unknown antigens for the first time.

4.6 HIAR in frozen sections

Fresh frozen sections are widely used for immunohistochemical studies, because (1) they preserve antigenicity well, (2) they provide reproducible results because the fixation time is precisely controlled and the fixation is uniform throughout the sections, and (3) they allow antigen localization within a short time for pathological diagnosis. We introduced new fixative, 10% formalin containing 25 mM CaCl_2 in 0.1 M HEPES-NaOH buffer (pH 7.4) that is more appropriate for the fixation of fresh frozen sections compared with buffered 10% formalin, because it has a stronger fixation ability and can crosslink proteins more rapidly and stabilize membranes, the extraction of antigens during fixation is minimized, and an excellent tissue structure is maintained after HIAR [29]. After heating in 20 mM Tris-HCl (pH 9.0) for 30 min or in 20 mM citrate buffer (pH 3.0), antigens in the nuclei, other cell organelles, cytoplasm, membranes, and extracellular matrix were clearly visible, even if they showed no immunoreactions without heating.

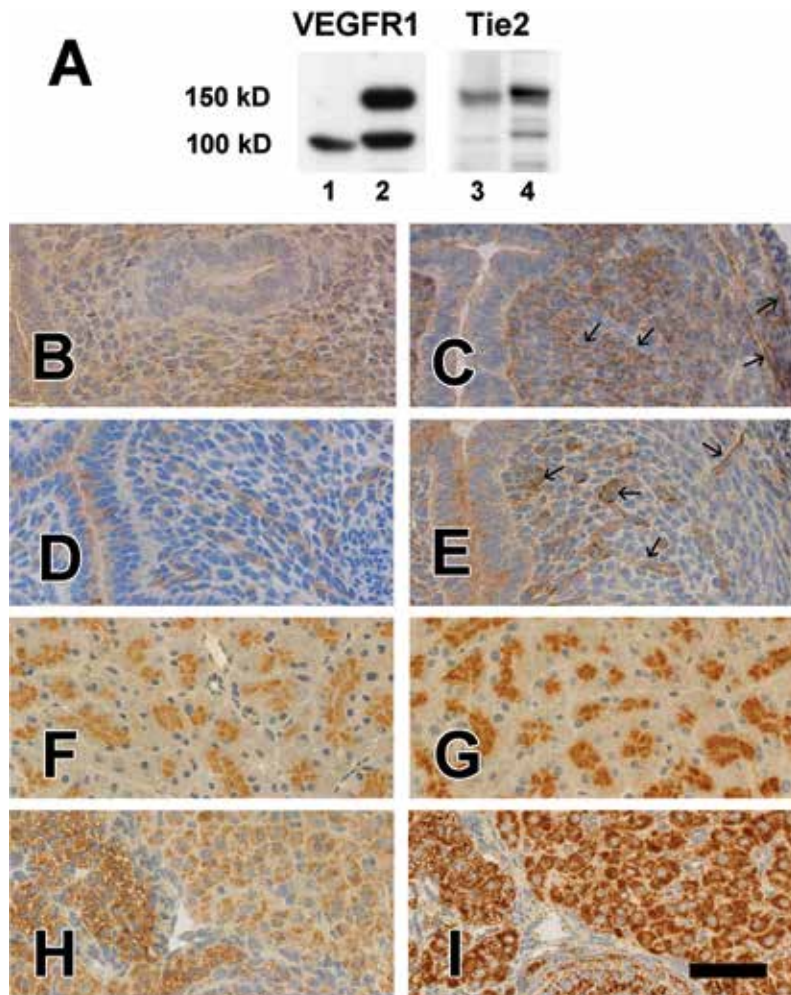


Figure 3. Antigen retrieval for highly masked epitopes with disulfide bonds in paraffin and frozen sections. A. VEGFR₁ and Tie 2 expressions in the uteri of 10-day-old mice were demonstrated using Western blotting. VEGFR₁ and Tie 2 proteins were analyzed after treatment with 2-mercaptoethanol (lines 2 and 4) or without the treatment (lines 1 and 3), respectively. Membrane bound VEGFR₁ (150 kD) shows no reaction to the antibody without reduction of disulfide bonds, whereas soluble VEGFR₁ (100 kD) binds to the antibody independence of reduction (lines 1 and 2). Tie 2 antibody shows strong immunoreaction to Tie 2 protein-reduced disulfide bonds (lines 3 and 4). B–E. Immunostaining of VEGFR₁ (B and C) and Tie 2 (D and E) in the frozen sections of 10-day-old mouse uteri. Fresh frozen sections were fixed with 10% formalin containing 25 mM CaCl₂ in 0.1 M HEPES buffer (pH 7.4) for 5 min, treated with 0.1 M dithiothreitol (DTT)/20 mM Tris-HCl (pH 9.0) for 1 h and then with 0.1 M iodoacetamide/0.1 M Tris-HCl (pH 9.0) for 15 min (C and E); B and D, sections without reduction. The sections were then heated in 20 mM Tris-HCl (pH 9.0) for 30 min at 95°C and immunostained with the antibodies. The stroma shows diffuse VEGFR₁ immunostaining which may be based on the soluble VEGFR₁ in non-reduced section (B), while vasculatures (arrows) and basal membrane of epithelial cells exhibit positive VEGFR₁-immunostaining which may be corresponded to the membrane-bound VEGFR₁ (C). Clear Tie 2-immunostaining is recognized in the endothelial cells of vasculatures (arrows) in the reduced section (E) but not in the non-reduced section (D). F–I. Immunohistochemistry in paraffin sections. Clathrin was detected in the mouse pancreas after reduction with DTT (G) or without reduction (F) followed by heating in 20 mM Tris-HCl (pH 9.0). Tom 20 was immunostained in the mouse ovary after reduction with DTT (I) or without reduction (H) followed by heating. Bar = 50 μm.

4.7 Antigen retrieval for highly masked epitopes with disulfide bonds

Few antigens that reduced disulfide bonds react with antibodies when they are analyzed using Western blotting (Figure 3A), whereas they reveal negative immunostaining even if the tissues were fixed with formaldehyde or other physical

fixatives followed by heating (**Figure 3B** and **D**). In such cases, the epitopes should be located in a highly folded portion of the antigen protein that may be stabilized with disulfide bonds to form stable secondary and tertiary structures. The reduction of disulfide bonds using dithiothreitol or 2-mercaptoethanol prior to heat treatment yields strong immunoreactions (**Figure 3C** and **E**) [28, 30]. In addition, when epitopes are covered by neighboring heat-resistant polypeptides, the accessibility of antibodies to the epitopes is also inhibited. When immunostaining is performed using old FFEP or using sections on a slide glass stored for a long time, the samples should be oxidized to produce many disulfide bonds in the tissues. The reduction and cleavage of disulfide bonds may be effective for such specimens (**Figure 3F–I**).

5. HIAR in immunoelectron microscopy

Immunoelectron microscopy is a powerful technique for observing the localization of antigens in cell organelles and for studying the relationship between antigens and other macromolecules. Three main immunoelectron microscopy methods have been used to localize antigens: the pre-embedding method, the post-embedding method, and cryoultramicrotomy. Although fixation is one of the most important aspects of sample preparation for all three methods, the choices of fixatives and tissue processing procedures are limited unlike light microscopy, because of the need to satisfy compatible requirements, such as conservation of fine structure, immobilization of antigen minimizing the diffusion, and conservation of immunoreaction. In general, fixatives that allow good morphological findings and precise antigen localization through the rapid and tight crosslinking of macromolecules also severely inhibit antigen-antibody interactions.

Fixatives containing formaldehyde as the main crosslinking reagent are popular for immunoelectron microscopy using the pre-embedding method, since antibody penetration into the cells is an important factor for this method; formaldehyde solution, PLP (periodate-lysine-paraformaldehyde) [31], and a mixture of formaldehyde and a low concentration (0.05–0.5%) of glutaraldehyde. For the post-embedding method, a mixture of formaldehyde and a low concentration of glutaraldehyde is frequently used to preserve the fine structure and membrane structures, since dehydration and resin embedding are performed without osmium tetroxide post-fixation. A short period of perfusion fixation with glutaraldehyde is also applied for the post-embedding method. The suitable fixatives, fixing periods, and temperatures of fixatives have been determined by trial and error for each antigen independent of the staining methods.

In this section, a standardized fixation method that yields positive immunoreactions for the pre-embedding and the post-embedding methods after HIAR will be described and discussed how HIAR is also effective for some routinely processed materials for the electron microscopy that are fixed with glutaraldehyde and osmium tetroxide and embedded in epoxy resins.

5.1 Standardized fixative

We introduced a standardized fixative that can yield positive immunoreactions for many antigens in electron microscopy after HIAR [32]. Tissues were fixed with 4% formaldehyde containing 2.5 mM CaCl₂ and 1.25 mM MgCl₂ in 0.1 M HEPES-NaOH buffer (pH 7.4) for 2 h at room temperature and then with the same fixative composition in 0.1 M HEPES buffer-NaOH buffer (pH 8.5) overnight at room temperature. The vehicle osmolarity of the fixatives was adjusted to 300–330 mOsm by adding sucrose or glucose. Formaldehyde containing CaCl₂ and MgCl₂ was shown to

be the best fixative, producing a rapid and complete fixation that minimizes diffusion artifacts (the divalent cations are well known to act as stabilizers of membrane structures). In addition, tissues were fixed using two steps: first at pH 7.4 and then at pH 8.5. This method preserves the cellular fine structures because the crosslinking reaction produced by formaldehyde progresses rapidly at a basic pH. Fixation was then performed at room temperature to enable a faster reaction than that possible at 4°C.

5.2 Pre-embedding method

Although the pre-embedding method is the most popular and the simplest method for immunoelectron microscopy, HIAR has only been applied for the detection of a few antigens. Frozen sections or vibratome sections from specimens fixed with formaldehyde or a mixture of formaldehyde and glutaraldehyde were heated in various solutions such as citrate buffer (pH 6.0), Tris-HCl buffer (pH 9.0 or pH 10.0), or citraconic anhydride solution (pH 7.4) for different periods for each antigen [33–36]. Yamashita reported that 4% formaldehyde containing 25 mM CaCl₂ in 0.1 M cacodylate buffer (pH 7.4) was a suitable fixative for the pre-embedding method by applying HIAR for several antigens [4].

We applied the pre-embedding method to tissues fixed using the standardized fixative described above. Frozen sections (about 15 µm) were mounted on a slide glass and then heated in 20 mM Tris-HCl (pH 9.0) containing 10% sucrose for 2–4 h at 70°C. Immunostaining was performed using (horseradish peroxidase) HRP-labeled antibodies and antigen localization was visualized with 3,3'-diaminobenzidine (DAB). Most of the antigens that were examined showed negative immunoreactions without heat treatment, but they produced strong immunoreaction after heating (**Figure 4**). Since endogenous immunoglobulins are inactivated after heat treatment (**Figure 4A and B**), the immunoreactions can be clearly detected even in the mouse tissues using mouse monoclonal antibodies. Tris-HCl buffer (pH 9.0) is effective for most antigens but citrate buffer (pH 6.0 or pH 3.0) yields strong reaction for a few antigens with basic isoelectric points, such as vascular endothelial cell growth factor (VEGF). Therefore, the selection of suitable solutions for each antigen should be examined using FFEP sections or frozen sections on light microscopy.

The positively immunostained sections were then post-fixed with 1% osmium tetroxide in 0.1 M phosphate buffer (pH 7.4) for 30 min, dehydrated with ethanol, and then embedded in epoxy resin. All antigens detected in frozen sections on light microscopy were localized using the pre-embedding method preserving fine structures (**Figure 5**).

5.3 Post-embedding method

The post-embedding method provides more reproducible and reliable immunostaining results than the pre-embedding method, which produces a limited and heterogeneous penetration of antibodies into the tissues, since immunoreactions occur on the surfaces of ultrathin sections. Furthermore, immunoreactions on ultrathin sections permit the counting of immunogold particles, enabling semi-quantitative analyses, and the simultaneous staining of multiple antigens. Although the post-embedding method has these advantages, it has only been used for a limited number of antigens because antigenicity is frequently lost during the dehydration and embedding procedures. Specimens embedded in acrylic resins without osmication show a disrupted membrane structure and poorly contrasted cell organelles.

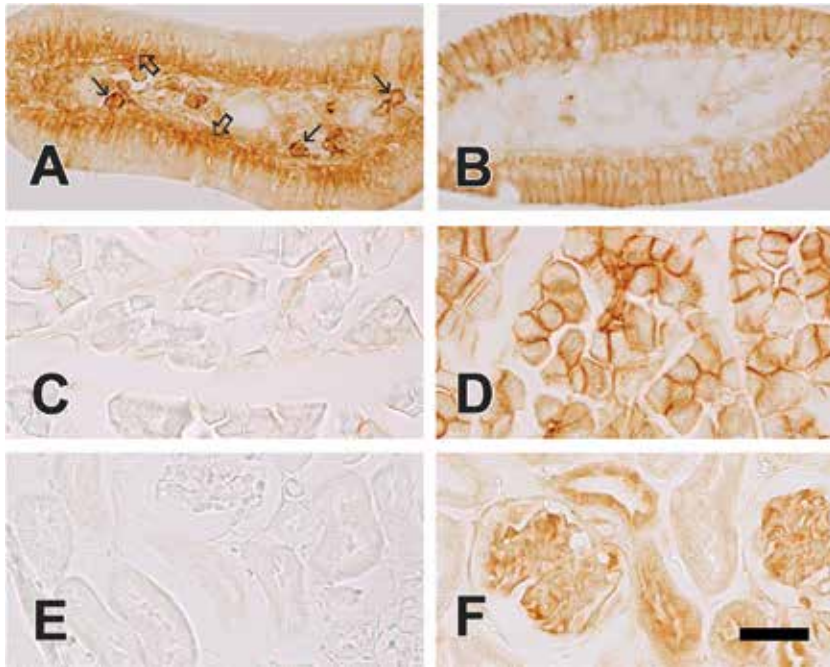


Figure 4.

HIAR in frozen sections from specimens fixed with the standardized fixative. Mouse tissues were fixed with the standardized fixative and immersed in 10, 15, and 20% sucrose and then frozen. Frozen sections (15 μ m) were immunostained with anti-E-cadherin monoclonal antibody in the small intestine (A and B), anti- β -catenin monoclonal antibody in the pancreas (C and D), and anti-claudin 5 polyclonal antibody in the kidney (E and F) after heating in 10 mM Tris-HCl buffer (pH 9.0) containing 10% sucrose for 3 h at 70°C (B, D, and F) or without heating (A, C, and E). Endogenous mouse immunoglobulins are seen in the lamina propria mucosa (arrows) and plasma cells (outline arrows), but E-cadherin immunoreactions is not detected without heating (A). However, the endogenous immunoglobulin immunostaining is negative and E-cadherin is clearly localized along the lateral membrane of intestinal epithelium after heating; the junctional complexes show strong immunoreactions (B). β -Catenin immunoreaction is present along the lateral membrane of pancreatic acinar cells (D) but not in the section without heating (C). After heating, claudin-5 is localized in the glomeruli and distal tubules in the kidney (F). Bar = 50 μ m.

Several investigators have applied HIAR to the post-embedding method and have reported its usefulness [37–39]. Tissues were fixed with a mixture of formaldehyde and glutaraldehyde or formaldehyde alone and embedded in acryl resins; then, ultrathin sections were heated in various solutions. We attempted to establish a standardized method for immunoelectron microscopy that would satisfy the following requirements: (1) the preservation of fine cell structures with good image contrast in tissues embedded in acryl resins without OsO_4 post-fixation, (2) the application of HIAR to obtain a high labeling density, and (3) a simple and reproducible method that does not require special equipment [32, 39].

Tissues were fixed with the standardized fixative and dehydrated with dimethylformamide (DMF) on ice and embedded in the LR-White resin, since DMF may reduce abrupt osmotic pressure changes in the tissues and the extraction of membrane lipids. The resin was polymerized for 24 h at 55°C. Ultrathin sections mounted on a nickel grid were heated in 0.5 M Tris-HCl buffer (pH 9.0) for 1–2 h at 95°C. After immunogold labeling, the sections were treated with 2% glutaraldehyde containing 0.05% tannic acid in 0.1 M phosphate buffer (pH 5.5) for 5 min and with 1% OsO_4 /0.1 M phosphate buffer (pH 7.4) for 5 min and then double stained with uranyl acetate and lead citrate. This method yielded strong and reproducible immunoreactions for many soluble, membrane bound, and filamentous proteins (**Figure 6**), [32, 39]. Furthermore, tannic

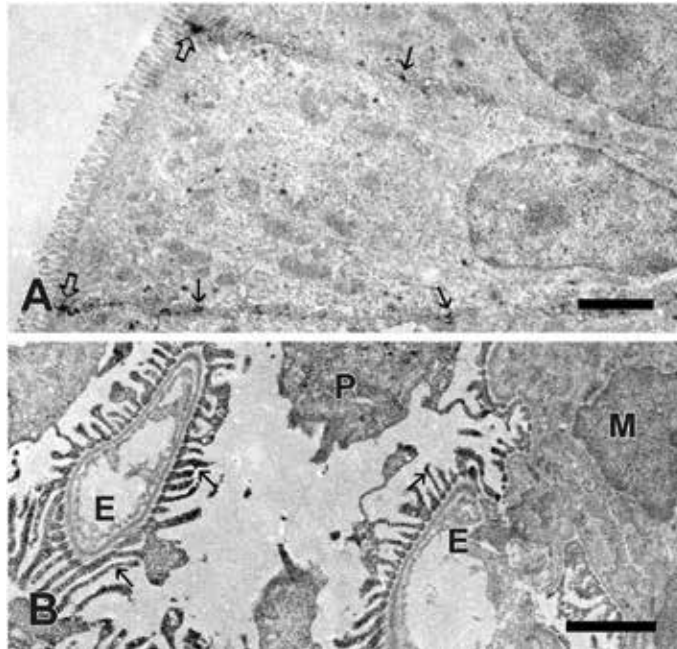


Figure 5. HIAR for immunoelectron microscopy with the pre-embedding method. Frozen sections immunostained with anti-E-cadherin antibody (A) and anti-claudin-5 antibody (B) demonstrated in **Figure 4** were post-fixed with osmium tetroxide, dehydrated in ethanol, and then embedded in the epoxy resin. A. Immunoreaction for E-cadherin is seen in the adherence junction (outline arrows) and spotty reaction (arrows) is present in the lateral membrane of intestinal epithelium. B. Claudin-5 is localized in the foot processes of podocyte (arrows) in the renal glomerulus: P, podocyte; E, endothelial cells; and M, mesangial cell. Bar = 2 μ m.

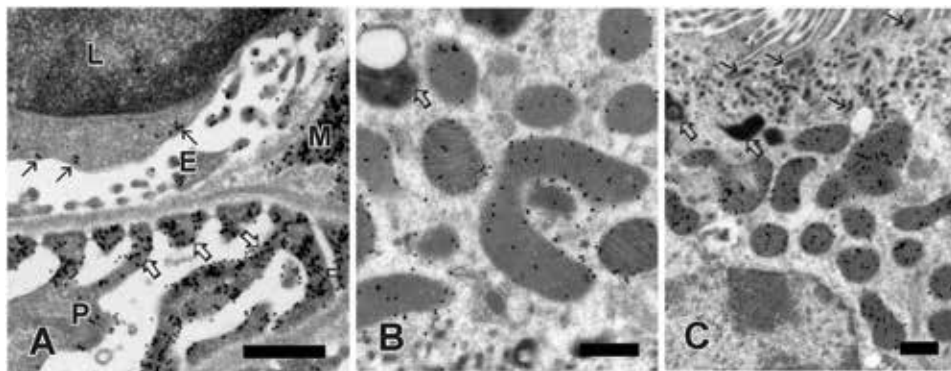


Figure 6. HIAR for immunoelectron microscopy with the post-embedding method. Mouse kidney was fixed with the standardized fixative and then embedded in LR-White resin. Ultrathin sections were heated in 0.5 M Tris-HCl (pH 9.0) for 1 h at 95°C and treated with anti- β -actin/TBS (A), Tom 20/10 mM Tris-HCl (pH 7.4) containing 50 mM NaCl (B), and anti-mortalin (mitochondrial 70 kD heat shock protein)/TBS (C) and then treated with colloidal gold-labeled secondary antibodies/TBS. A. Strong β -actin immunoreactions are seen in the foot processes of podocyte (P) (outline arrows) and in the cytoplasm of mesangial cell (M). Lymphocyte (L) shows potty reactions beneath the cell membrane (arrows). B. Tom 20 is localized along the mitochondria but not recognized in the lysosome (outline arrow). C. Mitochondria show mortalin immunoreaction, whereas lysosomes (outline arrows), apical canaliculi (arrows), and nucleus are negative for staining. Bars = 500 nm.

acid treatment followed by osmium tetroxide treatment produced good contrasted images. The cellular membranes produced a positive image and the cell organelles, such as mitochondria, the Golgi complexes, secretory granules, and lysosomes, were well

contrasted. Nucleic acids (chromatins, nucleoli, and ribosomes), intracellular filaments (actin filaments, 10 nm filaments, and microtubules), and collagen fibers were well visualized.

5.4 Osmicated and epon-embedded specimens

Archives of materials embedded in epoxy resins are collected in many histology and pathology laboratories and in hospitals for morphological analyses, and these archives are expected to provide valuable data if they can be used for immunohistochemical studies. However, conventionally processed specimens for transmission electron microscopy have been regarded as unsuitable for immunoelectron microscopy using post-embedding methods for the following reasons: (1) Glutaraldehyde significantly suppresses antigen-antibody interactions and HIAR is ineffective for most antigens. (2) Osmium tetroxide severely inhibits immunoreactions by cleaving polypeptides and oxidizing methionine and cysteine [17]. (3) Epoxy resins produce tight three-dimensional crosslinks that suppress antigen-antibody interactions.

A limited number of antigens can be successfully detected on sections from conventionally processed materials. One method involves the oxidation and removal of osmium by treating ultrathin sections with sodium metaperiodate aqueous solution [40]. Another method involves the partial removal of epoxy resins by treating the sections with hydrogen peroxide or sodium/potassium ethoxide [41, 42]. The combined use of partial desaturation and heat treatment has also been examined. Borson and Skjorten polymerized the epoxy resin to reduce copolymerization between the proteins and the resin and to make a porous polymer for applying HIAR to glutaraldehyde-fixed and epon-embedded materials [43]. We have also demonstrated that HIAR is effective for post-embedding immunoelectron microscopy using conventionally processed epon blocks, contrary to presumptions that antigen detection would be a special case in these specimens [44].

5.4.1 Frozen sections fixed with glutaraldehyde and osmium tetroxide

The effectiveness of HIAR in the post-embedding method using conventionally processed epon-embedded specimens was systematically examined for 18 antibodies. Frozen sections fixed with 2% glutaraldehyde for 30 min at room temperature or with 2% glutaraldehyde for 30 min followed by 1% osmium tetroxide for 30 min at room temperature were dehydrated with ethanol and then rehydrated to elucidate the validity of HIAR for avoiding the effects of epoxy resin embedment. In another experiment, frozen sections fixed with glutaraldehyde and osmium tetroxide were treated with sodium metaperiodate, since this reagent has been reported to be effective for osmicated materials, as described above.

After autoclaving in Tris-HCl buffer (pH 9.0), 7 of the 18 antibodies exhibited a strong immunoreaction in frozen sections fixed with glutaraldehyde and osmium tetroxide, whereas heating revealed almost no effect on the sections fixed with glutaraldehyde alone (**Table 1; Figure 7**). Treatment with sodium metaperiodate was ineffective for the antigen retrieval of all the antibodies (**Table 1**). The mechanisms of HIAR in the frozen sections fixed with glutaraldehyde and osmium tetroxide were assumed to be as follows [44]. Osmium tetroxide binds to ethylene bonds formed by glutaraldehyde fixation, i.e., $-\text{CH}=\text{CH}-\text{CH}=\text{N}-\text{R}$ (**Figure 2c**). Heat treatment removes the osmium tetroxide additives and forms 1, 2-diols (**Figure 2d**), since the black color fades in frozen sections fixed with glutaraldehyde and osmium tetroxide after autoclaving. The cleaving of the double bonds should extend the antigen polypeptides and increase the flexibility of the polypeptides. However, the morphology in the frozen tissues fixed with glutaraldehyde and osmium

tetroxide was more disrupted after autoclaving, compared with those fixed with glutaraldehyde alone or 4% formaldehyde containing 25 mM CaCl₂. The reason may be as follows. Osmium tetroxide treatment induces polypeptide fragmentation (**Figure 2c** and **d**), and heating extracts the fragments after crosslink cleavage by glutaraldehyde.

5.4.2 HIAR in epon-embedded materials

Partial deresination with sodium ethoxide was required for light microscopy using semi-thin epon sections. After autoclaving in 100 mM Tris-HCl (pH 9.0) for 10 min, six of the seven antibodies that showed positive immunoreactions in the frozen sections exhibited clear localizations in the semi-thin sections. α -Amylase (**Figure 8A** and **B**), clathrin (**Figure 8C**), and claudin-5 (**Figure 8D**), which all showed positive immunoreactions in the semi-thin sections, were localized on ultrathin sections using colloidal gold-labeled antibodies. For HIAR, ultrathin sections were heated in 500 mM Tris-HCl buffer (pH 9.0) for 1–3 h at 95°C. Although heat treatment was essential for the detection of antigens on ultrathin sections, heat treatment reduced the electron density of ribosomes, chromatins,

	GA-EtOH		GA-OsO ₄ -EtOH		
	Non	Autoclave	Non	NaIO ₄	Autoclave
PCNA	0	1	0	0	2
Clathrin	0	0–1	0	0	3
GFAP	0	0–1	0	0	3
Occludin	0	0–1	0	0	3
Tom 20	0	0–1	0	0	3
Claudin-5	0	0	0	0	2
α -Amylase	0–1	1	0	0–1	2
NRP1	0	0	0		1
β -Catenin	0–1	0	0		0
E-Cadherin	0	0–1	0		0
Desmin	0	0–1	0		0
Caveolin	0	0	0		0
VEGFR2	0–1	0	0		0
ER α	0	1–2	0		0–1
AnR	0	0	0		0
β -Actin	1	1	0		0
γ -GTP	1	1	0		0

Fresh frozen sections were fixed with 2% glutaraldehyde/0.1 M phosphate buffer (pH 7.4) for 30 min (GA-EtOH) or fixed with 2% glutaraldehyde/0.1 M phosphate buffer (pH 7.4) for 30 min and further fixed with 1% osmium tetroxide/0.1 M phosphate buffer (pH 7.4) for 30 min (GA-OsO₄-EtOH). Some sections fixed with glutaraldehyde and osmium tetroxide were further treated with 1% sodium metaperiodate aqueous solution for 5 min (NaIO₄); all sections were hydrated with ethanol and then rehydrated after fixation. The fixed sections were immunostained after autoclaving in 20 mM Tris-HCl (pH 9.0) at 120°C for 10 min (autoclave) or without heat treatment (Non). Immunostaining was scored as followed: 3, strong; 2, moderate; 1, weak; 0–1, faint; and 0, negative.

Table 1. HIAR in frozen sections prepared from specimens fixed with glutaraldehyde or glutaraldehyde and osmium tetroxide.

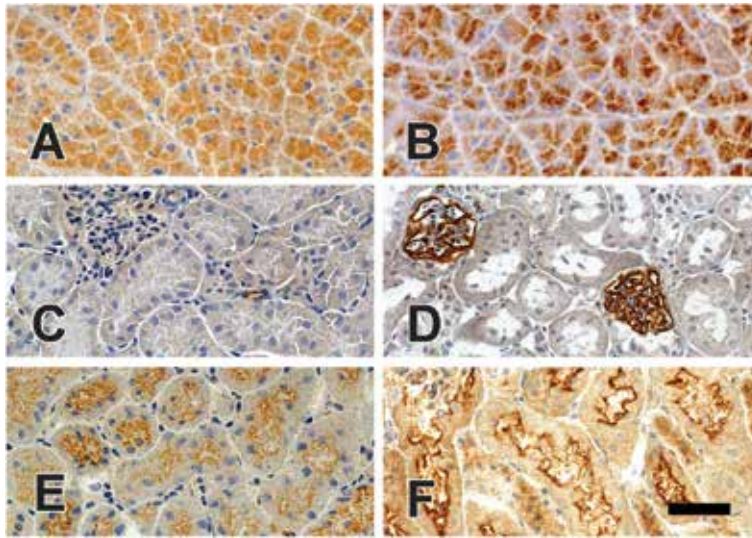


Figure 7.

HIAR in frozen sections fixed with glutaraldehyde and osmium tetroxide. Fresh frozen sections (6 μm) from mouse tissues were fixed with 2% glutaraldehyde in 0.1 M phosphate buffer (pH 7.4) for 30 min at room temperature (A, C, and E) and successively with 1% osmium tetroxide in 0.1 M phosphate buffer (pH 7.4) for 30 min at room temperature (B, D, and F). The sections were autoclaved in 20 mM Tris-HCl (pH 9.0) for 10 min at 120°C. They were then immunostained with anti- α -amylase antibody in the pancreas (A and B), anti-claudin-5 antibody in the kidney (C and D), and anti-clathrin antibody in the kidney (E and F). Although negative or weak immunostaining is seen in the sections fixed with glutaraldehyde after autoclave (A, C, and E), strong α -amylase immunoreactions are recognized in the apical cytoplasm of pancreatic acinar cells (B) and clear claudin-5 and clathrin immunoreactions are observed in the glomeruli (D) and in the apical cytoplasm of proximal tubular cells in the kidney (F), respectively. Bar = 50 μm .

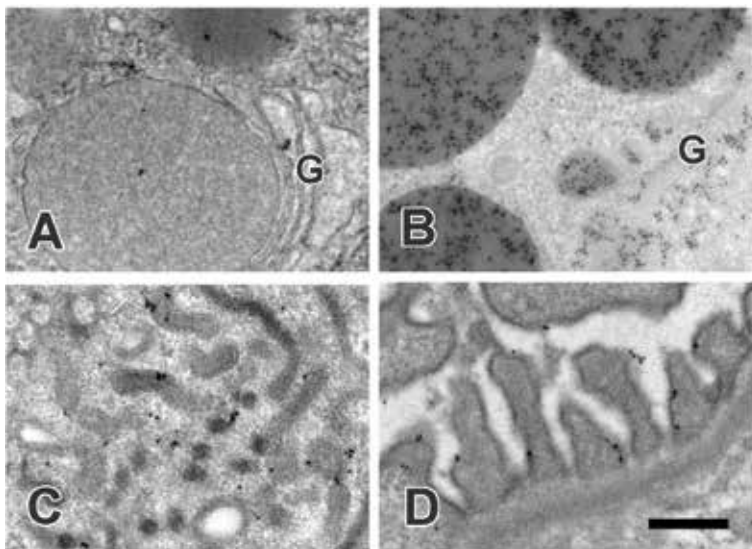


Figure 8.

HIAR for the specimens fixed with glutaraldehyde and osmium tetroxide, embedded in epoxy resin. Mouse tissues were fixed with 2% glutaraldehyde/0.1 M phosphate buffer (pH 7.4) for 3 h at 4°C and post-fixed with 1% osmium tetroxide/0.1 M phosphate buffer (pH 7.4) for 1 h and then embedded in the epoxy resin. Ultrathin sections were heated in 0.5 M Tris-HCl (pH 9.0) for 2 h at 95°C. α -Amylase is localized in the Golgi apparatus (G), condensing vacuole and secretory granules in the exocrine pancreas after heat treatment (B), whereas no reaction is seen in the sections without heating (A). Immunoreaction for clathrin is recognized in the apical canalliculi of renal proximal tubular cell (C). Claudin-5 is localized along the membrane of podocyte foot processes in the glomerulus (D). Bar = 500 nm.

intracellular membranes, and secretory granules in the exocrine pancreas. The partial removal of epoxy resins with sodium ethoxide followed by autoclaving revealed the disruption of the fine structure and no reproducible immunolabeling.

These results indicated that archived epon-embedded specimens could be a useful resource for immunohistochemical studies at both the light and electron microscopy levels, since they provide excellent morphology and detailed antigen localization compared with paraffin-embedded materials.

6. Effects of diluents on antibodies in immunohistochemistry

The relationship between epitopes and paratopes of antibodies is thought to be similar to that between keys and keyholes. However, since these structures change their conformations to form a final specific and tight binding after antigen-antibody association, conservation of the flexibility of their polypeptide chains should be important. Although hydrogen bonds, hydrophobic forces, electrostatic forces, and van der Waals forces all participate in the final tight binding, electrostatic forces are important for the initial contact and association of antigen and antibody molecules (i.e., the net charges of each molecule and the neighboring charges of antigens). Buffer type, ionic strength, pH, and the presence of detergents in solutions are likely to exert strong influences on the antigen-antibody reaction. Although many kinds of diluents are commercially available for immunohistochemistry and Western blotting and yield good results with low background staining and a high sensitivity for some antigens, systematic studies of antibody diluents for immunohistochemistry have not been performed. In this section, the effects of dilution solutions for primary antibodies on immunostaining for light and electron microscopy are described.

6.1 Kind of dilution buffers

Fifteen monoclonal antibodies were diluted in 10 mM phosphate buffer (pH 7.4) containing 150 mM NaCl (PBS), 10 mM Tris-HCl buffer (pH 7.4) containing 150 mM NaCl (TBS), or 10 mM FEPES-NaOH buffer (pH 7.4) containing 150 mM NaCl (HBS); 1% bovine serum albumin (BSA) (final concentration) was added to each solution. Paraffin sections from mouse tissues fixed with formaldehyde were immunostained after autoclaving in 20 mM Tris-HCl buffer (pH 9.0) for 10 min. The sections were treated with the primary antibodies diluted with the solutions overnight at 4°C and successively with Envision HRR (Dakocytomation) for 1 h at room temperature. As shown in **Table 2**, all the antibodies diluted with TBS showed stronger immunoreactions than those diluted with PBS or HBS [45]. Although the reasons are unclear, the binding of phosphate ion (a larger ion) to positively charged regions of epitopes and paratopes may reduce the flexibility of peptide chains.

6.2 Ionic strength of dilution solution

Fifteen monoclonal antibodies were diluted in 1% BSA/10 mM Tris-HCl buffer (pH 7.4) containing 50 mM NaCl, 150 mM NaCl, or 300 mM NaCl. After autoclaving, the paraffin sections were treated with the primary antibodies overnight and then with Envision HRR for 1 h at room temperature. The results are shown in **Table 2**. Most of the antibodies showed strong immunostaining when they were diluted with a buffer containing 50 mM NaCl [45]. However, monoclonal antibodies to proliferating cell nuclear antigen (PCNA) showed the strongest immunostaining when diluted with a buffer containing 300 mM NaCl, and monoclonal antibodies to glial fibrillary

Antibodies	Clones and subclasses	Dilution buffer type			mM NaCl/10 mM TB		
		PBS	TBS	HBS	50	150	300
PCNA	PC10; IgG2a	1	2	2	1	2	2-3
ER α	D12; IgG2a	3	2	2	2	2	2
ER α	ID5; IgG1	1	1-2	1	2	1-2	1
S-100	M2A10; IgG1	1	2	1-2	3	2	1
Mortalin	JG1; IgG3	3	3	3	3	3	3
HSP 70	sc-27; IgG2a	1	2	2	3	2	1-2
α -Synuclein	42; IgG1	2	2	2	2	2	2
GFAP	6F2; IgG1	2	2	1	1	2	2
Desmin	D33; IgG1	1	2	1	1	2	2
β -Actin	AC-74; IgG2a	2	2	2	1	2	1-2
Clathrin	X22; IgG1	1	2	2-3	3	2	1
E-Cadherin	36B5; Ig1	1	2	2	3	2	1
β -Catenin	sc-763; IgG1	1	2	1	3	2	1
γ -GTP	5B9; IgG1	1	2	2	3	2	1
CASGM	170-5; IgG1	2	2	2	3	2	1

FFPE sections (6 μ m) of mouse tissues were autoclaved in 20 mM Tris-HCl (pH 9.0) for 10 min and then immunostained with monoclonal antibodies. Antibodies were diluted with 150 mM NaCl/10 mM phosphate buffer (pH 7.4) (PBS), 150 mM NaCl/10 mM Tris-HCl (pH 7.4) (TBS), or 150 mM NaCl/10 mM HEPES buffer (pH 7.4) (HBS). The antibodies were also diluted with 10 mM Tris-HCl (pH 7.4) containing 50 mM, 150 mM, or 300 mM NaCl. Immunostaining was scored as followed: 3, strong; 2, moderate; and 1, weak.

Table 2.
Effects of diluents for monoclonal antibodies on immunohistochemistry.

acidic protein (GFAP) and β -actin diluted with 150 mM yielded the strongest immunostaining. Polyclonal antibodies to nuclear transcription factors such as estrogen receptor (ER) α , androgen receptor (AnR), glucocorticoid receptor, and p300 yielded stronger immunostaining when diluted with a buffer containing 150 or 300 mM NaCl than that using a buffer containing 50 mM NaCl (not shown). These results suggest that the net charges of antibodies and antigens influence the contact of these proteins, and the net neighboring charges of antigens also affect the interactions. Nuclear antigens are associated with highly acidic nucleic acid, and β -actin and GFAP bundles are composed of β -actin and GFAP proteins with acidic isoelectric points. Dilution solution with a high ionic strength may reduce the net charges around the antigens and antigen molecules, allowing antibodies to come in contact with their respective antigens.

6.3 Immunolectron microscopy

In immunohistochemistry using HRP-labeled antibodies, the staining intensity can be increased using highly sensitive reaction solutions and a longer enzyme reaction time. However, the intensification of immunoreactions is difficult in the post-embedding method and ultracryotomy using colloidal gold-labeled secondary antibody. Instead, the selection of diluents for the antibodies may be more important for obtaining a high labeling density with a low background staining compared

with light microscopy, whereas almost no studies have been performed for immunoelectron microscopy.

We examined the effect of diluents of several antibodies for the post-embedding method using specimens fixed with the standardized fixative and embedded in LR-White resin [39, 41]. Glutaraldehyde and osmium tetroxide fixed and epon-embedded specimens were also used for a few antibodies. After HIAR, ultrathin sections were immunostained using antibodies diluted in the following solutions: PBS, TBS, 10 mM Tris-HCl (pH 7.4) containing 50 mM NaCl, Can Get Signal A (Toyobo Co.), and Can Get Signal B (Toyobo Co.); 1% BSA (final concentration) was then added to the diluents. In general, diluents that produced strong immunoreactions on light microscopy also produced a high labeling density of colloidal gold-labeled antibody. Anti-claudin-5 polyclonal antibody showed the strongest immunoreaction when it was diluted with Can Get Signal A for both LR-White-embedded materials and epon-embedded materials (**Figure 8D**). Can Get Signal A also showed the strongest immunoreactions when used as the diluent for E-cadherin monoclonal antibody. Monoclonal antibodies to β -catenin, β -actin, and clathrin showed a high labeling density when diluted in TBS. Polyclonal antibody to Tom 20 diluted with 50 mM NaCl/10 mM Tris-HCl (**Figure 6B**) or Can Get Signal B showed strong immunostaining. TBS was a better diluent for colloidal gold-labeled secondary antibodies than PBS.

7. Concluding remarks

The main mechanisms of HIAR are cleavage of chemical crosslinks formed by formaldehyde and extend of polypeptides chains to expose epitopes. Highly masked epitopes in heat-stable proteins can be exposed with reduction of disulfide bond followed by heating. Heating also cleaves crosslinks formed by double fixation with glutaraldehyde and osmium tetroxide. The principle of HIAR is applicable for immunoelectron microscopy using the post-embedding and pre-embedding methods, in which tissues are fixed with a standardized fixative described in this text. The association of exposed epitopes and antibodies under a suitable solution are also important for each immunohistochemical reaction.

Abbreviations

AnR	androgen receptor
BSA	bovine serum albumin
CAGSM	common antigen of secretory granule membrane
DAB	3,3' diaminobenzidine
ER α	estrogen receptor α
FFPE	formalin-fixed and paraffin embedded
GFAP	glial fibrillary acidic protein
γ -GTP	γ -glutamyl transpeptidase
HIAR	heat-induced antigen retrieval
HRP	horseradish peroxidase
HSP	heat shock protein
NRP	neuropilin
PBS	phosphate-buffered saline (10 mM phosphate buffer (pH 7.4) containing 150 mM NaCl)
PCNA	proliferating cell nuclear antigen

Tom	translocase of outer mitochondrial protein
VEGF	vascular endothelial cell growth factor
VEGFR	VEGF receptor
TBS	Tris-buffered saline (10 mM Tris-HCl buffer (pH 7.4) containing 150 mM NaCl)

Author details

Shuji Yamashita

Keio University School of Medicine, Japan

*Address all correspondence to: shuji@z5.keio.jp

IntechOpen

© 2018 The Author(s). Licensee IntechOpen. This chapter is distributed under the terms of the Creative Commons Attribution License (<http://creativecommons.org/licenses/by/3.0>), which permits unrestricted use, distribution, and reproduction in any medium, provided the original work is properly cited. 

References

- [1] Shi SR, Key ME, Kalra KL. Antigen retrieval in formalin-fixed, paraffin-embedded tissues: An enhancement method for immunohistochemical staining based on microwave oven heating of tissue sections. *Journal of Histochemistry and Cytochemistry*. 1991;**39**:741-748
- [2] Yamashita S, Okada Y. Mechanisms of heat-induced antigen retrieval: Analyses in vitro employing SDS-PAGE and immunohistochemistry. *Journal of Histochemistry and Cytochemistry*. 2005;**53**:13-21
- [3] Emoto K, Yamashita S, Okada Y. Mechanisms of heat-induced antigen retrieval: Does pH or ionic strength of solution play a role for refolding of antigens? *The Journal of Histochemistry and Cytochemistry*. 2005;**53**:1311-1321
- [4] Yamashita S. Heat-induced antigen retrieval: Mechanisms and application to histochemistry. *Progress in Histochemistry and Cytochemistry*. 2007;**41**:141-200
- [5] Shi SR, Taylor CR. Extraction of DNA/RNA from formalin-fixed, paraffin-embedded formalin-fixed, paraffin-embedded tissues based on the antigen retrieval principle. In: Shi SR, Taylor CR, editors. *Antigen Retrieval Immunohistochemistry Based Research and Diagnostics*. New Jersey: John Wiley & Sons, Inc; 2012. pp. 47-71
- [6] Gustafsson OJ, Arentz G, Hoffman P. Proteomic developments in the analysis of formalin-fixed tissue. *Biochimica et Biophysica Acta*. 2015;**1854**:559-580
- [7] Metz B, Kersten GFA, Hoogerhout P, Brugghe HF, Timmermans HAM, Jong A, et al. Identification of formaldehyde-induced modifications in proteins. *Journal of Biological Chemistry*. 2004;**279**:6235-6243
- [8] Sutherland BS, Toews J, Kast J. Utility of formaldehyde cross-linking and mass spectrometry in the study of protein-protein interactions. *Journal of Mass Spectrometry*. 2008;**43**:699-713
- [9] Toews J, Rogalski JC, Kast J. Accessibility governs the reactivity of basic residues in formaldehyde-induced protein modification. *Analytica Chimica Acta*. 2010;**676**:60-67
- [10] Fox CH, Johnson FB, Roller PP. Formaldehyde fixation. *Journal of Histochemistry and Cytochemistry*. 1985;**33**:845-853
- [11] Mason JT, O'Leary TJ. Effects of formaldehyde fixation on protein secondary structure: A calorimetric and infrared spectroscopic investigation. *Journal of Histochemistry and Cytochemistry*. 1991;**39**:225-229
- [12] Sompuram SR, Vani K, Messana E, Bogen SA. A molecular mechanism of formalin fixation and antigen retrieval. *American Journal of Clinical Pathology*. 2004;**121**:190-199
- [13] Fowler CB, O'Leary TJ, Mason JT. Modeling formalin fixation and histological processing with ribonuclease A: Effects of ethanol dehydration on reversal of formaldehyde cross-links. *Laboratory Investigation*. 2008;**88**:785-791
- [14] Sabatini DD, Bensch K, Barrenett RJ. Cytochemistry and electron microscopy. The preservation of cellular ultrastructure and enzymatic activity by aldehyde fixation. *Journal of Cell Biology*; **163**(17):19-58
- [15] Kawahara J, Ohmori T, Ohkubo T, Hattori S, Kawamura M. The structure of glutaraldehyde in aqueous solution determined by ultraviolet absorption and light scattering. *Analytical Biochemistry*. 1991;**201**:94-98

- [16] Migneault I, Dartiguenave C, Bertrand MJ, Waldron KC. Glutaraldehyde: behavior in aqueous solution, reaction with proteins, and application to enzyme crosslinking. *BioTechniques*. 2004;**37**:798-802
- [17] Deetz JS, Berhrman EJ. Reaction of osmium reagents with amino acids and proteins. Reactivity of amino acid residues and peptide bond cleavage. *International Journal of Peptide and Protein Research*. 1981;**17**:495-500
- [18] Hopwood D, Yeaman G, Milne G. Differentiating the effects of microwave and heat on on tissue proteins and their crosslinking by formaldehyde. *Histochemical Journal*. 1988;**20**:341-346
- [19] Rait VK, O'Leary TJ, Mason JT. Modeling formalin fixation and antigen retrieval with bovine pancreatic ribonuclease A: I-structural and functional alterations. *Laboratory Investigation*. 2004;**84**:292-299
- [20] Shi SR, Imam SA, Young L, Cote RJ, Taylor CR. Antigen retrieval immunochemistry under the influence of pH using monoclonal antibodies. *Journal of Histochemistry and Cytochemistry*. 1995;**43**:193-201
- [21] Pileri SA, Roncador G, Ceccarelli C, Piccioli M, Briskomatis A, Sabattini E, et al. Antigen retrieval techniques in immunohistochemistry: Comparison of different methods. *Journal of Pathology*. 1997;**183**:116-123
- [22] Kim SH, Kook MC, Shin YK, Park SH, Song HG. Evaluation of antigen retrieval buffer systems. *Journal of Molecular Histology*. 2004;**35**:409-416
- [23] Kajiya H, Takekoshi S, Egashira N, Miyakosh T, Serizawa T, Teramoto A, et al. Selection of buffer pH by the isoelectric point of antigen for the efficient heat-induced epitope retrieval; re-appraisal for nuclear protein pathobiology. *Histochemistry and Cell Biology*. 2009;**132**:659-667
- [24] Yamashita S. pH or ionic strength of antigen retrieval solution: A potential role for refolding during feat treatment. In: Shi SR, Taylor CR, editors. *Antigen Retrieval Immunohistochemistry Based Research and Diagnostics*. New Jersey: John Wiley & Sons Inc; 2010. pp. 303-321
- [25] Klockenbusch C, Kast J. Optimization of formaldehyde cross-linking for protein interaction analysis of non-tagged integrin β 1. *Journal of Biomedicine and Biotechnology*. 2010;**2010**:927585. DOI: 1155/2010/927585
- [26] Hoffman EA, Frey BL, Smith LM, Auble DT. Formaldehyde crosslinking: A tool for the study of chromatin complexes. *Journal of Biological Chemistry*. 2015;**290**:26404-26411
- [27] Namimatsu S, Ghazizadeh M, Sugisaki Y. Reversing the effects of formalin fixation with citraconic anhydride and heat: A universal antigen retrieval method. *Journal of Histochemistry and Cytochemistry*. 2005;**53**:3-11
- [28] Yamashita S, Kudo A, Kawakami H, Okada Y. Mechanisms of angiogenic suppression in uteri exposed to diethylstilbestrol neonatally in the mouse. *Biology of Reproduction*. 2013;**88**:116:1-13
- [29] Yamashita S, Okada Y. Application of heat-induced antigen retrieval to aldehyde-fixed fresh frozen sections. *Journal of Histochemistry and Cytochemistry*. 2005;**53**:1421-1432
- [30] Yamashita S, Katsumata O. Heat-induced antigen retrieval in immunohistochemistry. Mechanisms and applications. In: Pellicciari C, Biggiogera M, editors. *Methods in Molecular Biology 1560, Histochemistry of Single Molecules, Methods and Protocols*. New York: Humana Press; 2017. pp. 147-161

- [31] McLean IW, Nakane PK. Peroxidase-lysine-paraformaldehyde fixative. *The Journal of Histochemistry and Cytochemistry*. 1974;**22**:1077-1083
- [32] Yamashita S, Katsumata O, Okada Y. Establishment of a standardized post-embedding method for immunoelectron microscopy by applying heat-induced antigen retrieval. *Journal of Electron Microscopy*. 2009;**58**:267-279
- [33] Dai W, Sato S, Ishizaki M, Wakamatsu K, Namimatsu S, Sugisaki Y, et al. A new antigen retrieval method using citraconic anhydride for immunoelectron microscopy: Localization of surfactant protein C (proSP-C) in the type II alveolar epithelial cells. *Journal of Submicroscopic Cytology and Pathology*. 2004;**36**:219-222
- [34] Ashour F, Deuchars J. Electron microscopic localisation of P2X4 receptor subunit immunoreactivity to pre- and post-synaptic neuronal elements and glial processes in the dorsal vagal complex of the rat. *Brain Research*. 2004;**1026**:44-55
- [35] Katsumata O, Mori M, Sawane Y, Niimura T, Ito A, Okamoto H, et al. Cellular and subcellular localization of ADP-ribosylation factor 6 in mouse peripheral tissues. *Histochemistry and Cell Biology*. 2017;**148**:577-590
- [36] Hann CR, Springett MJ, Johnson DH. Antigen retrieval of basement membrane proteins from archival eye tissues. *Journal of Histochemistry and Cytochemistry*. 2001;**49**:475-482
- [37] Xiao JC, Adam A, Ruck P, Kaiserling E. A comparison of methods for heat-mediated antigen retrieval for immunoelectron microscopy: Demonstration of cytokeratin No. 18 in normal and neoplastic hepatocytes. *Biotechnic and Histochemistry*. 1996;**71**:278-285
- [38] Saito N, Konishi K, Takeda H, Kato M, Sugiyama T, Asaka M. Antigen retrieval trial for post-embedding immunoelectron microscopy by heating with several unmasking solutions. *Journal of Histochemistry and Cytochemistry*. 2003;**51**:989-994
- [39] Yamashita S. Post-embedding mammalian tissue for immunoelectron microscopy: A standardized procedure based on heat-induced antigen retrieval. In: Schwartzbach SW, Skalli O, Schikorski T, editors. *Methods in Molecular Biology 1474, High-Resolution Imaging of Cellular Proteins, Methods and Protocols*. New York: Humana Press; 2016. pp. 279-290
- [40] Bendayan M, Zollner M. Ultrastructural localization of antigenic sites on osmium-fixed tissues applying the protein A-gold technique. *Journal of Histochemistry and Cytochemistry*. 1983;**31**:101-109
- [41] Rocken C, Roessner A. An evaluation of antigen retrieval procedures for immunoelectron microscopic classification of amyloid deposits. *Journal of Histochemistry and Cytochemistry*. 1999;**47**:1385-1394
- [42] Coleman RA, Liu J, Wade JB. Use of anti-fluorophore antibody to achieve high-sensitivity immunolocalizations of transporters and ion channels. *Journal of Histochemistry and Cytochemistry*. 2006;**54**:817-827
- [43] Brorson SH, Skjorten F. Improved technique for immunoelectron microscopy. How to prepare epoxy resin to obtain approximately the same immunogold labeling for epoxy sections as for acrylic sections without any etching. *Micron*. 1996;**27**:203-209
- [44] Yamashita S, Okada Y. Heat-induced antigen retrieval in conventionally processed epon-embedded specimens:

Procedures and mechanisms. *Journal of Histochemistry and Cytochemistry*. 2014;**62**:584-597

[45] Yamashita S. Immunoelectron microscopy with the post-embedding method based on heat-induced antigen retrieval: Techniques and mechanisms. *Kenbikyo*. 2014;**49**:124-131 (in Japanese)

Section 2

Use of
Immunohistochemistry in
Disease Detection

Immune Cell Profiling in Cancer Using Multiplex Immunofluorescence and Digital Analysis Approaches

Edwin Roger Parra

Abstract

During the last years, multiplex immunofluorescence (mIF) has emerged as a very powerful tool in multiple epitope detection to study tumor tissues. This revolutionary technology is providing an important visual technique for tumor examination in formalin-fixed paraffin-embedded specimens for a better understanding of tumor microenvironment, new treatment discoveries, cancer prevention, as well as translational studies. The aim of this chapter is to highlight the use of tyramide signal amplification methodology in mIF and image analysis to identify several proteins at the same time in one single tissue and their spatial distribution in different tumor specimens including whole sections, core needle biopsies, and tissue microarrays. This type of methodology associated with image analysis can perform high-quality throughput assay in translational research studies to be applied in cancer prevention and treatments.

Keywords: tyramide signal amplification, conventional IHC protocol, immunoprofiling, cancer tissues, image analysis, spatial analysis

1. Introduction

In the last years, novel and effective immunotherapies for patients with different tumor types are becoming clinically important, because of the remarkable clinical efficacy observed with several immune checkpoint inhibitors such as cytotoxic T lymphocyte antigen 4 (CTLA-4) and the programmed death receptor 1 (PD-1) or its ligand (PD-L1) [1–12]. Whereas anti-CTLA-4 antibodies (ipilimumab and tremelimumab), anti-PD-1 antibodies (nivolumab and pembrolizumab), and anti-PD-L1 antibodies (atezolizumab, avelumab, and durvalumab) have produced remarkable results, increasing the survival prognosis in many cancer types, it is still unknown why some tumors do not respond to or relapse after this type of treatment. In this way, increased observations suggest that tumors rich in tumor-associated immune cells (TAICs) may respond to therapies targeting immune system inhibitory or stimulatory mechanisms, and tumors with non-TAICs may require additional interventions aimed at promoting optimal inflammation and innate immune activation in the tumor microenvironment [13–15]. Indeed, characterization of different immune checkpoints as well as tumor microenvironment in patients with cancer has become

a fundamental step in providing evidence for the presence of distinct immunologic phenotypes, based on the presence or absence of various immune cells [1, 16, 17] that can predict the response to the therapy. In this way, the study of immune checkpoints and TAICs and their interaction prompt the need for multiplexed analyses of tumor tissues. To address this need, in the last years, multiplex imaging platforms have emerged as an important tool to provide critical information about cancer microenvironment, prognosis, therapy, and relapse [18–22]. Different components in the tumor microenvironment can be examined simultaneously using multiplex methodologies, providing insight into biological cross-talk present at the tumor-host interface and from subcellular levels to entered cell populations. In addition, the precision of these new techniques can be used to evaluate the special distribution of multiple biomarkers detected simultaneously, and their coexpressions or interactions between cells are becoming a essential tool to study tumor tissues [22] and to ultimately enhance disease diagnosis and better inform timely patient care [23].

Multiplex technologies are being used to identify the presence of multiple biological markers as immune checkpoint and TAICs on a single tissue sample [24]. The multiplex imaging techniques provide unique biological information that in many cases cannot be obtained by other imaging methods or by single immunohistochemistry (IHC) techniques. As mentioned, individual cells can be accessed with extraordinary fidelity equal to that achievable in the bulk population, such that even rare cell populations can be studied to understand their important role in translational research, and this knowledge can be applied in cancer prevention and treatment. In this chapter, we will discuss one of the most reliable and a very well-known methodology to identify simultaneous biomarkers in formalin-fixed, paraffin-embedded (FFPE) specimens as well as its imaging analysis platform as an important tool for potential application in future cancer immunotherapy biomarker discoveries.

2. Tyramide signal amplification for multiplex staining in FFPE tissues

Tyramide signal amplification (TSA) was described in the 1990s by Bobrow and colleagues [25, 26]. It is an enzyme-linked signal amplification method that is used to detect and localize low copy number of proteins present in tissues by conventional IHC protocol, using, most commonly, alkaline phosphatase or horseradish peroxidase (HRP) enzymatic reaction to catalyze the deposition of tyramide-labeled molecules at the site of probe or epitope detection. Tyramides are conjugated to biotin or fluorescent labels and revealed by streptavidin-HRP system [27, 28]. The HRP catalyzes the formation of tyramide into highly reactive tyramide radicals that covalently bind to electron-rich tyrosine moieties close to the epitope of interest on FFPE tissue. Tissue surfaces with anchored biotinylated tyramide must be further treated with fluorescent- or enzyme-tagged proteins that have a high affinity for biotin, such as streptavidin, before microscopic visualization [27, 28]. The detection of the proteins is increased more than ten times compared to standard biotin-based staining methods [29].

Perkin Elmer developed the Opal™ workflow (**Figure 1**), which allows simultaneous staining of multiple biomarkers within a single paraffin tissue section. Multiplex immunofluorescence (mIF) allows researchers to use antibodies raised in the same species, and different panels combined with different targets can be created using this technology [21, 27]. The approach, in the manual protocol, involves detection with fluorescent TSA reagents, followed by microwave treatment that removes the primary and secondary antibodies between cycles and any nonspecific staining that reduces tissue autofluorescence for each antibody cycle. The correct ordering of the different antibodies in a panel is still challenging and is only solved by trial and error to obtain a perfect staining. In the automated protocol using Leica Bond RX or another

autostainer, the time of staining is reduced drastically when compared with manual staining. The possibilities for mIF are expanding our knowledge of tumor immune contexture (**Figure 2**) in different types of cancers. Mapping the tumor microenvironment and the predictive and/or prognostic value of immune checkpoint expression on malignant cells and TAICs has been carried out in patients with melanoma, lung cancer, breast cancer, gastric cancer, Hodgkin lymphoma, and others by mIF [30–34]. Similar to other multiplex techniques, in the TSA mIF method, our experience showed that the approach to different targets requires diligent optimization, first in conventional chromogenic IHC validation and then in the simplex IF, before mIF

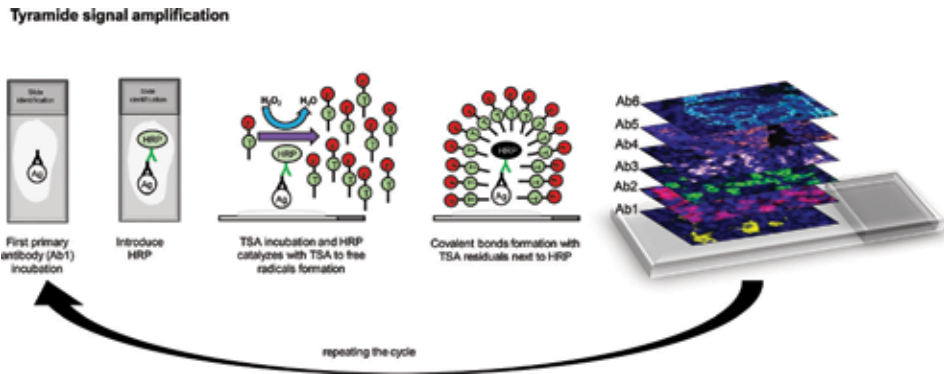


Figure 1. *Tyramide signal amplification workflow. After primary antibody (Ab), the HRP-conjugated secondary antibody binds to an unconjugated primary antibody specific to the target/antigen of interest. Detection is ultimately achieved with a fluorophore-conjugated tyramide molecule that serves as the substrate for HRP. Activated tyramide forms covalent bonds with tyrosine residues on or neighboring the protein of interest and is permanently deposited upon the site of the antigen. The method allows for serial cycles of the primary/secondary antibody pairs, while preserving the antigen-associated fluorescence signal, making this process amenable to multiple rounds of staining in a sequential fashion.*

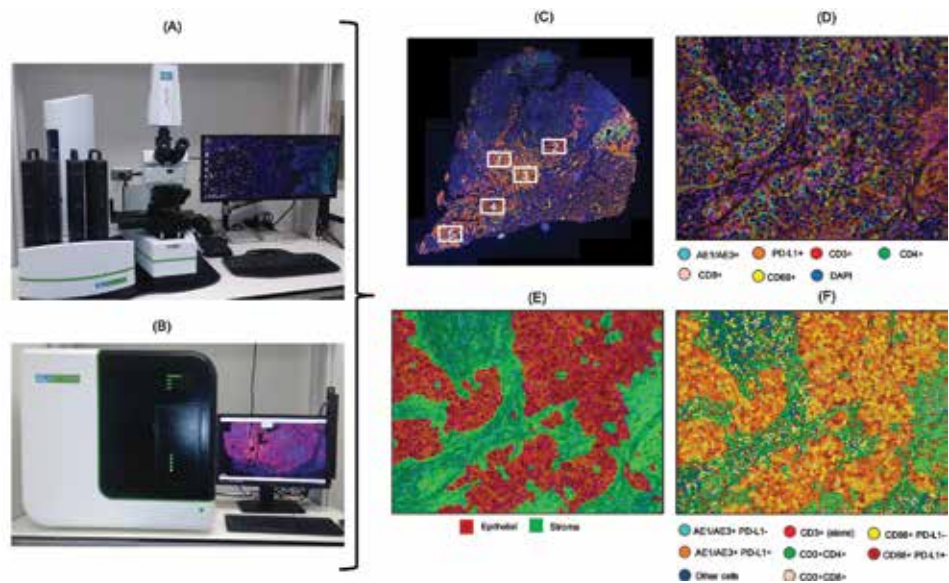


Figure 2. *(A) Vectra® and (B) Polaris™ scanner systems, (C) low magnification image, showing the selection of five intratumoral areas of interest to be analyzed, (D) composite image of lung cancer tissue showing seven color markers to identify different cell populations, (E) tissue segmentation (epithelial and stromal compartments), and (F) cell populations' immune phenotyping.*

staining in control tissues. The use of specific, very well-standardized, and validated antibodies, as well as the careful use of other components, as right antibody titration, incubation time, and antigen retrieval during staining, is important to obtain good and reproducible results using different panels [27]. The use of very well-known control tissues during each staining and for each created panel that allows all the markers is important and essential to detect possible staining errors during the process in each mIF panel. Properties of the FFPE material, such as sample age, method of preservation, storage conditions, and tissue type, are very important factors to be considered to obtain high-quality mIF staining and good data. Pathologists play a key role in making sure that tissue samples collected are appropriate for diagnostic and research purposes. The tissues need to be processed adequately, that is, fixed in 10% formalin and stored in good conditions to avoid antigenic deterioration that can influence the process when targeting several proteins using this methodology. Type of tissue, is another important factor to be considered, sometimes as a limitation factor for a quality staining with this technique. We observed that some tissues that have abundant fat as breast tissue or cartilage in some type of cancers or bone component that were submitted a decalcification procedures, are more challenges during the mIF staining, showing frequently artifacts of staining like background, folds, caused by tissue detached and unspecific or not clear staining on the cells, causes by the decalcification procedures. Antibodies with very good performance in decalcified tissues are limited, and those need an exhaustive validation in IHC before creating a new panel to stain these samples. No less important, the size of the sample is another factor to be considered during mIF staining; small biopsies as core needle biopsies (CNBs) less than 1.0 × 0.2 cm are more challenging and have high probability to be lost during standard mIF staining than bigger tissues as whole sections (~1.0 × 1.0 cm). The minimum number of malignant tumor cells required for mIF marker analysis has not been well established and is another factor to be considered during staining and analysis.

Specimen type	Size (cm)	Viable tumor cells (N)	Necrosis (%)	Fat/cartilage/bone (%)	Adequacy for mIF staining*
Whole section	>1.0 × 1.0	>100	0 or <10	0 or <10 of any component	100% in our series
Whole section	>1.0 × 1.0	>100	0 or >10	>50 of any component	80% in our series
Small biopsies	>1.0 × 0.2	>100	0 or <10	0 or <5 of any component	100% in our series
Small biopsies	<1.0 × 0.2	>100	<10	<50 of any component	70% in our series
Small biopsies	<1.0 × 0.2	<100	>10	>50 of any component	50% in our series
TMA (by core)	>0.1	>100	0 or <5	0 or <5 of any component	100% in our series

A preliminary quality control to establish the samples by a pathologist is strongly recommended to optimize the preparation of tissue for multiplex immunofluorescence staining and ultimately to guaranty a quality data. Each case needs to be considered separately and can be influenced by several characteristics. In general, the quality of the samples including the fixation process of the FFPE tissues, storage and cutting procedures, will influence the quality of multiplex staining (). There are, however, according to our experience, different tissue characteristics that need to be considered as challenges for staining and analysis, and these are considered sometimes as limitations of the staining. By understanding much better these tissue limitations, we can avoid wasted effort, resources, and funds of the laboratory as well as preserve the high-quality data obtained by this technique.*

Table 1.
Quality criteria's samples for multiplex immunofluorescence.

According our experience, samples with at least more than 100 malignant cells are preferred, to avoid errors in the interpretations of different markers, especially when the targets of study are malignant cells. Necrotic areas in more than 50% of the entire sample can compromise the quality of the staining and when compromise the quality of the sample and the staining need to be considered judiciously by the pathology as excluded criteria to preserve the quality of the analysis and data (**Table 1**). The quality control of pathology, as a first step, is essential to avoid wasted effort, resources, and funds of the laboratory and to preserve the high-quality data obtained by this methodology.

3. Image approaches and data analysis

Although the methodology of TSA is available for FFPE material and can enable multiparametric readouts from a single tissue section, they sometimes have limited scalability and throughput, related to limited number of markers allowed per panel compared with other multiplex methodologies like imaging mass cytometry and multiplexed ion beam imaging [35, 36]. The scanner system (**Figure 2**) Vectra® [27] from PerkinElmer provides high quality of scanning with high-resolution and multiband filter cubes that provide greater flexibility associated with the multispectral camera, to match with the sample. The new generation of scanner Polaris™ (PerkinElmer) scan system supports multiple filters using tunable LED excitation, similar to confocal microscope, and the captured signals are assembled in a composite image [37]. After acquiring the panoramic low-magnification images at $\times 4$ or $\times 10$, the specimens can be sampled using different ROI sizes by the phenochart (PerkinElmer) software viewer to scan high-resolution images at $\times 20$ or $\times 40$. Although, the scanner system Vectra®-Polaris™ can capture different regions of interest (ROIs) using the filters and the multispectral camera at high quality resolution [36], it is still impossible to accelerate the process of scanning or scan the whole tissue section as a unique image for the analysis. The time for scanning the sample is variable and depends on the number of markers used in the panel, number of ROIs captured per sample, and size of the ROI and can take from minutes to several hours according these parameters [38] (**Table 2**). According our experience, the TSA

Magnification	Scanner		ROI (Vectra®)/(Polaris™) (seven markers)
	Vectra® (Time/ minutes)	Polaris™ (Time/ minutes)	
4×*	~9	–	Panoramic view
10×*	~18	~13	Panoramic view
20×	~6	~5	1×1 (669×500 μm)/(931×698 μm)
20×	~12	~14	2×2 (1338×1000 μm)/(1862×1396 μm)
20×	~22	~35	3×3 (2007×1500 μm)/(2793×2094 μm)
40×	~4	~8	1×1 (334×250 μm)/(465×249 μm)
40×	~10	~20	2×2 (669×500 μm)/(931×698 μm)
40×	~19	~36	3×3 (1004×750 μm)/(1396×1047 μm)

The time for scanning the sample is variable and depends on the number of markers used in the panel, number of regions of interest (ROI) captured per sample, and size of the ROI using Vectra® or Polaris™ system, as well as whether the system stores the image locally or in a server. Available only in Vectra®.

Table 2.
 Approximate time for image scanning using Vectra® or the Polaris™ scanner system.

Vendor	Program name	Method	Availability
PerkinElmer	InForm	Color-based colocalization, tissue, cell segmentation	Licensed
Definiens	Tissue Studio	Imaging segmentation, marker intensity measurement, and statistical analysis	Licensed
Indica Labs	HALO	Membrane, colocalization, immune cell proximity, spatial analysis	Licensed
Visiopharm	Visimoph Tissuemorph	Signal intensity, area, counting objects, statistical analysis	Licensed
Spot Imagine	Spot advanced	Color-based colocalization	Licensed
FARSIGHT	Nucleus Editor	Multichannel-based object identification/ toolkit	Free
NIH	Image J	Color-based, user interactive segmentation	Free
HistoRx	AQUAnalysis	Signal intensity per unit area and per layer	Licensed
CompuCyte	iCyte	Nucleus segmentation or phantom contouring, measuring associated signals	Licensed

Table 3.
Image analysis software systems available for multiplex immunofluorescence.

staining system for mIF when combined with multispectral image analysis software, such as InForm (PerkinElmer), can provide a powerful tool for analysis of multiple markers in one single slide [21, 39]. However, there are many available software in the market that can be used for the analysis of mIF images generated by the InForm software from the Vectra®-Polaris™ scanner systems, and it is important to know that the InForm software is essential to generate the individual unmixed tyramide fluorochrome with a positive signal without noise or aberrant background staining and with high resolution performance across the different ROIs from the scanning systems [40]. For the analysis, image analysis software need to be accessible (**Table 3**), with easy automated capabilities of detection, including tissue segmentation, compartmentalization of the staining (e.g., nuclear, membranous, or cytoplasmic) (**Figure 2**), and spatial colocalization of cell distribution, critically important to study different markers included in different panels (**Figure 3**). In the same way, comprehensive evaluation using this different image analysis software is needed not only for clear antigen demarcation and good staining procedures but also for good interpretation of the results. Pathologists are very important and need to standardize the possible interobserved variation [41, 42] when using different image analysis platforms during the colocalization of proteins.

4. Multiplex immunofluorescence staining from translational research

Despite the evolution in the last years, in different levels of cancer research, concerning prevention, diagnosis, therapeutic options, and follow-up methods, cancer diseases are still the major public health problem worldwide [43]. Profiling immune cells is currently a powerful metric for tumor subclassification and predicting clinical outcomes. A great variety of cancer research screening tools is applied to diagnose tumors and has been established for different tumors. Simultaneous quantification of more than one biomarker at the same time has become more and more interesting in cancer research using different multiplex technologies. Multiplex TSA can allow different biomarkers in one single slide, targeting different

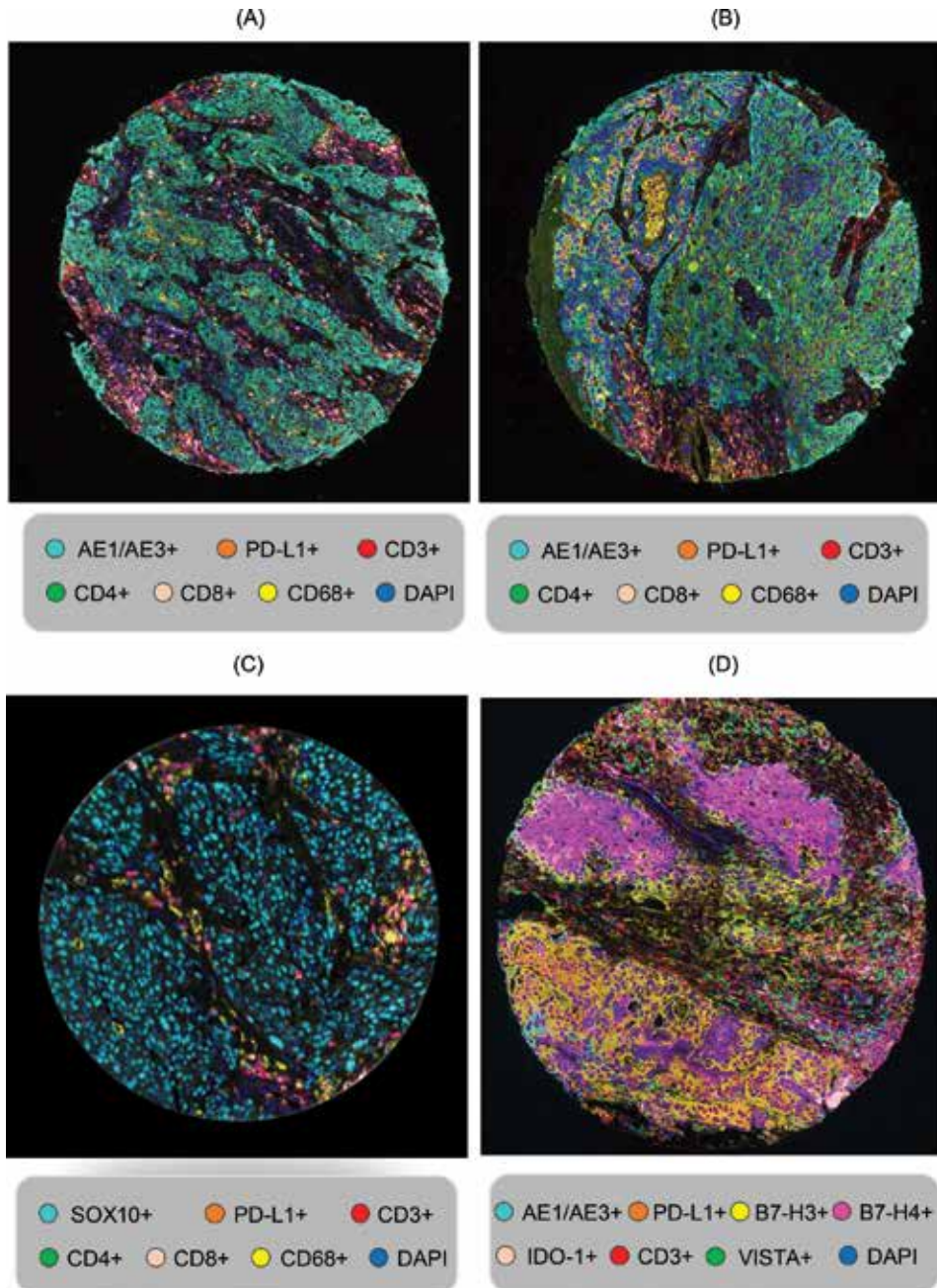


Figure 3. Microphotographs of representative examples of multiplex immunofluorescence in tumor tissues using different markers, (A) lung adenocarcinoma, (B) lung squamous cell carcinoma, (C) malignant melanoma, and (D) lung squamous cell carcinoma. $\times 20$ magnification.

systemic processes, such as inflammation, immunecheckpoints, angiogenesis, or cell death using tumor markers (**Figure 3**), to improve cancer prevention, diagnostic accuracy, and treatment. We demonstrated that this method can offer important advantages, such as high-throughput performance, low material requirement, wide range of applications, and cost- and time-effective multiplex for several parameters in different panels [23, 44, 45]. Several biomarkers can be cancer-specific since malignant cells of different histologic types can produce different patterns of

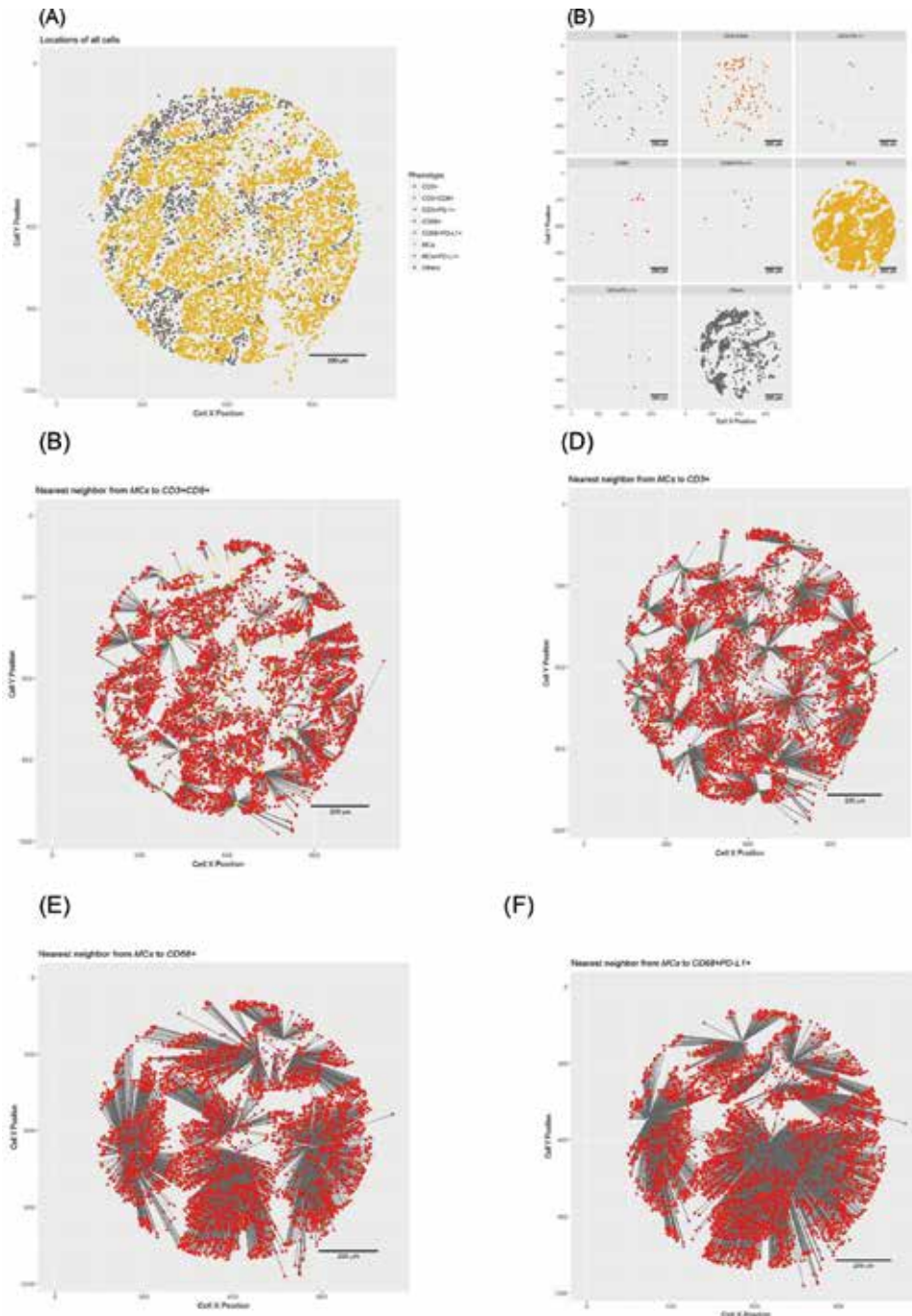


Figure 4. Microphotographs of representative examples of spatial-distribution visualization of different phenotypes analyzed. (A) distribution of individual cells using X and Y positions, (B) spatial localization of selected cells, and (C to F) distance measurements between malignant cells (MCs) and different cell populations.

proangiogenic factors, growth factors, and immune cells that are tumor related. The study of biomarker panels (Figure 3) and its spatial distribution (Figure 4) can be used for early diagnosis and assessment of therapy response [46]. This methodology can represent an ideal method to realize personalized therapies using efficient mIF panels and help to understand much better the cancer microenvironment,

highlighting the benefit for exploring immune evasion mechanisms and finding potential biomarkers that allow researchers to assess the mechanism of action and predict and track response [47].

5. Conclusion

The detection of multiple markers in the same tissue section can provide important and efficient means to apply this technology in disease diagnosis, prevention, and translational research. Multiplex immunofluorescence platforms have emerged more and more from translational research labs toward the clinic, increasing the opportunity to study and understand much better the tumor-immune interactions. This methodology and different image analysis strategies can give important information about immune cells' coexpression and their spatial-pattern distribution in the tumor microenvironment. Development of multiplex immunofluorescence based-TSA system requires a very well-trained multidisciplinary team including pathologists, oncologists, and immunologists. In addition, this methodology requires automation to provide efficient and fast information as well as easy analysis methodologies for research pathologists that currently use this method.

Acknowledgements

The author would like to acknowledge the people that work in the laboratory of multiplex immunofluorescence, Mei Jang, Tong Li, Aerole Tanhemon, and Barbara Mino; the pathology team that work in the multiplex image analysis; as well as the chair of the Department of Translational Molecular Pathology, Dr. Ignacio Wistuba.

Conflict of interest


The author does not have any type of competing interest.

Author details

Edwin Roger Parra
Department of Translational Molecular Pathology, The University of Texas MD
Anderson Cancer Center, Houston, Texas, USA

*Address all correspondence to: erparra@mdanderson.org

IntechOpen

© 2018 The Author(s). Licensee IntechOpen. This chapter is distributed under the terms of the Creative Commons Attribution License (<http://creativecommons.org/licenses/by/3.0>), which permits unrestricted use, distribution, and reproduction in any medium, provided the original work is properly cited. 

References

- [1] Topalian SL, Hodi FS, Brahmer JR, Gettinger SN, Smith DC, McDermott DF, et al. Safety, activity, and immune correlates of anti-PD-1 antibody in cancer. *The New England Journal of Medicine*. 2012;**366**(26):2443-2454
- [2] Hamid O, Robert C, Daud A, Hodi FS, Hwu WJ, Kefford R, et al. Safety and tumor responses with lambrolizumab (anti-PD-1) in melanoma. *The New England Journal of Medicine*. 2013;**369**(2):134-144
- [3] Wolchok JD, Kluger H, Callahan MK, Postow MA, Rizvi NA, Lesokhin AM, et al. Nivolumab plus ipilimumab in advanced melanoma. *The New England Journal of Medicine*. 2013;**369**(2):122-133
- [4] Ansell SM, Lesokhin AM, Borrello I, Halwani A, Scott EC, Gutierrez M, et al. PD-1 blockade with nivolumab in relapsed or refractory Hodgkin's lymphoma. *The New England Journal of Medicine*. 2015;**372**(4):311-319
- [5] Brahmer JR, Hammers H, Lipson EJ. Nivolumab: targeting PD-1 to bolster antitumor immunity. *Future Oncology*. 2015;**11**(9):1307-1326
- [6] Herbst RS, Soria JC, Kowanetz M, Fine GD, Hamid O, Gordon MS, et al. Predictive correlates of response to the anti-PD-L1 antibody MPDL3280A in cancer patients. *Nature*. 2014;**515**(7528):563-567
- [7] Gettinger S, Herbst RS. B7-H1/PD-1 blockade therapy in non-small cell lung cancer: Current status and future direction. *Cancer Journal*. 2014;**20**(4):281-289
- [8] Robert C, Long GV, Brady B, Dutriaux C, Maio M, Mortier L, et al. Nivolumab in previously untreated melanoma without BRAF mutation. *The New England Journal of Medicine*. 2015;**372**(4):320-330
- [9] Sunshine J, Taube JM. PD-1/PD-L1 inhibitors. *Current Opinion in Pharmacology*. 2015;**23**:32-38
- [10] Gettinger SN, Horn L, Gandhi L, Spigel DR, Antonia SJ, Rizvi NA, et al. Overall survival and long-term safety of nivolumab (anti-programmed death 1 antibody, BMS-936558, ONO-4538) in patients with previously treated advanced non-small-cell lung cancer. *Journal of Clinical Oncology*. 2015;**33**(18):2004-2012
- [11] Dong H, Strome SE, Salomao DR, Tamura H, Hirano F, Flies DB, et al. Tumor-associated B7-H1 promotes T-cell apoptosis: A potential mechanism of immune evasion. *Nature Medicine*. 2002;**8**(8):793-800
- [12] Ishida Y, Agata Y, Shibahara K, Honjo T. Induced expression of PD-1, a novel member of the immunoglobulin gene superfamily, upon programmed cell death. *The EMBO Journal*. 1992;**11**(11):3887-3895
- [13] Kershaw MH, Westwood JA, Darcy PK. Gene-engineered T cells for cancer therapy. *Nature Reviews Cancer*. 2013;**13**(8):525-541
- [14] Kalbasi A, June CH, Haas N, Vapiwala N. Radiation and immunotherapy: A synergistic combination. *The Journal of Clinical Investigation*. 2013;**123**(7):2756-2763
- [15] Gajewski TF, Schreiber H, Fu YX. Innate and adaptive immune cells in the tumor microenvironment. *Nature Immunology*. 2013;**14**(10):1014-1022
- [16] Teng MW, Ngiow SF, Ribas A, Smyth MJ. Classifying cancers based on

T-cell infiltration and PD-L1. *Cancer Research*. 2015;**75**(11):2139-2145

[17] Tumeh PC, Harview CL, Yearley JH, Shintaku IP, Taylor EJ, Robert L, et al. PD-1 blockade induces responses by inhibiting adaptive immune resistance. *Nature*. 2014;**515**(7528):568-571

[18] Steiner C, Ducret A, Tille JC, Thomas M, McKee TA, Rubbia-Brandt L, et al. Applications of mass spectrometry for quantitative protein analysis in formalin-fixed paraffin-embedded tissues. *Proteomics*. 2014;**14**(4-5):441-451

[19] Stauber J, MacAleese L, Franck J, Claude E, Snel M, Kaletas BK, et al. On-tissue protein identification and imaging by MALDI-ion mobility mass spectrometry. *Journal of the American Society for Mass Spectrometry*. 2010;**21**(3):338-347

[20] Sood A, Miller AM, Brogi E, Sui Y, Armenia J, McDonough E, et al. Multiplexed immunofluorescence delineates proteomic cancer cell states associated with metabolism. *JCI Insight*. 2016;**1**(6):1-14

[21] Gorris MAJ, Halilovic A, Rabold K, van Duffelen A, Wickramasinghe IN, Verweij D, et al. Eight-color multiplex immunohistochemistry for simultaneous detection of multiple immune checkpoint molecules within the tumor microenvironment. *Journal of Immunology*. 2018;**200**(1):347-354

[22] Rost S, Giltneane J, Bordeaux JM, Hitzman C, Koeppen H, Liu SD. Multiplexed ion beam imaging analysis for quantitation of protein expression in cancer tissue sections. *Laboratory Investigation*. 2017;**97**(8):992-1003

[23] Parra ER. Novel platforms of multiplexed immunofluorescence for study of paraffin tumor tissues. *Journal*

of Cancer Treatment & Diagnosis. 2018;**2**(1):43-53

[24] Dixon AR, Bathany C, Tsuei M, White J, Barald KF, Takayama S. Recent developments in multiplexing techniques for immunohistochemistry. *Expert Review of Molecular Diagnostics*. 2015;**15**(9):1171-1186

[25] Bobrow MN, Harris TD, Shaughnessy KJ, Litt GJ. Catalyzed reporter deposition, a novel method of signal amplification. Application to immunoassays. *Journal of Immunological Methods*. 1989;**125**(1-2):279-285

[26] Bobrow MN, Shaughnessy KJ, Litt GJ. Catalyzed reporter deposition, a novel method of signal amplification. II. Application to membrane immunoassays. *Journal of Immunological Methods*. 1991;**137**(1):103-112

[27] Parra ER, Uraoka N, Jiang M, Cook P, Gibbons D, Forget MA, et al. Validation of multiplex immunofluorescence panels using multispectral microscopy for immune-profiling of formalin-fixed and paraffin-embedded human tumor tissues. *Scientific Reports*. 2017;**7**(1):13380

[28] Stack EC, Wang C, Roman KA, Hoyt CC. Multiplexed immunohistochemistry, imaging, and quantitation: A review, with an assessment of tyramide signal amplification, multispectral imaging and multiplex analysis. *Methods*. 2014;**70**(1):46-58

[29] Faget L, Hnasko TS. Tyramide signal amplification for immunofluorescent enhancement. *Methods in Molecular Biology*. 2015;**1318**:161-172

[30] Ju X, Shen R, Huang P, Zhai J, Qian X, Wang Q, et al. Predictive relevance of

PD-L1 expression with pre-existing TILs in gastric cancer. *Oncotarget*. 2017;**8**(59):99372-99381

[31] Carey CD, Gusenleitner D, Lipschitz M, Roemer MGM, Stack EC, Gjini E, et al. Topological analysis reveals a PD-L1-associated microenvironmental niche for Reed-Sternberg cells in Hodgkin lymphoma. *Blood*. 2017;**130**(22):2420-2430

[32] Edwards J, Wilmott JS, Madore J, Gide TN, Quek C, Tasker A, et al. CD103+ tumor-resident CD8+ T cells are associated with improved survival in immunotherapy naïve melanoma patients and expand significantly during anti-PD1 treatment. *Clinical Cancer Research*. 2018;**24**(13):3036-3045

[33] Buisseret L, Pommey S, Allard B, Garaud S, Bergeron M, Cousineau I, et al. Clinical significance of CD73 in triple-negative breast cancer: Multiplex analysis of a phase III clinical trial. *Annals of Oncology*. 2018;**29**(4):1056-1062

[34] Parra ER, Villalobos P, Behrens C, Jiang M, Pataer A, Swisher SG, et al. Effect of neoadjuvant chemotherapy on the immune microenvironment in non-small cell lung carcinomas as determined by multiplex immunofluorescence and image analysis approaches. *Journal for ImmunoTherapy of Cancer* . 2018;**6**(1):48

[35] Blom S, Paavolainen L, Bychkov D, Turkki R, Maki-Teeri P, Hemmes A, et al. Systems pathology by multiplexed immunohistochemistry and whole-slide digital image analysis. *Scientific Reports*. 2017;**7**(1):15580

[36] Isse K, Lesniak A, Grama K, Roysam B, Minervini MI, Demetris AJ. Digital transplantation pathology: Combining whole slide imaging, multiplex staining and automated image analysis.

American Journal of Transplantation. 2012;**12**(1):27-37

[37] Sanderson MJ, Smith I, Parker I, Bootman MD. *Fluorescence microscopy*. Cold Spring Harbor Protocol. 2014;**2014**(10):pdb top071795

[38] Spindel S, Sapsford KE. Evaluation of optical detection platforms for multiplexed detection of proteins and the need for point-of-care biosensors for clinical use. *Sensors (Basel)*. 2014;**14**(12):22313-22341

[39] Feng Z, Puri S, Moudgil T, Wood W, Hoyt CC, Wang C, et al. Multispectral imaging of formalin-fixed tissue predicts ability to generate tumor-infiltrating lymphocytes from melanoma. *Journal for ImmunoTherapy of Cancer*. 2015;**3**:47

[40] Bobrow MN, Litt GJ, Shaughnessy KJ, Mayer PC, Conlon J. The use of catalyzed reporter deposition as a means of signal amplification in a variety of formats. *Journal of Immunological Methods*. 1992;**150**(1-2):145-149

[41] Huang W, Hennrick K, Drew S. A colorful future of quantitative pathology: Validation of Vectra technology using chromogenic multiplexed immunohistochemistry and prostate tissue microarrays. *Human Pathology*. 2013;**44**(1):29-38

[42] Nederlof M, Watanabe S, Burnip B, Taylor DL, Critchley-Thorne R. High-throughput profiling of tissue and tissue model microarrays: Combined transmitted light and 3-color fluorescence digital pathology. *Journal of Pathology Informatics*. 2011;**2**:50

[43] Siegel RL, Miller KD, Jemal A. *Cancer statistics, 2017*. CA: A Cancer Journal for Clinicians. 2017;**67**(1):7-30

[44] Stack EC, Foukas PG, Lee PP. Multiplexed tissue biomarker imaging.

Journal for ImmunoTherapy of Cancer.
2016;**4**:9

[45] Bolognesi MM, Manzoni M, Scalia CR, Zannella S, Bosisio FM, Faretta M, et al. Multiplex staining by sequential immunostaining and antibody removal on routine tissue sections. *The Journal of Histochemistry and Cytochemistry*. 2017;**65**(8):431-444

[46] Parra ER. Novel technology to assess programmed death-ligand 1 expression by multiplex immunofluorescence and image analysis. *Applied Immunohistochemistry & Molecular Morphology*. 2018;**26**(2):e22-ee4

[47] Barua S, Fang P, Sharma A, Fujimoto J, Wistuba I, Rao AUK, et al. Spatial interaction of tumor cells and regulatory T cells correlates with survival in non-small cell lung cancer. *Lung Cancer*. 2018;**117**:73-79

Low-Specificity and High-Sensitivity Immunostaining for Demonstrating Pathogens in Formalin-Fixed, Paraffin-Embedded Sections

Yutaka Tsutsumi

Abstract

The present review describes a part of the author's own experience in applying immunoperoxidase staining to routine histopathological diagnosis. The target disorder was focused on infection. In the practice of pathology diagnosis services, it is important for us diagnostic pathologists to judge whether the lesion is caused by an infection or not. When an infectious disease is highly likely, the visualization of pathogens within the inflammatory lesion is required to suggest a causative agent. Two main approaches the author would like to introduce include (1) the use of commercially available antisera showing wide cross-reactivity to a variety of bacteria and (2) the use of diluted patients' sera. These immunohistochemical studies employing "low-specificity" and "high-sensitivity" probes are useful for confirming the localization of pathogen within the infectious lesion.

Keywords: infectious diseases, diagnostic immunohistochemistry, specificity, sensitivity, commercial antiserum, patient's serum, paraffin section

1. Introduction

Infectious diseases kill a significant number of people in the world. Of the top 10 leading causes of death in low-income countries in 2016, pneumonia, diarrheal diseases, acquired immune deficiency syndrome (AIDS), malaria, and tuberculosis are listed up. More than half of deaths in low-income countries were due to communicable diseases, maternal causes, conditions arising during pregnancy and childbirth, and nutritional deficiencies, while such causes shared less than 7% of deaths in high-income countries [1]. It is no double to say that the detection of infectious agents in the lesion is essential for the histopathological diagnosis of infectious diseases [2, 3]. For the correct diagnosis and appropriate treatment of the patient, immunohistochemical demonstration of pathogens within the lesion must be suitable and desirable [4–10].

Needless to say, the most important factor, the "life," in the immunohistochemical analysis should be a high-specificity antibody for exactly demonstrating the corresponding antigen. A variety of immunohistochemical techniques for

increasing the sensitivity of detection have been developed, in order to localize the antigens under highly specific and highly sensitive conditions in routinely processed (formalin-fixed, paraffin-embedded) sections [11–13]. Immunohistochemical approach is quite fitted to the histopathological diagnosis of infectious diseases, since the antigens of the pathogen are absent from the human tissue specimens [4, 7–10].

However, pathogens express multiple antigens, and the antigens are often cross-reactive among different pathogens [14]. The pathogen in a single category further reveals a variety of serum types [15]. It is more difficult for us pathologists than expected to detect a certain pathogen using a single antibody [4, 7]. It is next to impossible to prepare and keep specific antibodies in hand for immunohistochemical diagnosis in a single institution simply because there are too many species of microbes pathogenic to humans. We have a limited number of commercially available antibodies against pathogens. Useful commercial antibodies may soon disappear from the market because of a simple reason: the dead stock [16].

In the routine practice of histopathological services using hematoxylin and eosin (H&E) staining, it is often the situation that the pathologists are requested to judge if the lesion is infective or not. Namely, the presence of some sort of pathogenic organisms within the lesion should be shown with the maximal priority in making the diagnosis, and the detailed identification of the species name should be analyzed using different technologies afterward. For example, if a lesion showing massive necrosis is experienced, we must comment that the necrosis is infective in origin or tumor-related. In such a situation, an antibody widely cross-reactive to bacteria but unreactive to human tissue is valuable. A monoclonal antibody H9 (a gift of Prof. Shigeru Kamiya, Department of Microbiology, Kyorin University School of Medicine, Mitaka, Tokyo) against bacteria-specific heat shock protein (HSP)-60, not cross-reactive animal mitochondrial HSP-60, is quite valuable [7, 17], but it is not commercially available. Lipopolysaccharide (LPS) or endotoxin, located in the outer layer of the bacterial wall, should be the good marker of Gram-negative bacteria (refer to **Figure 11**) [18], but it is practically difficult for us to get a monoclonal or polyclonal antibody detecting widely cross-reactive LPS.

In order to visualize pathogens in formalin-fixed, paraffin-embedded sections, we do not necessarily need to prepare antibodies with high specificity [4, 7, 19]. The author routinely uses four kinds of commercially available rabbit antisera raised against *Bacillus Calmette-Guérin* (BCG; *Mycobacterium bovis*), *Bacillus cereus* (*B. cereus*), *Treponema pallidum* (*T. pallidum*), and *Escherichia coli* (*E. coli*) [16, 19]. For immunoperoxidase staining, the amino acid polymer technique or indirect immunoperoxidase method is employed. Immunostaining using these low-specificity antimicrobial antisera commonly yields clear high-sensitivity signals with low background, because of poor cross-reactivity of bacterial antigens to human cells and tissues.

The second approach for detecting unknown pathogens in the histopathological sections is the use of patient's serum [4, 7, 8, 20–23]. Patients' sera diluted at 1:500 or 1:1000 become convenient probes for indirect immunoperoxidase localization of pathogens in formalin-fixed, paraffin-embedded sections, particularly when cellular tissue reactions have been confirmed under the microscope. Serum antibody titer should be high in the recovery or chronic stage of illness. The existence of inflammatory tissue reaction, such as an abscess or granuloma, indicates that immune cells in the patient have been activated against the causative pathogen. The second approach is of high value for protozoan and helminthic disorders.

2. Commercially available antibodies against pathogens: the author's experience

In **Table 1**, commercially available antibodies against pathogens are listed up, simply for the convenience of the readers. The catalog is solely based on the author's experience, so that the antibodies may not be most suitable for detecting pathogens in routinely prepared sections [8, 19]. Some antibodies may be no longer available, simply because of limited market. The specificity of the antibodies is categorized

Pathogen	Type (clone)	Company	Dilution	Pretreatment	Specificity
Antibacterial antibody					
<i>Actinomyces</i>	Mo (396AN1)	DSHB	1:5	CB6	High
<i>Bacillus cereus</i>	Rabbit	Abcam	1:500	CB6	Low
<i>Bartonella henselae</i>	Mo (H2A10)	Biocare	1:100	EDTA	High
BCG	Rabbit	Dako	1:5000	None	Low
<i>Campylobacter jejuni</i>	Mo (4080)	Novocastra	1:50	CB6	Moderate
<i>Chlamydia trachomatis</i>	Mo (B104.1)	Biomedica	1:5	CB6	High
<i>Escherichia coli</i>	Rabbit	Dako	1:20,000	PK	Low
<i>E. coli</i>	Mo (MAB706)	Millipore	1:50	CB6	High
<i>E. coli</i> (LPS)	Mo (2D7/1)	Abcam	1:5000	CB6	Moderate
<i>Enterococcus</i>	Rabbit	Abcam	1:2000	None	Moderate
<i>Helicobacter pylori</i>	Rabbit	Dako	1:50	PK	Moderate
<i>Helicobacter pylori</i>	Mo (UCL3R)	Novocastra	1:100	EDTA	High
<i>Klebsiella pneumoniae</i>	Mo (70–2)	Monosan	1:300	None	High
<i>Legionella pneumophila</i>	Rabbit	Denka Seiken	1:500	EDTA	High
<i>Mycobacterium tuberculosis</i>	Mo (MAB738)	Chemicon	1:3000	EDTA	High
<i>M. tuberculosis</i> (MPT64)	Rabbit	Abcam	1:800	CB6	High
<i>Pneumococcus</i>	Mo (128/390)	Chemicon	1:1000	None	Moderate
Pneumolysin	Mo (9.1/2/3/6)	Novocastra	1:50	EDTA	High
Protein A	Mo (SPA-27)	Sigma	1:100	PK	Moderate
Protein G	Rabbit	Abcam	1:500	PK	Moderate
<i>Pseudomonas aeruginosa</i>	Mo (B11)	Biogenesis	1:800	EDTA	High
<i>Staphylococcus</i>	Mo (STAPH11–248.2)	Chemicon	1:500	PK	Moderate
<i>Streptococcus</i>	Goat	BioReagents	1:500	PK	Moderate
<i>Treponema pallidum</i>	Rabbit	Biocare	1:1000	EDTA	Low
<i>Treponema pallidum</i>	Mo (J010J)	Thermo	1:50	CB6	High
Antifungal antibody					
<i>Aspergillus</i>	Rabbit	Biocare	1:200	EDTA	Moderate

Pathogen	Type (clone)	Company	Dilution	Pretreatment	Specificity
<i>Aspergillus</i>	Mo (WF-AF-1)	Thermo	1:50	EDTA	High
<i>Candida</i>	Rabbit	Unitika	1:8000	PK	Moderate
<i>Candida</i>	Mo (MaB806)	Chemicon	1:400	Pepsin	High
<i>Cryptococcus</i>	Rabbit	Dako	1:500	None	Moderate
<i>Pneumocystis</i>	Mo (3F6)	Dako	1:100	CB6	High
<i>Rhizopus</i>	Mo (WSSA-RA-1)	Thermo	1:50	CB6	High
Antiviral antibody					
Adenovirus	Mo (M58 + M73)	Abcam	1:400	PK	High
BK virus	Mo (5E6)	Abnova	1:500	CB6	High
Cytomegalovirus	Mo (CCH2 + DDG9)	Dako	1:200	EDTA	High
EB virus (LMP1)	Mo (CS1-CS4)	Dako	1:50	PK	High
EB virus (EBNA2)	Mo (PE2)	Dako	1:100	EDTA	High
Influenza virus A	Mo (1331)	AbD	1:100	PK	High
Influenza virus A	Mo (1A52.9)	Acris	1:100	PK	High
Influenza virus B	Guinea pig	Denka Seiken	1:100	EDTA	High
HBs antigen	Goat	Bioss	1:2000	PK	High
HBs antigen	Mo (HB-024)	Japan Biotest	1:500	None	High
HBc antigen	Rabbit	Dako	1:15,000	EDTA	High
HBe antigen	Mo (BE-05)	Institute of Immunology	1:50	PK	High
HCV (NS3-NS4)	Mo (Tordji-22)	Signet	1:200	EDTA	High
HCV (NS3)	Mo (MMM33)	Novocastra	1:100	CB7	High
HCV (NS4)	Mo (5D4-10E7)	Abcam	1:300	EDTA	High
HCV (NS5a)	Mo (7-D4)	Fitzgerald	1:100	EDTA	High
HCV (core)	Mo (Aa70-Aa90)	Chemicon	1:100	EDTA	High
Herpes simplex virus-1	Rabbit	Dako	1:500	None	Moderate
Herpes simplex virus-2	Rabbit	Dako	1:1500	None	Moderate
HIV (p24)	Mo (kal-1)	Dako	1:1000	EDTA	High
HPV	Mo (K1H8)	Dako	1:500	CB6	High
HPV16	Mo (CamVir-1)	BioGenex	1:5000	EDTA	High
JC virus	Rabbit	Dako	1:300	CB7	High
Merkel cell polyomavirus	Mo (CM2B4)	Santa Cruz	1:100	EDTA	High
Measles virus	Rabbit	Novus	1:1000	EDTA	High
Mumps virus	Mo (MAB846)	Chemicon	1:400	EDTA	High
Norovirus (GII/4)	Rabbit	Denka Seiken	1:500	None	High
Parvovirus B19	Mo (R92.2.8)	Novocastra	1:1000	EDTA	High
RS virus	Mo (603705)	Novocastra	1:200	EDTA	High

Pathogen	Type (clone)	Company	Dilution	Pretreatment	Specificity
SV40 (T-antigen)	Mo (PAb416)	Millipore	1:100	EDTA	High
VZV	Mo (C90.2.8)	Novocastra	1:100	None	High
Antiprotozoan antibody					
<i>Toxoplasma gondii</i>	Rabbit	Abcam	1:200	CB6	High

Abbreviations: Mo, monoclonal antibody; PK, proteinase K; CB6, citrate buffer at pH 6 (heating); CB7, citrate buffer at pH 7 (heating); EDTA, ethylenediaminetetraacetic acid at pH 8 (heating); DSHB, Developmental Studies Hybridoma Bank; BCG, Bacillus Calmette-Guérin; EB, Epstein-Barr; HB, hepatitis B; HCV, hepatitis C virus; HIV, human immunodeficiency virus; HPV, human papillomavirus; RS, respiratory syncytial; SV40, simian virus 40; VZV, varicella-zoster virus

Antimicrobial antibodies the author is using are listed up for the readers' convenience.

Table 1.
 List of commercially available antibodies against pathogens: the author's experience.

into three grades: high, moderate, and low. Even when we use the high-specificity antibody for immunostaining, careful judgment is requested for the final identification of the causative microbe.

3. Application of commercially available antisera against BCG, *B. cereus*, *T. pallidum*, and *E. coli*

Immunoperoxidase application using four kinds of commercially available rabbit antisera raised against BCG, *B. cereus*, *T. pallidum*, and *E. coli* is described [4, 7, 8, 16, 19]. In this section, immunostaining application to mycobacterial infection, *B. cereus* pneumonia, syphilitic lesions, and *E. coli* infections is described. Although the specificity of the antisera is low, as described below, the respective causative pathogens were clearly demonstrated within the lesions.

3.1 Immunostaining for mycobacterial infections using BCG antiserum

Indirect immunoperoxidase staining using BCG rabbit antiserum (Dako/Agilent Technologies) diluted at a 1:5000 was highly sensitive for detecting mycobacteria in histopathological sections [4, 7, 8, 24, 25]. No pretreatment for antigen retrieval was given. Mycobacterial antigens were clearly demonstrable not only in caseous necrosis in active tuberculosis but also in a fibrous nodule of old calcified tuberculosis (**Figure 1**). BCG antigens were scarcely detectable in epithelioid granulomas. The BCG immunostaining was much more sensitive to detect mycobacteria than conventional acid-fast (Ziehl-Neelsen) staining, as indicated in **Table 2** [4, 24]. In BCG immunostaining, the judgment of positivity can be done easily and quickly, while it takes minutes or longer in case of conventional acid-fast staining. It is evident that the antiserum is reactive with mycobacterial antigenic substances on destroyed bacterial fragments. The BCG immunostaining was also applicable to demonstrating non-tuberculous mycobacteria and *Mycobacterium leprae*. **Figure 2** illustrates positive findings in opportunistic *Mycobacterium avium-intracellulare* (MAI) infection in AIDS and in lepromatous (multibacillary) leprosy in a biopsied skin lesion. No positivity was seen in tuberculoid (paucibacillary) leprosy.

The BCG antigens were extremely stable after prolonged fixation in formalin for a long period of time [19, 26]. **Figure 3** displays dense-positive signals in an exudative pulmonary tuberculosis lesion fixed in formalin for nearly 70 years.

3.2 Immunostaining for *B. cereus* pneumonia using *B. cereus* antiserum

B. cereus pneumonia is characterized by a lethal necrotic and hemorrhagic lesion infrequently seen in an immunocompromised or immunocompetent patient [27]. The autopsied lung was obtained from a female aged 60's long suffering from chronic lymphoplasmacytic leukemia. Gram-positive bacilli with spore formation

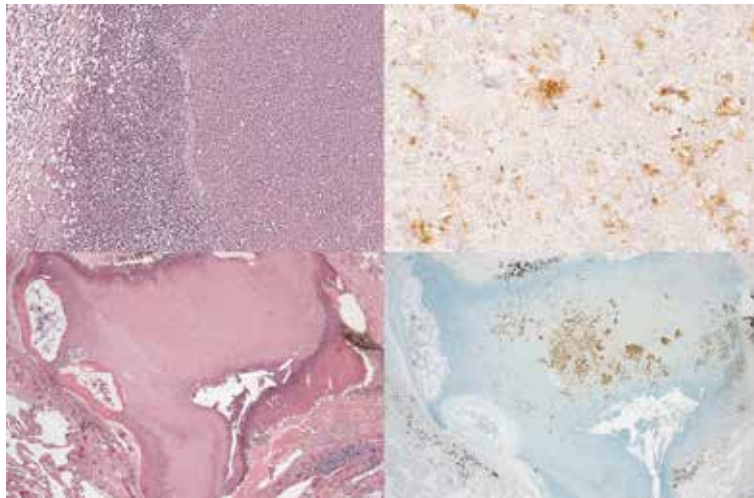


Figure 1. BCG immunostaining I (upper panels, cerebral tuberculoma; lower panels, old calcified nodule in the lung; left, H&E; right, BCG immunostaining). Mycobacterial antigens were clearly demonstrable not only in caseous necrosis but also in a fibrous nodule of old tuberculosis. Mycobacterial antigenic substances on destroyed bacterial fragments are detectable by the antiserum.

Disease	Acid-fast staining	BCG immunostaining
Tuberculosis		
Exudative lesion	5/6 (83%)	6/6 (100%)
Caseous granuloma	3/11 (27%)	5/11 (45%)
Non-caseous granuloma	0/6 (0%)	1/6 (17%)
Encapsulated caseous focus, non-calcified	0/9 (0%)	5/9 (56%)
Encapsulated caseous focus, calcified	0/11 (0%)	8/11 (73%)
Fibrous focus, calcified	0/1 (0%)	1/1 (100%)
<i>Total</i>	<i>8/44 (18%)</i>	<i>26/44 (59%)</i>
Leprosy		
Lepromatous leprosy (multibacillary form)	2/2 (100%)*	2/2 (100%)
Tuberculoid leprosy (paucibacillary form)	0/3 (0%)	0/3 (0%)
Sarcoid-type granuloma		
Sarcoidosis	0/7 (0%)	0/7 (0%)
Sarcoid-like reaction in lymph node	0/3 (0%)	0/3 (0%)

*Fite modification employing oil-xylene for deparaffinization required.
Acid-fast staining and BCG immunostaining were compared using three types of granulomatous lesions embedded in paraffin.

Table 2. Comparative detectability of mycobacteria with acid-fast staining and immunostaining for BCG antigens.

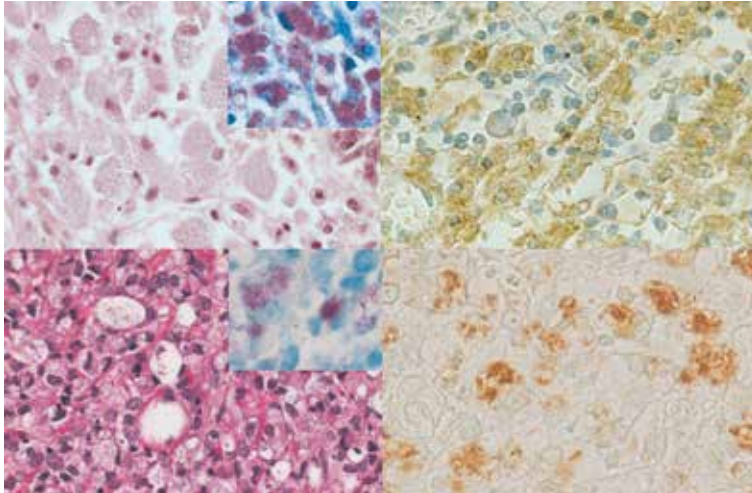


Figure 2. BCG immunostaining II (upper panels, non-tuberculous mycobacterial lymphadenitis in AIDS; lower panels, lepromatous leprosy; left, H&E; right, BCG immunostaining; inset, acid-fast staining). Striated histiocytes in *Mycobacterium avium-intracellulare* (MAI) infection in AIDS and globi in lepromatous (multibacillary) leprosy in a biopsied skin lesion are strongly labeled. Fite modification of acid-fast staining is requested for demonstrating *M. leprae*.

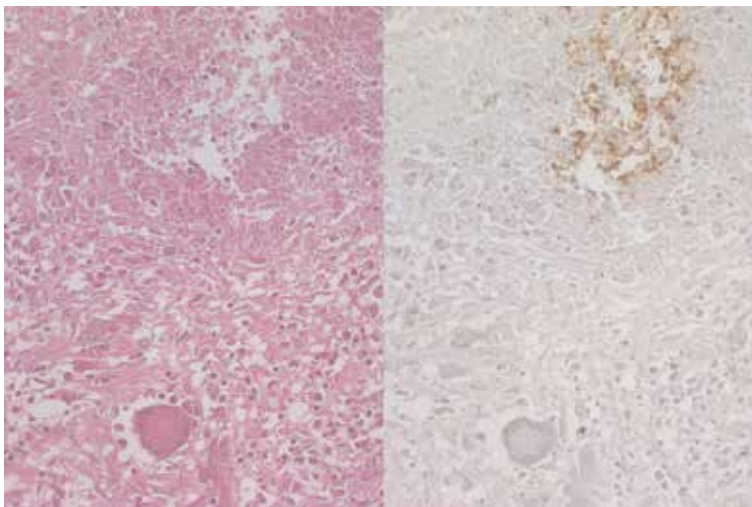


Figure 3. BCG immunostaining III (left, HE; right, BCG immunostaining). BCG antigens are very stable against fixation. Dense-positive signals are seen in a pulmonary exudative tuberculosis lesion fixed in formalin for 70 years. Of note is that the nuclei are poorly stained with hematoxylin due to prolonged fixation.

were multifocally clustered in the necrohemorrhagic lesion. Immunostaining (the amino acid polymer method, Simple Stain-Max, Nichirei, Tokyo, Japan) using *B. cereus* rabbit antiserum (Abcam) diluted at 1:500 after heat-induced antigen retrieval in 10 mM citrate buffer, pH 6, demonstrated positive signals on the spore of the bacilli (**Figure 4**) [8, 19, 28]. Similar findings were obtained in case of opportunistic soft tissue gangrene caused by *B. cereus* [9].

3.3 Immunostaining for syphilitic lesions using *T. pallidum* antiserum

Warthin-Starry's silver method is technically difficult, frequently with a false-negative result in case of treponemal infection. In contrast, immunostaining

(Simple Stain-Max, Nichirei) using *T. pallidum* rabbit antiserum (Biocare) diluted at 1:1000, after heat-induced antigen retrieval in 1 mM EDTA solution, pH 8, is highly sensitive and reproducible in demonstrating long coiled microbes among the lesion [4, 7–10, 19]. **Figure 5** illustrates a neck skin papule richly infiltrated by plasma cells, biopsied from a middle-aged Japanese male patient in a remission state of malignant lymphoma 2 years after chemotherapy. Clinicians suspected of skin recurrence of malignancy, but immunostaining clearly demonstrated dense infection of coiled bacteria in the epidermis. Plasma cell-rich appearance microscopically suggested the possibility of syphilis, and thus immunostaining for *T. pallidum* was

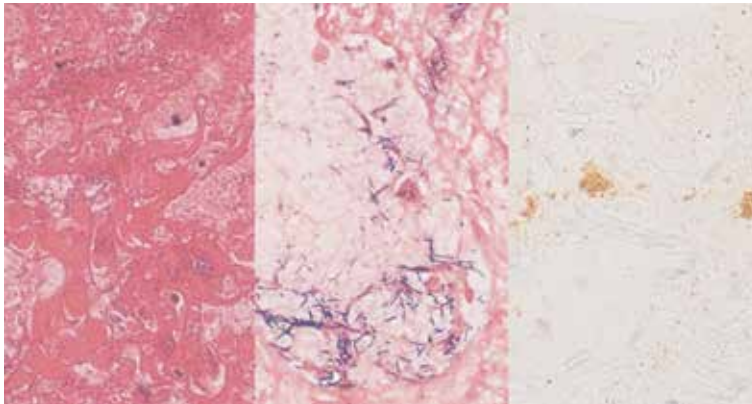


Figure 4. Lethal *B. cereus pneumonia* (left, H&E; center, Gram stain; right, immunostaining using *B. cereus* rabbit antiserum). Gram-positive rods are clustered in the necrohemorrhagic lung tissue, and *B. cereus* antigens are localized in the spore of the bacteria.

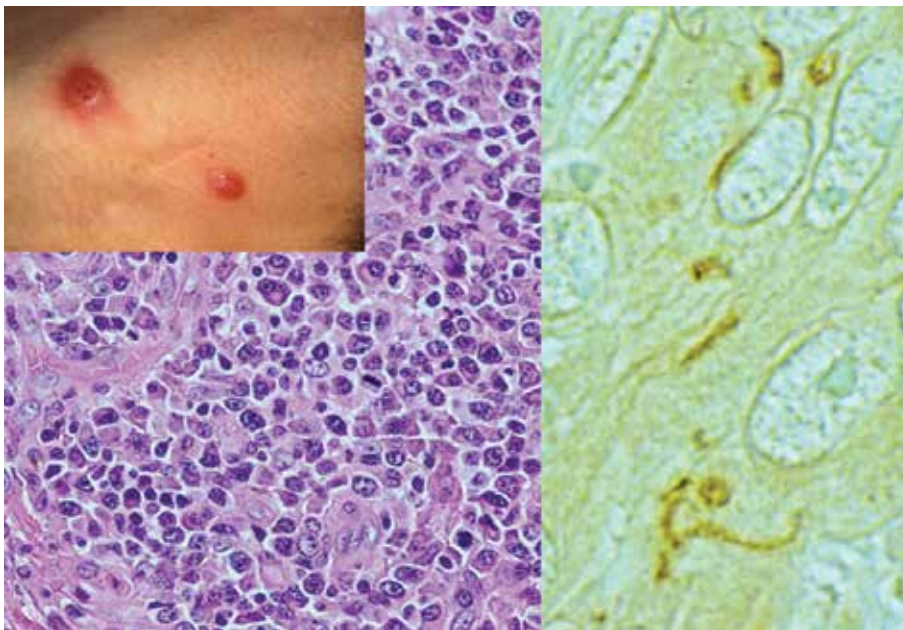


Figure 5. *T. pallidum* immunostaining I (left, H&E; right, immunostaining using *T. pallidum* antiserum; inset, gross appearance of skin eruption on the neck). The papular skin lesion in a middle-aged male is richly infiltrated by plasma cells, and thus the possibility of syphilis was suspected histopathologically. Immunostaining discloses infection of spiral-shaped long bacteria in the epidermis, confirming the diagnosis of clinically unsuspected syphilis.

performed. The diagnosis of stage II syphilis was subsequently confirmed by serological test for syphilis.

In **Figure 6**, a biopsied penile lesion with painless ulceration (chancre) in stage I and excised syphilitic granulomatous lymphadenitis in stage III are presented. In the penis, numerous spiral microbes were clustered mainly in the basal part of the squamous mucosa and around the dermal capillary vessels. In the stage III lesion with granulomatous reaction, coiled spirochetes were infrequently observed.

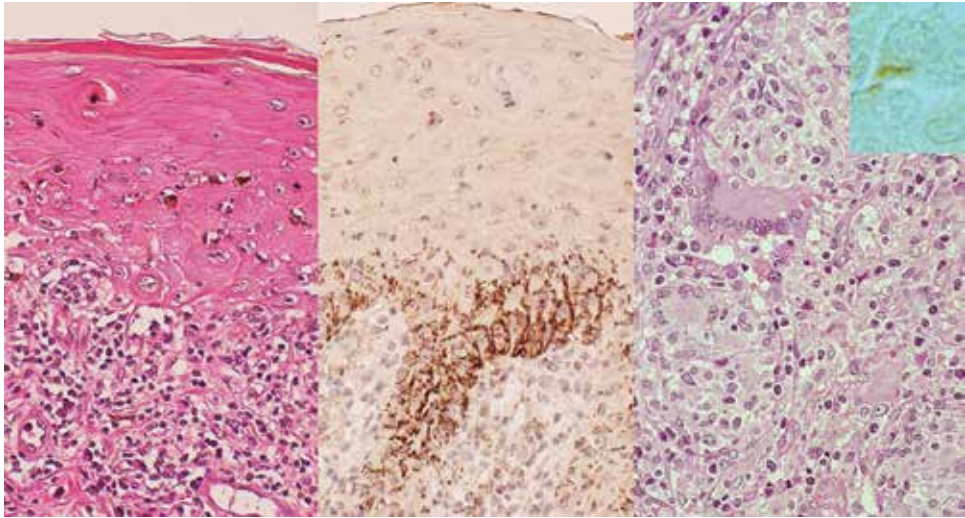


Figure 6. *T. pallidum* immunostaining II (left and center, stage I penile chancre; right, stage III syphilitic lymphadenitis; left and right, H&E; center and inset, immunostaining using *T. pallidum* antiserum). In the penis, numerous spiral microbes are clustered mainly in the basal part of the squamous mucosa and around the dermal capillary vessels. In the stage III lesion accompanying granulomatous reaction with multinucleated giant cells, coiled spirochetes are infrequently identified (inset).

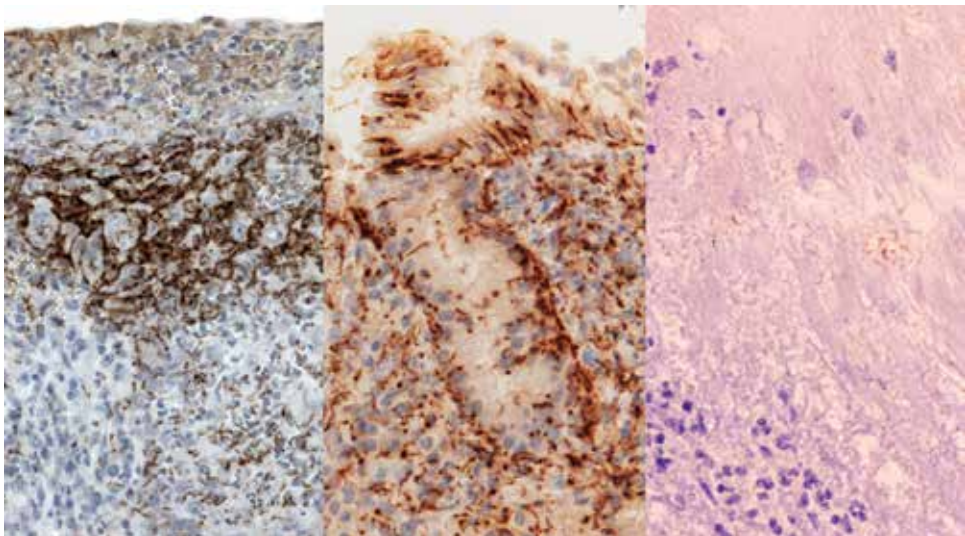


Figure 7. *T. pallidum* immunostaining III (left, tonsil; center, gastric mucosa; right, aortic valve). Immunohistochemical visualization of spirochetes in the biopsy specimens using *T. pallidum* antiserum significantly contributes to confirming the clinical and serological diagnosis of syphilis haphazardly affecting the tonsil, gastric mucosa, and aortic valve.

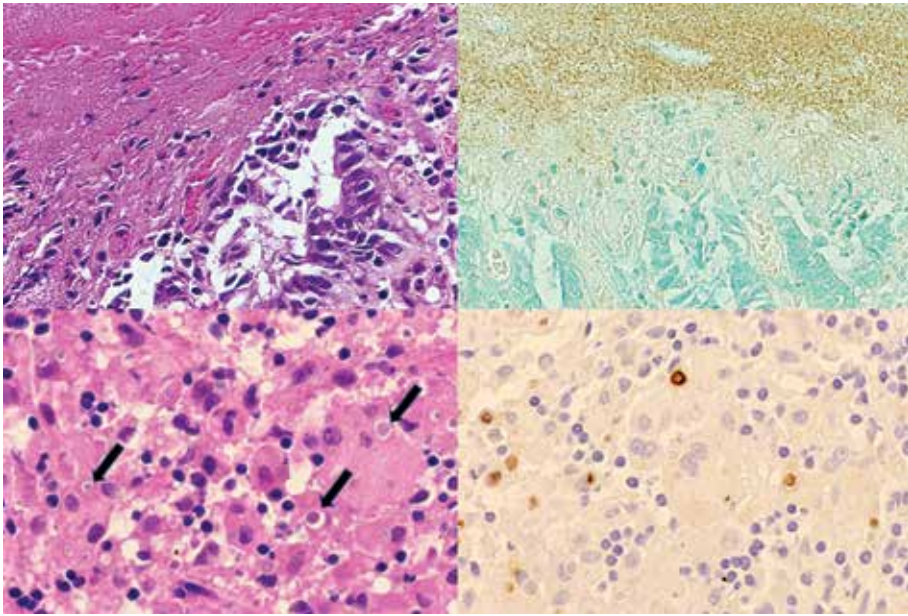


Figure 8. *E. coli* immunostaining I (upper panels, rectal erosion; lower panels, rectal malacoplakia; left, H&E; right, immunostaining using *E. coli* antiserum). *E. coli*-related antigens are detectable in eroded surface of rectal mucosa and in malacoplakia of the rectum. Michaelis-Gutmann bodies (arrows) in the cytoplasm of macrophages, the microscopic hallmark of malacoplakia, are round, basophilic, and immunoreactive to *E. coli* antigens.

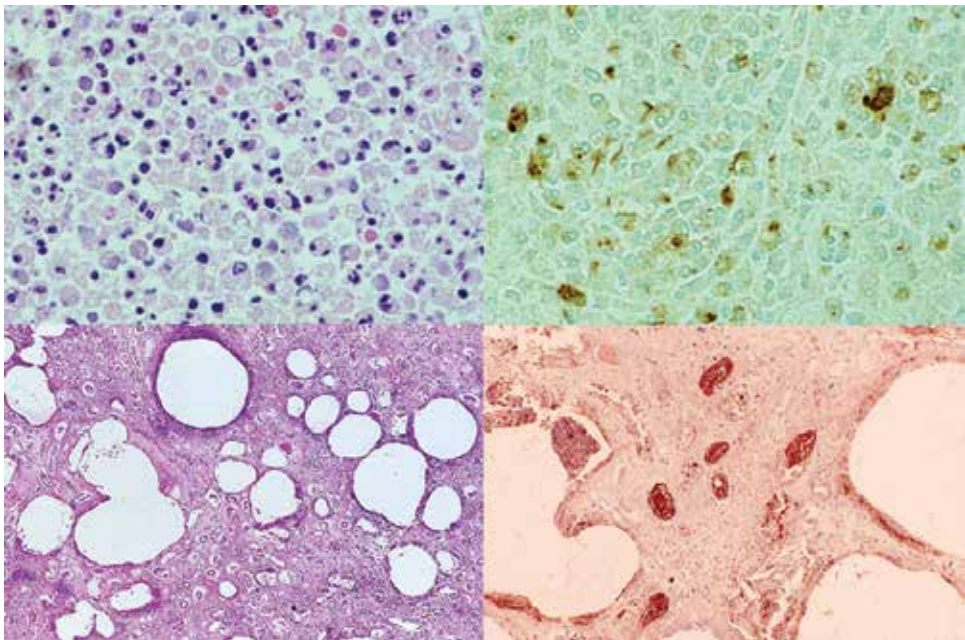


Figure 9. *E. coli* immunostaining II (upper panels, opportunistic *E. coli*-induced pneumonia; lower panels, *E. coli*-induced emphysematous pyelonephritis in a diabetic patient; left, H&E; right, immunostaining using *E. coli* antiserum). Positive rod-shaped signals are clearly seen in the cytoplasm of phagocytes in nosocomial bronchopneumonia and in severely affected kidney with numerous colonies of gas-forming bacteria.

Immunostaining was considerably supportive and useful in the clinical practice, when treponemal microbes were visualized in the tonsillar, gastric, and aortic valvular biopsy specimens (**Figure 7**).

3.4 Immunostaining for infection of *E. coli* and related bacteria using *E. coli* antiserum

Immunostaining (Simple Stain-Max, Nichirei) using *E. coli* rabbit antiserum (Dako) diluted at 1:20,000 after proteinase K pretreatment is applicable to demonstrating infection of *E. coli* or related enterobacteria in paraffin sections. *E. coli*-related antigens were immunodetected in colonic erosion and malacoplakia in the rectal mucosa (**Figure 8**) [4, 7, 8, 10, 28]. Malacoplakia is a variant of xanthogranulomatous inflammation caused by *E. coli*, and Michaelis-Gutmann bodies, a microscopic hallmark of malacoplakia, are immunoreactive for *E. coli* antigens [28]. *E. coli*-like organisms were immunohistochemically detected in xanthogranulomatous proctitis, cholecystitis, and cholangitis, as well as abscess-forming epididymitis [4, 29, 30]. Positive granular signals in *E. coli*-induced bronchopneumonia [31] and emphysematous pyelonephritis are illustrated in **Figure 9**.

4. Immunohistochemical demonstration of bacterial antigens using four kinds of antibacterial antisera with a wide cross-reactivity to a variety of bacteria

We diagnostic pathologists encounter lesions strongly suggestive of infection but with poor clinical information or with difficulty in microscopically supposing a causative pathogen. In such situations, immunostaining employing the abovementioned four kinds of rabbit antisera is worthy of application [8, 19]. We can prove the existence of pathogens in a certain part of the lesion. Background staining is negligible, whereas *B. cereus* antiserum may be cross-reactive to the nuclei of human cells in some cases (see **Figure 16**). In this type of application, we must abandon the specificity of immunostaining, and instead we welcome to accept the sensitivity of detection.

Regrettably enough, the availability of antisera against microbes from commercial sources has become limited. In fact, antisera against BCG and *E. coli* are no longer available from Dako (Agilent) company [16]. The author is afraid that this may hamper the standardization of immunohistochemical diagnosis of infectious diseases.

Table 3 summarizes reactivities of various microbes to the four kinds of rabbit antibacterial antisera.

4.1 *E. coli* antigens in leptospirosis

Hamster liver experimentally infected with *Leptospira interrogans* is shown in **Figure 10**. Not only *Leptospira* antiserum (the gift from Prof. Shinichi Yoshida, Department of Bacteriology, Faculty of Medical Sciences, Kyushu University, Fukuoka) but also *E. coli* antiserum were reactive to spiral-shaped bacteria in the hepatic sinusoid [19]. Pathogens phagocytized by activated Kupffer cells were visualized only by *Leptospira* antiserum [32]. *E. coli* antiserum was not cross-reactive with *T. pallidum* in the syphilitic lesion, while *T. pallidum* antiserum was unreactive with *Leptospira* in the hamster liver.

Bacterium	Anti- <i>B. cereus</i>	Anti-BCG	Anti- <i>T. pallidum</i>	Anti- <i>E. coli</i>
<i>Leptospira interrogans</i>	ND	–	–	+
<i>Serratia marcescens</i>	ND	–	+	+
<i>Brachyspira</i> sp.	+	+	+	+
Non-tuberculous <i>Mycobacterium</i>	ND	+	+	–
<i>Vibrio vulnificus</i>	+	+	+	+
<i>Bordetella pertussis</i>	+	+	+	–
<i>Haemophilus influenzae</i>	+	+	+	–
<i>Actinomyces israelii</i>	+	+	+	–
<i>Nocardia beijingensis</i>	+	+	+	–
<i>Bartonella henselae</i>	ND	+	+	–
<i>Corynebacterium kroppenstedtii</i>	+	+	+	(+)
<i>Klebsiella rhinoscleromatis</i>	+	(+)	–	–
<i>Propionibacterium acnes</i>	+	–	–	–
<i>Pseudomonas aeruginosa</i>	+	–	–	–
Gram-positive cocci causing				
Brain abscess	+	–	–	–
Chorioamnionitis	+	–	–	–

ND, not done, (+), focally positive.

Reactivities of various pathogens to commercial rabbit antisera against *B. cereus*, BCG, *T. pallidum*, and *E. coli* are summarized.

Table 3.
Reactivities of various microbes to the four kinds of rabbit antibacterial antisera.

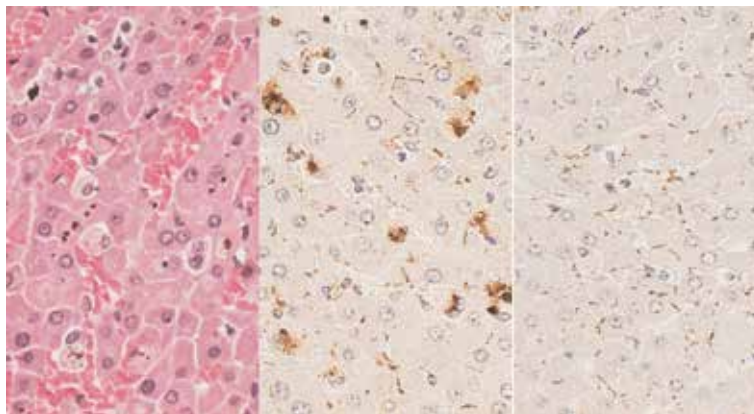


Figure 10.
Hamster liver in experimental leptospirosis (left, H&E; center, *Leptospira* antigens; right, *E. coli* antigens). Liver cell cords are disarranged due to infection of *Leptospira interrogans*. Not only *Leptospira* antiserum but also *E. coli* antiserum decorate spiral-shaped bacteria in the sinusoid. Pathogens phagocytized by activated Kupffer cells are visualized only by *Leptospira* antiserum.

4.2 Application to *Serratia* septicemia

Serratia marcescens, a red colony-forming Gram-negative rod usually showing low virulence, may cause opportunistic infection in immunosuppressed

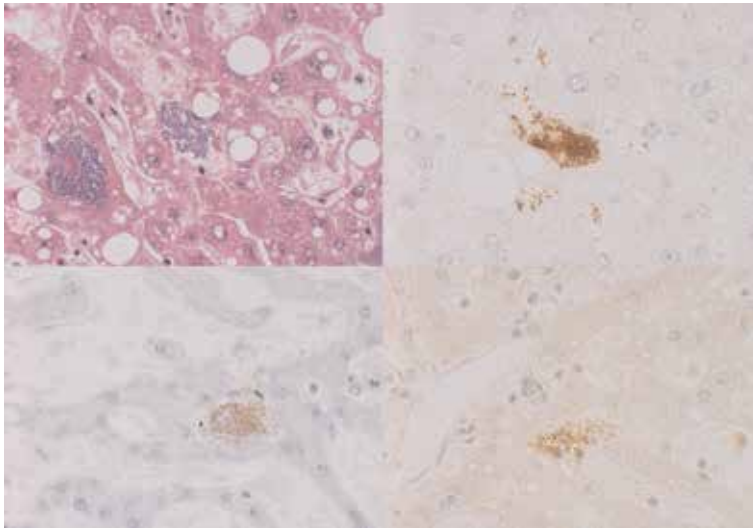


Figure 11. *Serratia marcescens* septicemia forming colonies in the sinusoid of autopsied liver (left upper, H&E; right upper, *E. coli* LPS; left lower, *E. coli* antigens; right lower, *T. pallidum* antigens). Colonies of Gram-negative microbes reveal positivity for both *E. coli* antigens and *T. pallidum* antigens, in addition to strong reactivity to monoclonal antibody 2D7/1 against *E. coli* LPS.

patients [33]. **Figure 11** illustrates the autopsied liver of a Japanese female aged 70's complicated by *S. marcescens* septicemia. Colonies of Gram-negative microbes were observed in the sinusoid of the liver. Comparative immunostaining disclosed positivity for both *E. coli* antigens and *T. pallidum* antigens, in addition to strong reactivity to monoclonal antibody 2D7/1 against *E. coli* LPS (Abcam) [19].

4.3 Application to intestinal spirochetosis

Intestinal spirochetosis is caused by localized infection of *Brachyspira aalborgi* or *B. pilosicoli* on the colonic mucosa. Basophilic brush border-like structures are recognized in H&E-stained sections [34]. It has been clarified that the brush border-like structures by zoonotic *B. pilosicoli* are much longer than those by *B. aalborgi* [35]. The surface-adherent bacteria were clearly visualized by immunostaining with *T. pallidum* monoclonal antibody (J010J), and the spirochete was also proven by immunostaining with antisera against *T. pallidum*, BCG, *E. coli*, and *B. cereus*, as shown in **Figure 12** [13, 19]. Antisera against *Leptospira* and *Helicobacter pylori* also cross-reacted to the pathogen.

4.4 Cross-reactivity to acid-fast bacilli

Non-tuberculous mycobacteria (*Mycobacterium avium-intracellulare*) in a caseous necrotic lesion of the lung were demonstrated not only by BCG antiserum but also by *T. pallidum* antiserum, as illustrated in **Figure 13** [19]. BCG antiserum was also strongly reactive with amorphous background substances, probably representing decayed bacterial proteins.

4.5 Application to *Vibrio vulnificus* infection

Gangrenous lesions in the extremity caused by lethal *Vibrio vulnificus* infection (flesh-eating disease) microscopically show active growth of Gram-negative

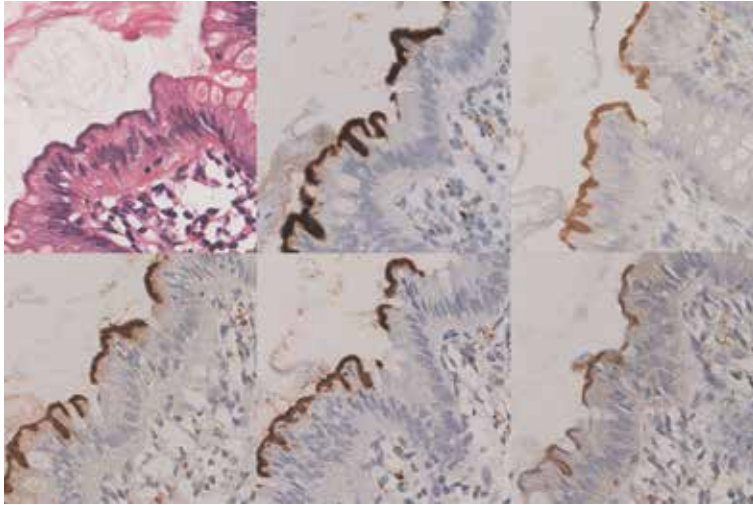


Figure 12. Intestinal spirochetosis (left upper, H&E; center upper, reactivity with *T. pallidum* monoclonal antibody Jo10]; right upper, reactivity with *T. pallidum* antiserum; left lower, BCG antigens; center lower, *E. coli* antigens; right lower, *Leptospira* antigens). The colonic mucosal surface-adherent, brush border-like basophilic bacteria (*Brachyspira aalborgi*) are visualized by monoclonal and polyclonal antibodies to *T. pallidum*, as well as by immunostaining with antisera to BCG, *E. coli*, and *Leptospira*.

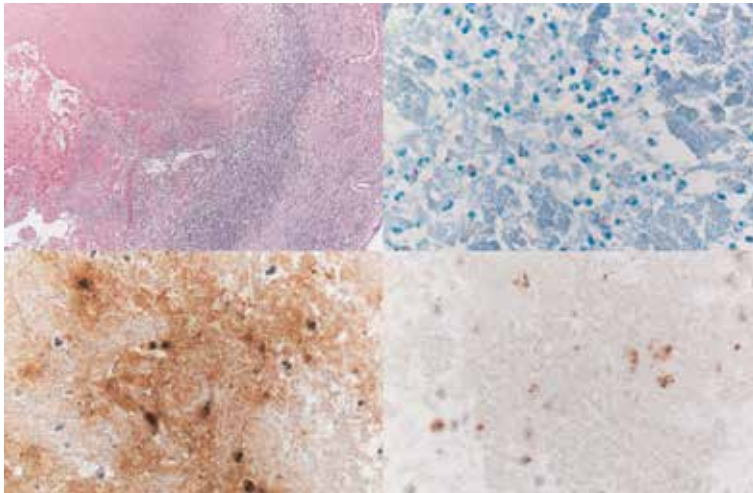


Figure 13. Non-tuberculous mycobacteriosis of the lung caused by *Mycobacterium avium-intracellulare* (left upper, H&E; right upper, acid-fast stain; left lower, BCG antigens; right lower, *T. pallidum* antigens). Acid-fast bacilli seen in caseous necrosis are labeled with both antisera. BCG antiserum also strongly reacts with background degradative substances.

bacteria in soft tissue [36]. The bacteria were immunolocalized with antisera against BCG, *B. cereus*, and *T. pallidum* (**Figure 14**) [8, 19]. *E. coli* antiserum was scarcely reactive.

4.6 Application to pertussis

Bordetella pertussis infection (pertussis) may cause severe illness leading the child to death [37]. The lung shows microscopic features of “atypical” pneumonia. The Gram-negative bacteria phagocytized by macrophages in alveoli of the autopsied

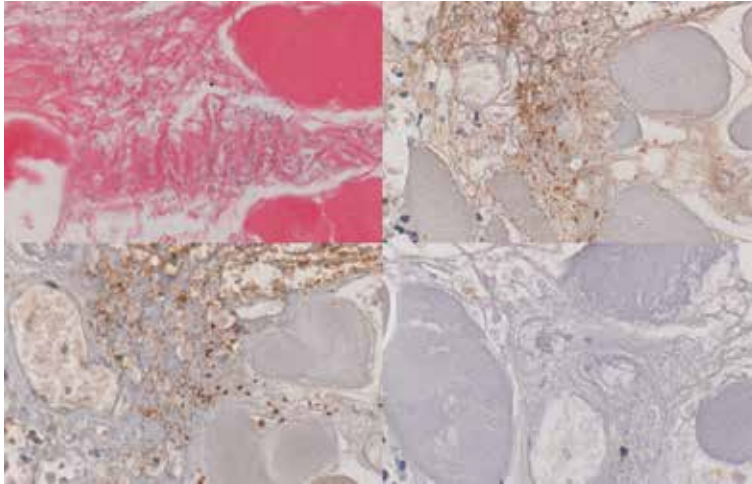


Figure 14. Gangrene of the extremity caused by *Vibrio vulnificus* infection (left upper, H&E; right upper, BCG antigens; left lower, *T. pallidum* antigens; right lower, *E. coli* antigens). Gram-negative bacteria growing among necrotic striated muscle fibers in the extremity are immunolocalized with antisera against BCG and *T. pallidum*. *E. coli* antiserum is scarcely reactive.

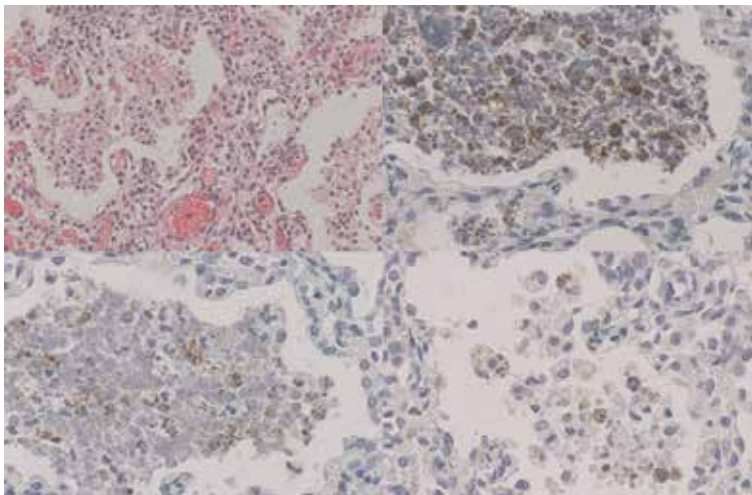


Figure 15. Autopsied lung in pertussis (left upper, H&E; right upper, BCG antigens; left lower, *B. cereus* antigens; right lower, *T. pallidum* antigens). The lung shows microscopic features of atypical pneumonia. *Bordetella pertussis* phagocytized by alveolar macrophages is demonstrable with antisera against BCG, *B. cereus*, and *T. pallidum*.

lung were positively immunostained with antisera against BCG, *B. cereus*, and *T. pallidum* (**Figure 15**) [19]. *E. coli* antiserum was scarcely reactive.

4.7 Application to *Haemophilus influenzae* infection

Haemophilus influenzae may cause tonsillar ulcer in children and young adults [38]. A biopsy material from the ulcerated tonsil of a young male revealed dense infection of Gram-negative rods on the ulcer base. Antisera against BCG, *B. cereus*, and *T. pallidum* demonstrated the pathogen (**Figure 16**) [19]. Again, *E. coli* antiserum was scarcely reactive.

4.8 Application to actinomycosis

Secondary dense infection of *Actinomyces israelii* is occasionally observed in biopsied sequestrum of the alveolar bone of the jaw [39]. Grocott-positive filamentous bacteria occupy the marrow space but with little inflammatory reaction. The microbes were visualized not only with *A. israelii* monoclonal antibody (396AN1) but also with antisera against BCG and *B. cereus* (**Figure 17**) [19]. Reactivity with antisera against *T. pallidum* and *E. coli* was faint.

4.9 Application to nocardiosis

Nocardiosis is caused by filamentous Gram-positive saprophytic bacteria, *Nocardia* spp., mainly in the lung. This weakly acid-fast aerobe infects mainly in the immunocompromised patients. *N. asteroides* is the most frequent isolate, but other species may also be encountered [40]. A subpleural nodule in the left upper lobe



Figure 16. Haemophilus influenzae-induced tonsillitis (left, H&E; center left, *B. cereus* antigens; center right, BCG antigens; right, *T. pallidum* antigens). Antisera against *B. cereus*, BCG, and *T. pallidum* demonstrate *H. influenzae* colonizing the tonsillar ulcer. *B. cereus* antigens are expressed with the strongest reactivity, while cross-reactivity to the nucleus of human cells is seen.

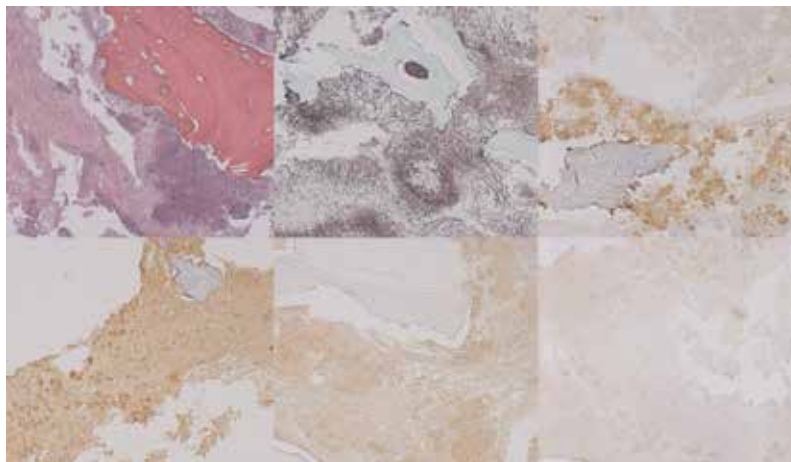


Figure 17. *Actinomyces israelii* colonizing the sequestration of the jaw bone (left upper, H&E; center upper, Grocott stain; right upper, reactivity with *A. israelii* monoclonal antibody 396AN1; left lower, *B. cereus* antigens; center lower, BCG antigens; right lower, *T. pallidum* antigens). The marrow space among dead bone trabeculae is occupied by Grocott-positive filamentous bacteria but with little inflammatory reaction. The pathogen is immunolocalized not only by the monoclonal antibody but also by antisera against *B. cereus* and BCG. *T. pallidum* antigens are scarcely expressed.

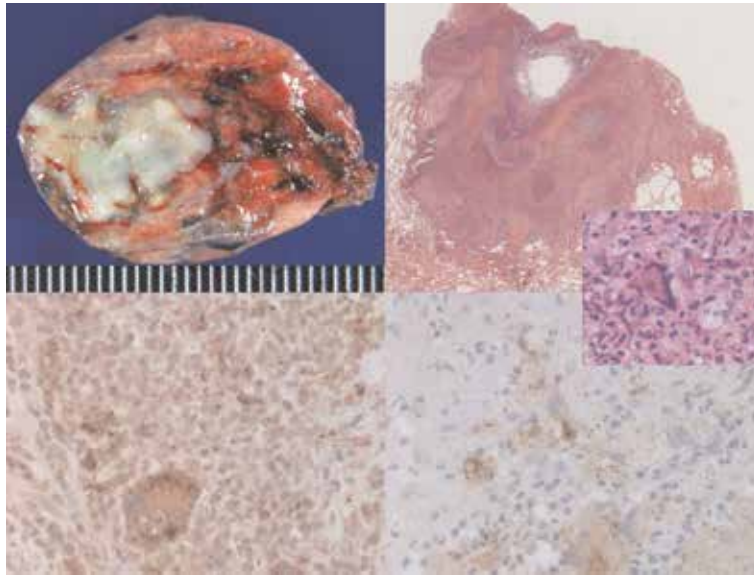


Figure 18. Pulmonary nocardiosis caused by *Nocardia beijingensis* (left upper, gross picture; right upper, low-powered H&E; inset, high-powered H&E; left lower, *B. cereus* antigens; right lower, BCG antigens). Subpleural abscess seen in a diabetic aged with steroid therapy was surgically excised. Necrotic lesions reveal focal clusters of foamy macrophages and a few multinucleated giant cells. Grocott stain failed to identify the pathogen. Antisera against *B. cereus* and BCG clearly demonstrate filamentous and aggregated microbes in the cytoplasm of foamy macrophages and giant cells.

was pointed out in a diabetic Japanese male aged 70's who also suffered from nephrotic syndrome with steroid administration. Video-assisted thoracic surgery disclosed necrotic nodule grossly resembling a tuberculous lesion. Microscopically, abscess formation with foamy cells clustering and occasional multinucleated giant cell reaction was confirmed, and *N. beijingensis* was isolated and molecularly confirmed by analyzing 16S ribosomal RNA. Grocott, periodic acid-Schiff, Gram, and Ziehl-Neelsen stains were all negative. Immunostaining using antisera against *B. cereus* and BCG clearly demonstrated filamentous or aggregated bacteria phagocytized by foamy cells and multinucleated giant cells (**Figure 18**). Some bacteria reacted to *T. pallidum* antiserum, while *E. coli* antiserum was unreactive.

4.10 Application to bartonellosis

Cervical lymphadenopathy in cat-scratch disease, infection of *Bartonella henselae*, is microscopically characterized by suppurative granuloma formation. Not only cat scratch but also bite by cat flea can provoke bartonellosis [41]. Splenic abscess is occasionally seen as systemic manifestation of cat-scratch disease [42]. Splenectomy was performed from a male patient aged 40's. Monoclonal antibody H2A10 to *B. henselae* (not cross-reactive to non-henselae *Bartonella*) [41] demonstrated a few microbes in the cytoplasm of macrophages accumulated in the abscess cavity. The positive findings were more easily obtained by immunostaining with antisera against BCG and *T. pallidum* (**Figure 19**) [19].

4.11 Application to granulomatous mastitis

Granulomatous mastitis is seen in childbearing women 2–4 years after breastfeeding [43]. The causative agent is lipophilic Gram-positive bacillus,

Corynebacterium kroppenstedtii, and the lesion is microscopically featured by lipid droplet-centered abscess or epithelioid granuloma. Antisera against BCG, *B. cereus*, and *T. pallidum* demonstrated bacterial cross-reactive antigens mainly in the lipid droplet surrounded by abscess and/or granuloma (**Figure 20**) [8, 16, 19]. The antigens were occasionally seen in the cytoplasm of macrophages clustered in the inflammatory lesion. *E. coli* antigens were infrequently seen in the lesion.

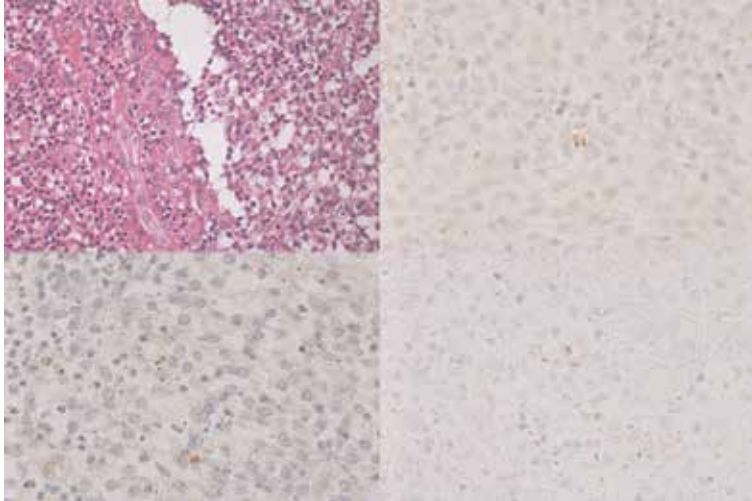


Figure 19. Splenic bartonellosis (left upper, H&E; right upper, reactivity with *Bartonella henselae* monoclonal antibody H2A10; left lower, BCG antigens; right lower, *T. pallidum* antigens). Suppurative granulomas are formed in the spleen. Macrophages in the abscess cavity focally reveal dot-like positive signals not only by the monoclonal antibody but also by antisera against BCG and *T. pallidum*. Of note is that more signals are seen with the two antisera than with the monoclonal antibody.

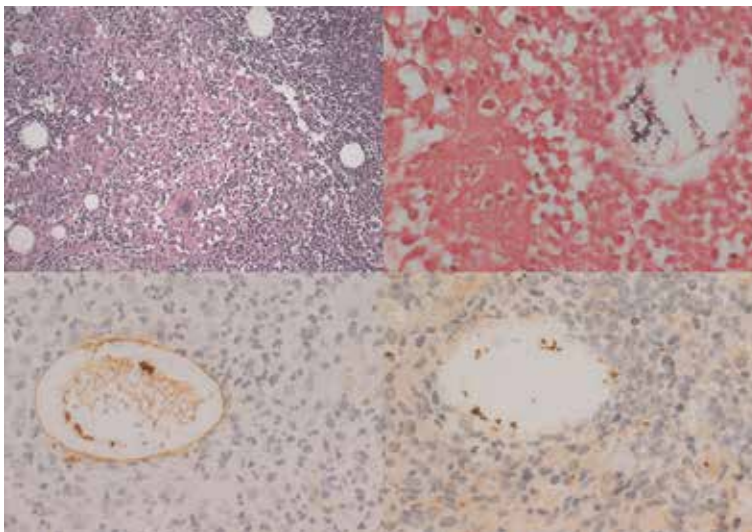


Figure 20. Granulomatous mastitis caused by *Corynebacterium kroppenstedtii* (left upper, H&E; right upper, Gram stain; left lower, BCG antigens; right lower, *T. pallidum* antigens). This lactation-related infection is microscopically featured by lipid droplet-centered abscess or epithelioid granuloma. Gram stain and immunostaining for BCG, *B. cereus*, and *T. pallidum* demonstrate bacterial colonies in the lipid droplet surrounded by inflammatory reactions.

It should be of note that the positive signals were identified at the site of the disease-specific lesion. Polymerase chain reaction (PCR) analysis using DNA extracted from paraffin sections confirmed the nucleotide sequence of *C. kroppenstedtii* [16].

4.12 Application to rhinoscleroma

Rhinoscleroma is localized and indolent infective nodule in the nasal cavity, endemic in Egypt, South America and eastern Europe. The main causative microbe has been reported to be *Klebsiella rhinoscleromatis*. Microscopically, foamy macrophages phagocytizing gram-negative rods, so-called Mickulicz cells, are observed in chronic inflammatory infiltrates [44]. A Japanese male aged 70's complained of a single elevated nodule in the nasal vestibule. Biopsy revealed localized infiltration of foamy macrophages in the background of chronic inflammation. Round vacuoles with short rod-like material were occasionally seen in the macrophages or Mickulicz cells [45]. Immunostaining disclosed positive findings with monoclonal antibody 70-2 against *Klebsiella* spp., and the antiserum against *B. cereus* gave similar positivity. Fewer cells were also reactive to BCG antiserum. Antisera against *T. pallidum* and *E. coli* failed to detect the intracellular microbes (**Figure 21**). Negativity to *E. coli* antiserum was an unexpected finding, because of the close relationship between the two enterobacteria.

4.13 Immunostaining with *B. cereus* antiserum showing the widest cross-reactivity among four

In certain lesions, *B. cereus* antiserum was reactive to the pathogen, while the other three antisera were poorly reactive. It is plausible that antiserum against *B. cereus*, a Gram-positive spore-forming rod, shows the widest cross-reactivity including Gram-positive bacteria. Bacterial microbes positive for *B. cereus*-related antigens were demonstrated in brain abscess, placental chorioamnionitis, and *Propionibacterium acnes*-induced folliculitis of the skin (**Figure 22**) (refer also to **Figure 45** for *P. acnes* folliculitis). Positive signals of *B. cereus* antigens in a lethal adult case of *Pseudomonas aeruginosa*-induced pneumonia/septicemia are demonstrated in **Figure 23** [19].



Figure 21. Rhinoscleroma caused by *Klebsiella rhinoscleromatis* (left upper: H&E, right upper: reactivity with monoclonal antibody 70-2 to *Klebsiella* spp., left lower: *B. cereus* antigens, right lower: *E. coli* antigens, inset: BCG antigens). Foamy macrophages with intracytoplasmic vacuoles containing short rod-like material (Mickulicz cells) are immunoreactive with monoclonal antibody 70-2 to *Klebsiella* spp. and *B. cereus* antiserum. Fewer cells are labeled with BCG antiserum, while *E. coli* antiserum is unreactive.

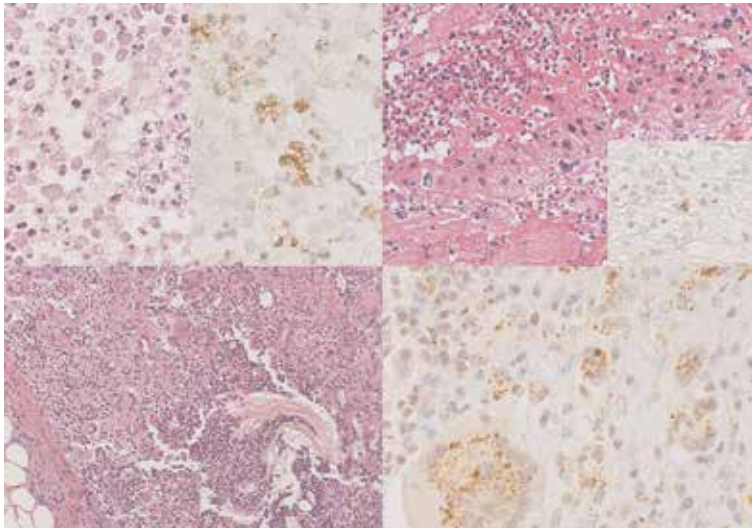


Figure 22. The widest cross-reactivity shown by *Bacillus cereus* antiserum (left upper, brain abscess; right upper, ascending chorioamnionitis of placenta; lower panels, *Propionibacterium acnes*-induced folliculitis of the chest, combination of H&E, and *B. cereus* immunostaining). Gram-positive bacterial microbes are visualized by immunostaining with *B. cereus* antiserum. No positivity is seen with BCG, *T. pallidum*, and *E. coli* antisera.



Figure 23. Lethal *Pseudomonas aeruginosa* pneumonia/septicemia (left, H&E; center, immunostaining using monoclonal antibody B11; right, immunostaining using *B. cereus* antiserum). Gram-negative bacilli grow along the alveolar septum, and no cellular reactions are noted. Immunoreactive signals are observed with the monoclonal antibody, as well as with *B. cereus* antiserum.

5. Use of patients' sera for demonstrating the target pathogens in paraffin sections

Sera of patients suffering from infectious diseases expectedly contain high-titer IgG-type antibodies against the causative microbe, particularly when inflammatory reactions such as abscess and granuloma are histopathologically confirmed in immunocompetent individuals. It is well known that 2 weeks is needed to have specific antibodies to be raised in the serum. The diluted patients' serum can be used as a probe for indirect immunoperoxidase staining on histopathologic specimens routinely embedded in paraffin [4, 7, 8, 20–23]. A variety of infectious microbes were demonstrable with reliable sensitivity but limited specificity, as indicated below. Endogenous human immunoglobulins (IgG) in formalin-fixed,

paraffin-embedded sections were scarcely detected by the peroxidase-labeled secondary antihuman immunoglobulins. High-sensitivity detection sequence such as the labeled polymer method naturally leads to high-background staining, because of the detection of endogenous immunoglobulins in sections. The method is simple, economic, useful, and beautiful for the histopathologic diagnosis of infectious diseases, and it is particularly suitable for the developing countries, since the patient's serum is free in charge. This approach is especially effective for detecting protozoa and helminth [22], because the specific antibodies are often commercially unavailable.

There are two situations. In some cases, the causative pathogen has been identified by clinical, laboratory, and/or histopathological analysis, and thus the specificity of the patient's serum can be expected before immunostaining. In other cases, the causative pathogen is unsettled yet or unknown. In the latter situation, the patient's serum functions as a low-specificity and high-sensitivity probe in immunostaining.

Table 4 summarizes patients' sera applicable to immunostaining in paraffin sections.

5.1 Methodology

Human tissues and organs, obtained either by biopsy, during surgery or at autopsy, were routinely fixed in 10% unbuffered or buffered formalin for 1 day to 4 weeks. The indirect immunoperoxidase technique was applied to deparaffinized sections [4, 7, 8, 20–23]. The serum of patient, principally not in an immunocompromised state, was diluted at 1:500 or 1:1000 and was incubated for 30 min or overnight. In case of protozoan infection, the presence of high-titer IgG antibodies in the patients' serum was commonly confirmed by immunofluorescence titration, as shown in **Table 4**. The serum from patients positive for human immunodeficiency virus (HIV) or hepatitis virus markers must not be utilized, in order to avoid biohazard. The serum of immunocompromised, non-HIV patients may be utilized after dilution at 1:5 or 1:10. The second layer reagent was horseradish peroxidase-labeled goat IgG to human immunoglobulins (Dako/Agilent) at a 1:50 dilution. Endogenous peroxidase activity was quenched in methanol containing 0.3% hydrogen peroxide for 20 min. No other pretreatment procedures such as proteinase digestion or heat-induced antigen retrieval were needed, but heating pretreatment was infrequently necessary for certain instances (e.g., the detection of free-living amoeba, *Balamuthia*; see below). Therefore, the author recommends introducing a heat-induced antigen retrieval procedure in 10 mM citrate buffer, pH 6, for immunostaining using silane (3-aminopropyltrimethoxysilane)-coated glass slides. After the diaminobenzidine coloring reaction, the nuclei were counterstained with 5% methyl green or Mayer's hematoxylin. When necessary, paraffin sections of related or unrelated infectious lesions were immunostained to confirm the cross-reactivity or specificity of the patients' serum.

It is of notice that IgG in the patients' serum may show cross-reactivity to related pathogens to certain or considerable degrees [4, 20, 21]. In bacterial and fungal infections, the sera often serve as pan-bacterial or pan-fungal probes. The cross-reactivity may result from the naturally acquired antibodies in healthy individuals [20]. In viral, protozoan, and helminthic infections, in contrast, high-grade specificity with limited cross-reactivity can be expected [22]. When the specificity of the sera of patients with parasitic infestation is known, it is sufficiently satisfactory to enable them to be employed as specific antibody reagents for the following new cases.

5.2 Immunostaining using sera of patients with established diagnosis

Here, the immunohistochemical application of sera of patients with established or fixed diagnosis is shown, including bacterial, fungal, viral, protozoan, and helminthic infections.

Infectious disease	Serum dilution	Comments
Tsutsugamushi disease (scrub typhus)	1:100	Immunoelectron microscopy performed
Staphylococcal pyoderma	1: 500	<i>Staphylococcus aureus</i> cultured
<i>Propionibacterium acnes</i> folliculitis	1:500	<i>P. acnes</i> -specific antigen PAC3 identified
Cutaneous sporotrichosis	1:500	Sporotrichin reaction positive
<i>Malassezia (Pityrosporum)</i> folliculitis	1:500	Multiple skin papules on the chest
Cutaneous alternariosis	1:500	Long-lasting skin lesion on the knee
Cutaneous cryptococcosis in leukemia	1:10	Chemotherapy with steroid administration
Hemorrhagic varicella	1:500 [*]	Bone marrow transplanted acute leukemia
Cutaneous leishmaniasis (African type)	1:1000	High immunofluorescence titer
Cutaneous leishmaniasis (Indian type)	1:1000	High immunofluorescence titer
Visceral leishmaniasis (liver biopsy)	1:500	High immunofluorescence titer
Acanthamebic encephalitis	1:500	Opportunistic infection in liver cirrhosis
Amebic dysentery	1:500 [*]	High immunofluorescent titer
Balamuthia encephalitis	1:500	<i>Balamuthia</i> DNA identified by PCR
Cerebral toxoplasmosis	1:1000 [*]	High immunofluorescence titer
Cryptosporidiosis in AIDS	1:1000 [*]	High immunofluorescence titer
Duodenal cystoisosporiasis	1:500	Chronic intractable diarrhea
Blastocystosis (cell block of cultured microbes)	1:500 [*]	High immunofluorescence titer
Cutaneous gnathostomiasis	1:500	Creeping disease on the abdominal skin
Extra-gastrointestinal (omental) anisakiasis	1:500	Positive with monoclonal antibody
Liver ascariasis (surgical material)	1:500	Ouchterlony's diffusion-in-gel test positive
Japanese schistosomiasis (colon)	1:200	Calcified ova seen (healed remote case)
Bilharziasis (colon biopsy)	1:500	Spine-forming ova seen in urine
Multilocular echinococcosis	1:200	Hepatectomy specimen in Hokkaido Island
Neurocysticercosis	1:20	Multiple brain nodules

^{*}High-titer sera were obtained from other immunocompetent patients.

Table 4.
Patients' sera applicable to immunostaining in paraffin sections.

5.2.1 Bacterial infection

5.2.1.1 Tsutsugamushi disease (scrub typhus)

Mite-borne Tsutsugamushi disease or scrub typhus endemic in Japan is caused by *Orientia tsutsugamushi* belonging to the family *Rickettsiaceae* [46]. Biopsy was performed from the mite-bite eschar, and hemophagocytic macrophages were clustered at the base of the ulcer. The diluted patient's serum gave positive granulated signals in the cytoplasm of the macrophages [23], and pre-embedding

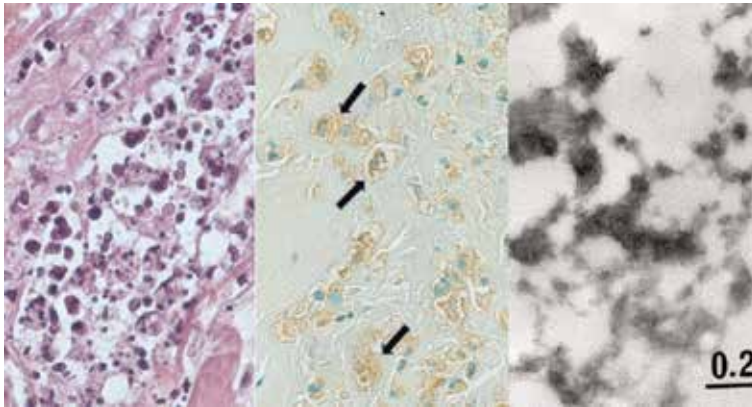


Figure 24. Mite-bite eschar in *Tsutsugamushi* disease or scrub typhus (left, H&E; center, reactivity with patient's own serum; right, pre-embedding immunoelectron microscopy using paraffin section). Hemophagocytic macrophages are clustered at the base of eschar. The patient's serum gave positive granulated signals in the cytoplasm of the macrophages (arrows), and pre-embedding immunoelectron microscopy disclosed densely labeled granular material measuring 2 μ m.

immunoelectron microscopy employing a paraffin section disclosed labeled granular material measuring 2 μ m (**Figure 24**) [47].

5.2.1.2 *Staphylococcal pyoderma*

Skin biopsy specimen from *Staphylococcus aureus*-induced pyoderma reveals diffuse dermal infiltration of neutrophils and macrophages. The patient's own serum detected coccoid bacteria phagocytized by the inflammatory cells (**Figure 25**) [20, 21, 23].

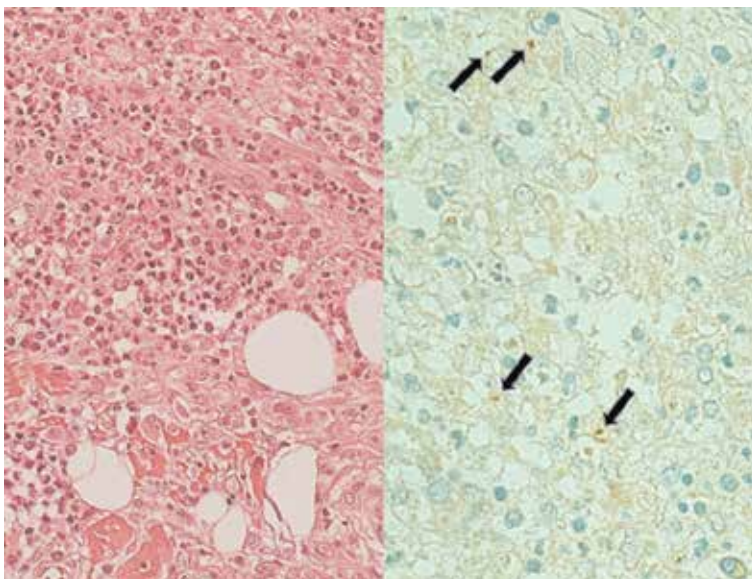


Figure 25. *Staphylococcus aureus*-induced pyoderma (left, H&E; right, reactivity with patient's own serum). The dermis reveals diffuse infiltration of neutrophils and macrophages. The patient's own serum detects coccoid bacteria phagocytized by the inflammatory cells (arrows).

5.2.2 Fungal infection

5.2.2.1 Sporotrichosis

Sporotrichosis, skin infection of a dimorphic fungus *Sporothrix schenckii* particularly endemic in tropical and subtropical areas, is mediated by traumatic inoculation from soil or plants [48]. Skin biopsy material of sporotrichosis shows suppurative granuloma formation in the dermis. Periodic acid-Schiff-reactive small yeast-like fungal cells phagocytized by macrophages or multinucleated giant cells were reactive with the patient's own serum (**Figure 26**) [20, 21, 23].

5.2.2.2 Malassezia folliculitis

Malassezia (Pityrosporum) folliculitis commonly seen on the face and upper portion of the trunk has been confused with acne vulgaris [49]. A dilated hair follicle in the biopsy material was infiltrated by neutrophils and epithelioid cells forming suppurative granuloma. The patient's own serum reacted to Grocott-positive yeast-like fungi in the lesion (**Figure 27**) [21, 23]. Malassezian bodies, a commensal in the hair follicle of normal seborrheic skin sampled from another patient, were strongly labeled with the same serum.

5.2.2.3 Cutaneous alternariosis

Alternaria is a nonpathogenic, melanin-forming fungus widely seen in the environment. Rarely, skin infection of *A. alternata* happens [50]. In a skin biopsy specimen from a young female, a few Grocott-reactive fungi were observed in the chronically inflamed dermis. The patient's own serum visualized the fungal microbes phagocytized by macrophages (**Figure 28**) [21, 23].

5.2.2.4 Cryptococcosis complicated in an immunocompromised state

Cutaneous lesions occur in 10-20% of life-threatening disseminated cryptococcosis seen in immunocompromised patients [51]. Opportunistic skin infection of *Cryptococcus neoformans* occurred in a young patient after chemotherapy and steroid

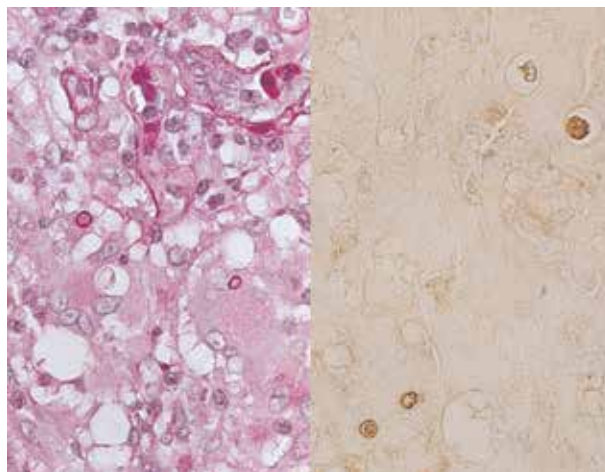


Figure 26. Sporotrichosis (left, periodic acid-Schiff reaction; right, reactivity with patient's own serum). Suppurative granulomas are formed in the dermis. Periodic acid-Schiff-reactive small yeast-like fungal cells are phagocytized by macrophages or multinucleated giant cells and are reactive with the patient's own serum.

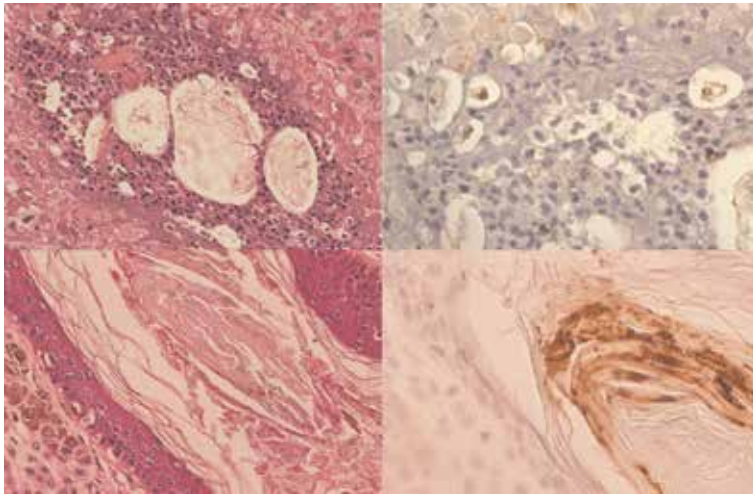


Figure 27. *Malassezia (Pityrosporum) folliculitis and commensal fungi in the hair follicle (upper panels, malassezial folliculitis; lower panels, a commensal in a normal hair follicle adjacent to intradermal nevus; left, H&E; right, reactivity with patient's serum). A dilated hair follicle in biopsy material is disrupted by suppurative granuloma formation. The patient's own serum reacted with yeast-like fungi infected in the lesion. Commensal malassezial cells in the hair follicle of normal seborrhic skin, sampled from another individual, are strongly labeled with the same serum.*

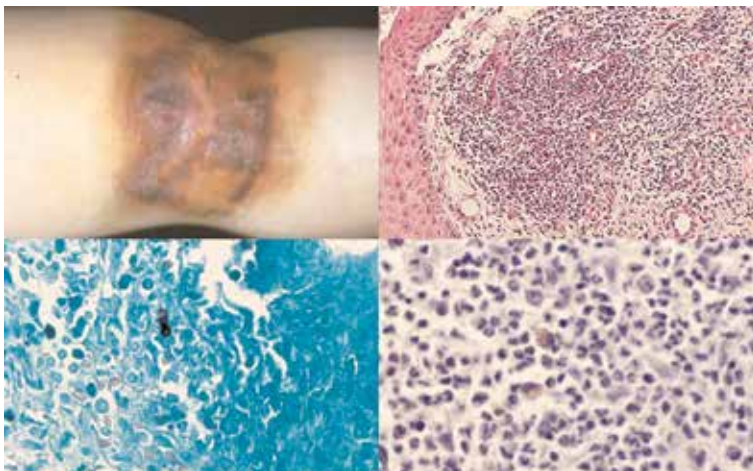


Figure 28. *Cutaneous alternariosis (left upper, gross appearance of the elbow; right upper, H&E; left lower, Grocott stain; right lower, reactivity with patient's own serum). Biopsy specimen from the brown-colored skin infiltrate contains a few Grocott-reactive fungi, *Alternaria alternata*, in the chronically inflamed dermis. The patient's own serum visualizes the fungal microbes phagocytized by macrophages.*

administration against acute lymphoblastic leukemia. Transparent yeasts were floating in mucoid material, and inflammatory reaction was poor. The patient's own serum diluted at 1:10 was weakly reactive to the pathogen (**Figure 29**) [20, 21, 23].

5.2.3 Viral infection

5.2.3.1 Hemorrhagic varicella

Biopsy was taken from the vesicular skin lesion of lethal hemorrhagic varicella (small pox). The patient was a young boy suffering from intractable acute

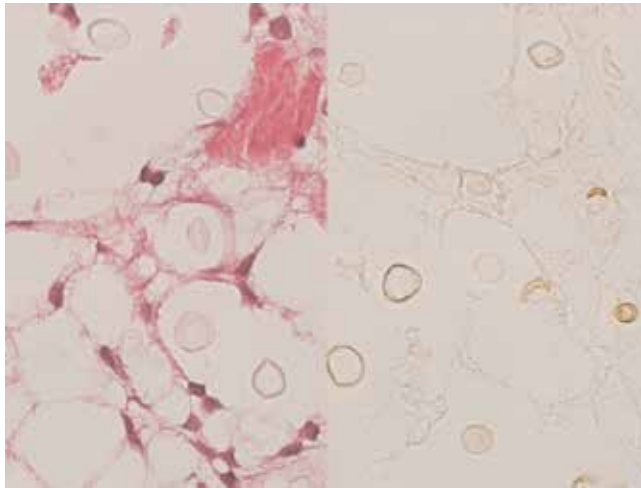


Figure 29. *Cutaneous cryptococcosis (left, H&E; right, reactivity with patient's own serum). Opportunistic skin infection of *Cryptococcus neoformans* in a treated leukemia case of the young microscopically reveals transparent yeasts floating in mucoid material. Inflammatory reaction is poor. The patient's own serum diluted at 1:10 weakly reacts to the pathogen.*

lymphoblastic leukemia treated with chemotherapy and bone marrow transplantation [52]. The 1:500 diluted serum of another adult patient with a recent history of varicella clearly reacted to the plasma membrane of acantholytic keratinocytes with intranuclear viral inclusion bodies, and the localization pattern was comparable with that of GP-1 antigen revealed by immunostaining using monoclonal antibody C90.2.8 (**Figure 30**) [21, 23]. The viral intranuclear inclusions remained unreactive. It is evident that antibodies raised in the infected patient were specific to GP-1 antigen of varicella-zoster virus, an immunodominant viral substance [53].

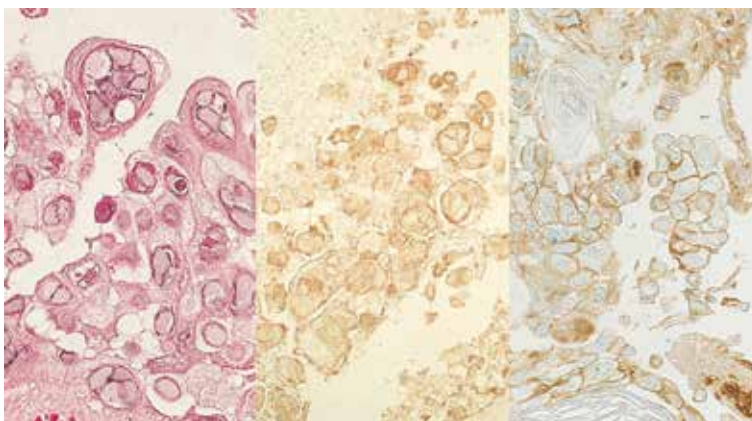


Figure 30. *Hemorrhagic varicella (left, H&E; center, reactivity with the serum of another patient; right, reactivity with monoclonal antibody C90.2.8 to GP-1 antigen of varicella-zoster virus). Biopsy was taken from a hemorrhagic vesicle, as lethal manifestation of opportunistic varicella-zoster virus infection in a leukemic boy after bone marrow transplantation. The diluted serum of another adult patient with a recent history of varicella clearly reacts to the plasma membrane of acantholytic keratinocytes with unreactive intranuclear viral inclusion bodies. The localization pattern is comparable with that of GP-1 antigen.*

5.2.4 Protozoan infection

5.2.4.1 Cutaneous leishmaniasis

Figure 31 demonstrates microscopic biopsy features of African-type cutaneous leishmaniasis (*Leishmania major* infection) [54]. Japanese men, a group of 5, volunteered afforestation on the Saharan desert in the Republic of Mali. Multiple ulcers were formed on the arms of all the members of the group. At the end of the work day, a large swarm of sandflies rushed at them. In a Japanese hospital, biopsy was taken from an ulcer on the arm of one of the members. The dermis was heavily infiltrated by macrophages full of granular microbes. The patient's own serum clearly demonstrated round pathogens in the cytoplasm of macrophages. In the biopsied older lesion seen in his friend, fewer pathogens were identified with immunostaining using the same serum [4, 8, 20–23].

Another form of cutaneous leishmaniasis, Indian type, is caused by *L. tropica* [55]. Solitary ulcer formation on the skin is characteristic of this clinical form. An aged Japanese patient stayed in India for months, and skin biopsy was performed in a Japanese hospital. Round pathogens were visualized in the cytoplasm of macrophages in the dermis by the patient's own serum (**Figure 32**) [22, 23]. Of note is that no cross-reactive staining was noted between the African and Indian types. Namely, the patient serum showed a very high specificity to the respective types of cutaneous leishmaniasis.

5.2.4.2 Acanthamebic keratitis

Acanthamebic keratitis is sight-threatening infection of the cornea by the genus *Acanthamoeba*, mostly seen in contact lens wearers [56]. A young male aged 10's, a soft contact lens user, complained of eye pain, and under the diagnosis of acanthamebic keratitis, superficial keratectomy was done. *Acanthamoeba* spp. was cultured. As shown in **Figure 33**, acanthamebic cysts and some trophozoites were identified in the corneal stroma by immunostaining using both the diluted serum of a patient of acanthamebic meningoencephalitis (see **Figure 49**) and a monoclonal

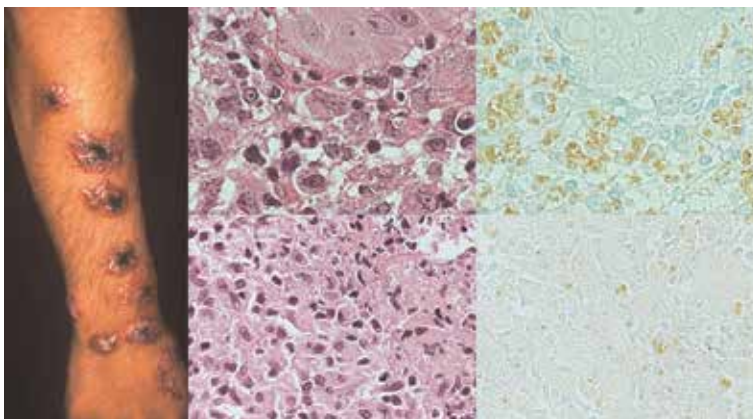


Figure 31. African-type cutaneous leishmaniasis (left, gross appearance of the forearm; upper panels, the patient of gross photograph; lower panels, an older lesion of his friend; center, H&E; right, reactivity with patient's serum). The Japanese men volunteered afforestation on the Saharan desert in the Republic of Mali. Biopsy was taken from ulcerated skin lesions. The patient's own serum demonstrates round pathogens (*Leishmania major*) in the cytoplasm of macrophages infiltrating in the dermis (upper panels). In the older lesion seen in his friend (lower panels), fewer pathogens are observed with immunostaining employing the same serum.

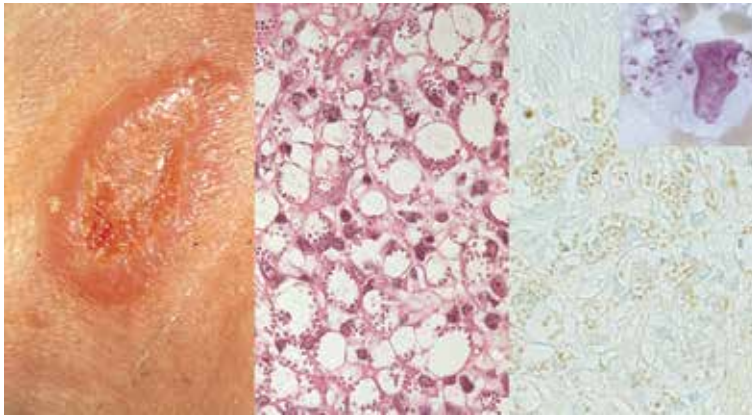


Figure 32.

Indian-type cutaneous leishmaniasis (left, gross appearance of the neck; center, H&E; right, reactivity with patient's own serum; inset, Giemsa stain on a stamp cytology preparation). Solitary skin ulcer is characteristic of this clinical form endemic in India. Biopsy specimen from a Japanese patient shows numerous round pathogens (*Leishmania tropica*) in the cytoplasm of macrophages in the dermis. The diluted patient's own serum visualizes the pathogen. Giemsa preparation demonstrates a pair of the nucleus and kinetoplast (smaller dot) in the protozoan cell.

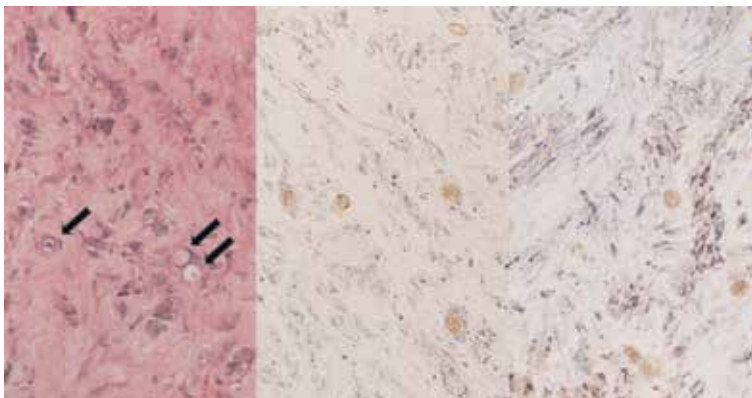


Figure 33.

Acanthamoebic keratitis (left, H&E; center, reactivity with the serum of patient of acanthamoebic meningoencephalitis; right, reactivity with monoclonal antibody ACA5 to *Acanthamoeba* sp.). Superficial keratectomy specimen from a young contact lens wearer reveals scattered amebic cysts (arrows) in the corneal stroma, and the microbes (cysts) are visualized by immunostaining using both the diluted patient's serum and the monoclonal antibody.

antibody ACA5 to *Acanthamoeba* spp. (a gift from Prof. Hiroshi Tachibana, Department of Infectious Diseases, Tokai University School of Medicine, Isehara) [57].

5.2.4.3 Amebic dysentery

Amebic dysentery, colonic infection of *Entamoeba histolytica*, is endemic in areas with poor sanitation and is often associated with AIDS [58]. Surgically resected colon specimen from an HIV-negative Japanese male patient demonstrated amebic trophozoites invading the ulcerated colon wall. As shown in **Figure 34**, the patient's own serum visualized the pathogen, and the localization was comparable with immunostaining using a monoclonal antibody EHK153 to *E. histolytica* (a gift from Prof. Yuji Tachibana, Department of Infectious Diseases, Tokai University School of Medicine, Isehara) [4, 20–23].

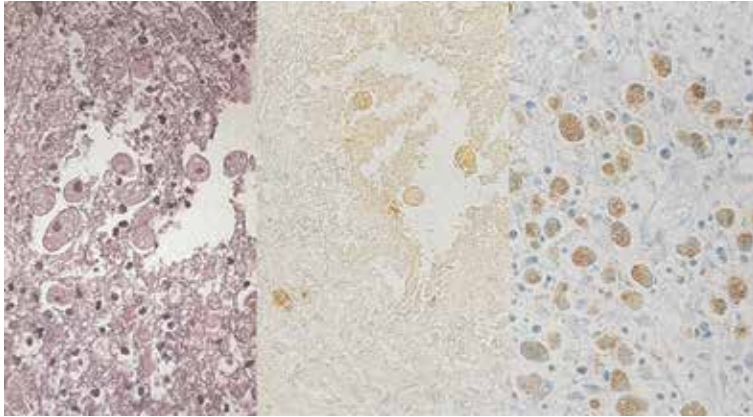


Figure 34. Amebic dysentery (left, H&E; center, reactivity with patient's own serum; right, reactivity with monoclonal antibody EHK153 to *E. histolytica*). Surgically resected colon specimen from an HIV-negative Japanese male demonstrates amebic trophozoites invading the ulcerated colon wall. The patient's own serum visualizes the pathogen, and the localization was comparable with immunostaining using the monoclonal antibody.

5.2.4.4 Toxoplasmosis

Cryptogenic and asymptomatic infection of *Toxoplasma gondii* is common throughout the world. In patients with compromised immune system, particularly in AIDS, the parasite is activated, resulting in lethal *Toxoplasma* encephalitis. When primary infection occurs in pregnant women without serum antibody, the placental tissue is infected, causing congenital toxoplasmosis in the fetus [59]. Ruptured protozoan cysts of AIDS-associated cerebral toxoplasmosis were reactive with the serum from a healthy individual serologically with high-titer IgG. The same serum decorated trophozoites of *T. gondii* dispersed in the meningeal space in an aged HIV-negative female with progressive supranuclear palsy, confirming the diagnosis of *Toxoplasma* meningitis (Figure 35) [21, 22].

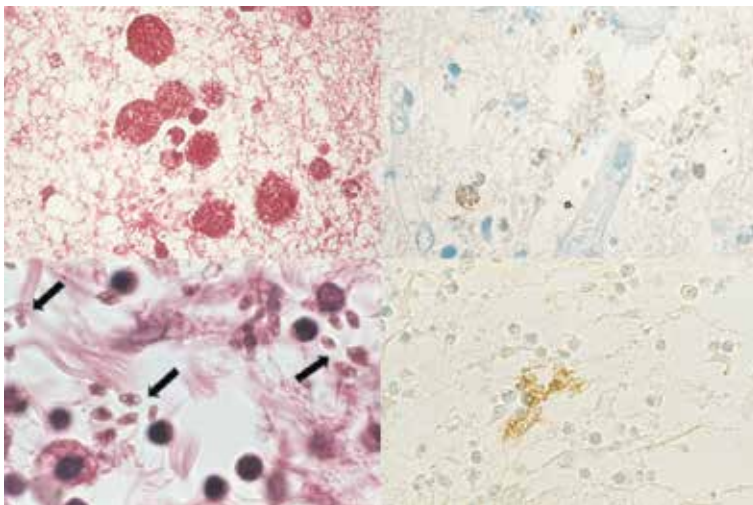


Figure 35. Toxoplasmosis (upper panels, toxoplasma encephalitis in AIDS; lower panels, toxoplasma meningitis in a non-AIDS patient; left, H&E; right, reactivity with the serum from a healthy individual serologically with high-titer IgG). Ruptured protozoan cysts in AIDS-associated cerebral toxoplasmosis are reactive with the serum. The same serum decorates trophozoites of *Toxoplasma gondii* (arrows) dispersed in the meningeal space in an aged HIV-negative female with progressive supranuclear palsy.

5.2.4.5 Cryptosporidiosis

Cryptosporidiosis is zoonotic and waterborne infection of *Cryptosporidium parvum*, preferentially involving small bowel mucosa. In immunocompetent individuals, self-limiting watery diarrhea occurs, while in AIDS patients, the infection provokes life-threatening intractable diarrhea without effective therapeutic agents in hand [60]. The high-titer patient serum was chosen from a stock of 1994 mass infection of *C. parvum* due to contamination in the water supply system, taking place in Hiratsuka, Kanagawa, Japan. Biopsy was performed from the terminal ileal mucosa of high school boy who complained of severe diarrhea after close contact with cows in a Hokkaido farm during the summer vacation. A Japanese AIDS patient died of intractable diarrhea, and autopsy revealed cryptosporidiosis on the small bowel mucosa. Immunostaining using the high-titer serum clearly demonstrated small dot-like positive signals along the brush border of the small bowel mucosa of both patients (**Figure 36**) [21–23].

5.2.4.6 Cystoisosporiasis

Cystoisospora (formerly called *Isospora*) *belli* infection causes intractable diarrhea in individuals who live in or have traveled to tropical poor sanitary areas. Infection in immunocompromised patients, particularly AIDS patients in Africa, is life-threatening [61]. *C. belli*-induced acalculous cholecystitis is a noteworthy finding [62]. Duodenal biopsy specimen was taken from a Japanese male patient with adult T-cell leukemia in Kyushu Island. Chronic active inflammation with villous atrophy represented intractable diarrhea seen in this patient. Large-sized schizonts of *C. belli* were observed among the columnar cells in H&E preparations, and they were visualized by immunostaining using the patient's own serum (**Figure 37**) [21, 23].

5.2.4.7 Blastocystosis

Blastocystis hominis belongs to an anaerobic parasite of uncertain taxonomy found in the human digestive tract, causing diarrhea when heavily infected. Vacuolated

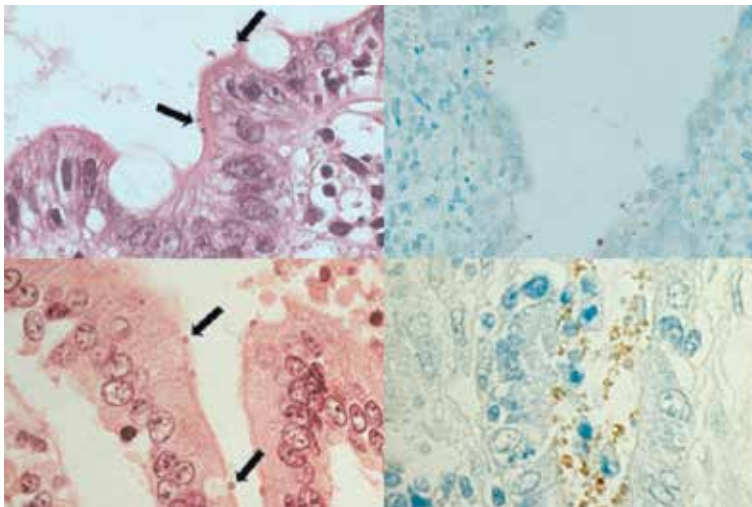


Figure 36. Cryptosporidiosis (upper panels, ileal mucosal biopsy from a young suffering from severe diarrhea after close contact with cows in a Hokkaido farm; lower panels, autopsied jejunum of an AIDS patient complaining of lethal diarrhea; left, H&E; right, reactivity with the serum of a cryptosporidiosis patient with high-titer IgG). The tiny microbes grow in the brush border of enterocytes (arrows). Immunostaining using the high-titer serum demonstrates dot-like positive signals on the apex of the columnar cells of both patients.

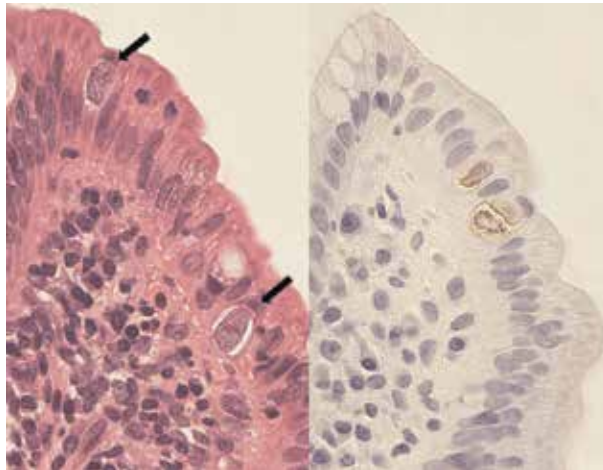


Figure 37. Cystoisosporiasis (left, H&E; right, reactivity with patient's own serum). Duodenal biopsy specimen was taken from a Japanese male patient with adult T-cell leukemia in Kyushu Island, complaining of severe diarrhea. Large-sized schizonts of *Cystoisospora belli* are scattered among the columnar cells (arrows). Immunostaining using patient's own serum decorates the microbe.

morphology and size variation are characteristic [63]. We encountered a patient with diarrhea and high-titer serum antibody to *B. hominis* [64]. The target of immunostaining was formalin-fixed, paraffin-embedded cell block preparations of cultured *B. hominis*. Cell wall positivity was clearly observed, as shown in **Figure 38** [21–23].

5.2.5 Helminthic infection

5.2.5.1 Gnathostomiasis

Infestation of *Gnathostoma* happens after eating undercooked or raw freshwater fish, frogs, birds, and reptiles, and migratory swelling of the skin (creeping disease) follows [65]. Cut surface of *G. hispidum* was identified in targeted abdominal skin biopsy from creeping disease, seen in a Japanese male patient aged 60's. The larval body is histologically featured by spiculated cuticles, well-developed muscle cells

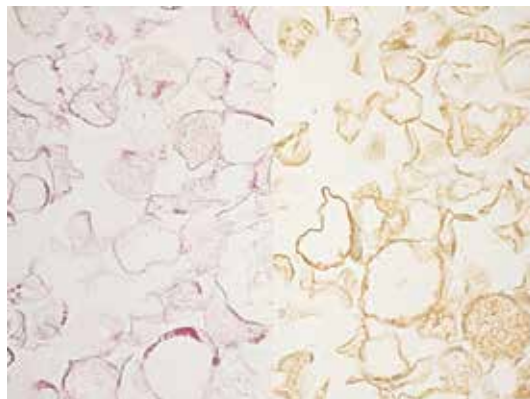


Figure 38. Blastocystosis (cultured *Blastocystis hominis* in cell block preparation: left, H&E; right, reactivity with the serum of a patient with serologically proven high-titer IgG). Cultured *B. hominis* reveals vacuolated morphology and size variation. The centrifuged pellet was fixed in formalin and embedded in paraffin to prepare cell blocks. The cell wall of the microbes is immunostained with the serum of a patient with diarrhea and high-titer serum antibody to *B. hominis*.

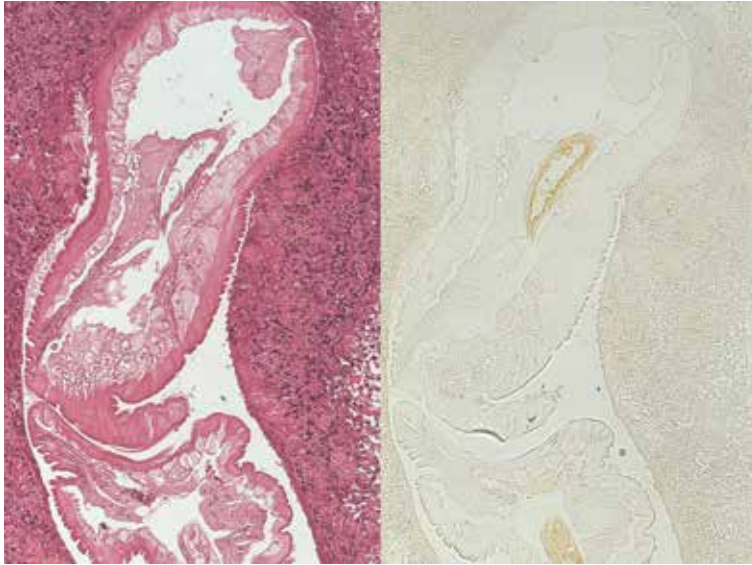


Figure 39. *Gnathostomiasis* (left, H&E; right, reactivity with patient's own serum). A Japanese male manifested creeping disease on the abdomen. Targeted biopsy reveals cut surfaces of *Gnathostoma hispidum* in the dermis. The larval body is histologically featured by spiculated cuticles, well-developed muscle cells with clear cytoplasm, eosinophilic lateral chords, and the centrally located gut. The patient's serum was solely reactive with the gut cells.

with clear cytoplasm, eosinophilic lateral chords, and the centrally located gut. The patient's serum was solely reactive with the gut cells (**Figure 39**) [21, 23].

5.2.5.2 *Ectopic anisakiasis*

Anisakis species belongs to a dolphin/whale ascarid. Anisakiasis is caused by the ingestion of a larval nematode in raw seafood dishes such as sushi and sashimi. Infestation occurs mainly in the stomach, but infrequently intestinal or extra-gastrointestinal anisakiasis is encountered [66]. A dead and decayed larval nematode was identified in the peritoneal (omental) nodule, and microscopic identification of the nematode species was impossible. The diagnosis of extra-gastrointestinal anisakiasis was made by distinct immunoreactivity with a monoclonal antibody An2 against *Anisakis simplex* (a gift from late Dr. Hajime Ishikura, Sapporo Medical University, Sapporo). The 1:500 diluted patient's own serum reacted weakly with the internal organs, especially the gut (**Figure 40**) [21].

5.2.5.3 *Schistosomiasis japonicum*

Schistosomiasis is caused by digenetic blood trematodes (fluke). Water snail-mediated three main species infest humans: *Schistosoma japonicum*, *S. haematobium*, and *S. mansoni*. Larvae (cercariae) show percutaneous infestation through intact skin. Paired adult worms of *S. japonicum* fix to the portal vein and provoke liver cirrhosis. The disease, rampant until the 1960s in certain areas of Japan, has been eradicated by 1976 [67]. Now, Mainland China and the Philippines are the main countries of epidemic [68]. We occasionally experience aged Japanese people accompanying calcified ova in the liver and colon. **Figure 41** demonstrates biopsied colonic mucosa with acid-fast *Schistosoma* ova in an aged asymptomatic male living in Kofu Basin, the historical endemic area. The patient's serum diluted at 1:200 reacted with the shell of the ovum [21].

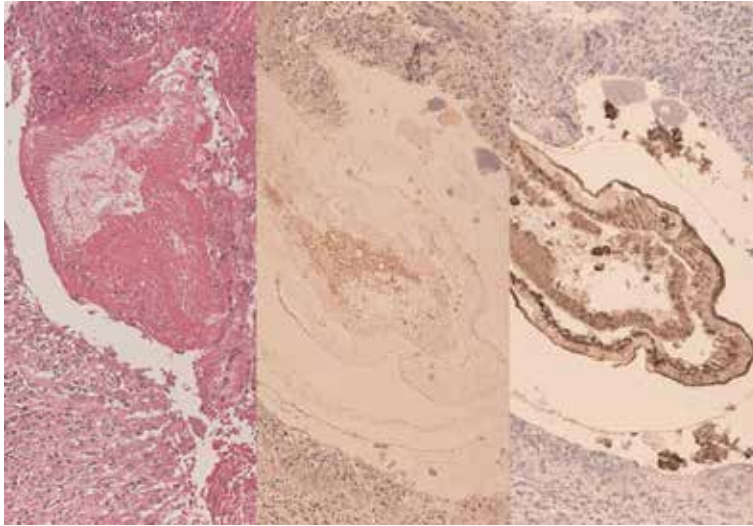


Figure 40. Ectopic anisakiasis (left, H&E; center, reactivity with patient's own serum; right, reactivity with monoclonal antibody An2 to *Anisakis simplex*). A dead and decayed larval nematode is seen in the omental nodule, and the diagnosis of extra-gastrointestinal anisakiasis was made by distinct immunoreactivity with the monoclonal antibody. The diluted patient's own serum reacts weakly with the internal organs, especially the gut.

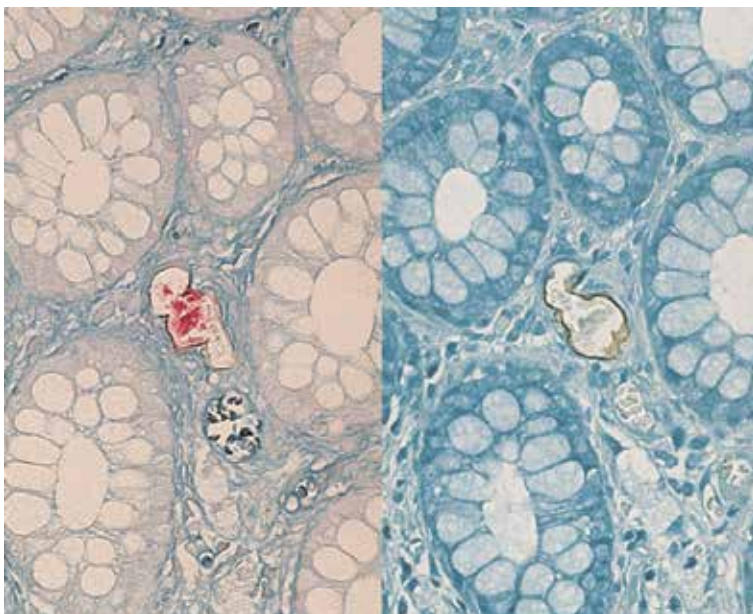


Figure 41. *Schistosomiasis japonicum* (left, acid-fast staining; right, reactivity with patient's own serum). In biopsied colonic mucosa of an asymptomatic individual living in a historical endemic area, acid-fast ova of *Schistosoma japonicum* are observed in the lamina propria mucosae. The patient's serum diluted at 1:200 reacts with the shell of the ovum.

5.2.5.4 Bilharziasis

Schistosoma haematobium infestation (bilharziasis) is endemic in sub-Saharan African continent. Infection occurs in fresh water in a short time (just for 10 min) when a larval form (cercaria) of *S. haematobium*, developing in the fresh water

snail, penetrates the intact skin. Paired adult worms, 1.5–2 cm in size, settle in paravascular pelvic veins, and ova are excreted from ulcers formed in the urinary bladder to the urine [69]. Ectopic egg tubercles (foreign body granulomas against eggs) may be formed in the uterine cervix, ureter, and rectosigmoid colon and even in the brain. Two young Japanese male patients with a history of staying in African continent complained of hematuria and presented ectopic egg tubercles in the sigmoid colon and in the brain, respectively. The multinucleated (miracidial) content of the egg was strongly labeled with the patient's own serum in both the biopsied colon and surgically resected cerebral lesion (**Figure 42**) [21, 23].

5.2.5.5 Multilocular echinococcosis

Multilocular (alveolar) echinococcosis, infestation of *Echinococcus multilocularis*, is endemic in Hokkaido, the northernmost island of Japan. This zoonotic parasitosis showing liver involvement is mainly mediated by ingestion of eggs excreted from red foxes [70]. The liver infested by *E. multilocularis* was surgically removed from a female patient aged 30's living in Hokkaido. The multilocular hydatid cyst wall was collapsed and embedded in the fibrous tissue. No protoscolex was seen in the lesion. The patient's serum diluted at 1:200 was reactive with the collapsed cyst wall component, while the intact hydatid cyst wall revealed negativity (**Figure 43**) [23].

5.2.5.6 Neurocysticercosis

Neurocysticercosis is infestation of *Cysticercus cellulosae*, a larval form of *Taenia solium* (tapeworm). Infestation occurs by ingesting *C. cellulosae* embedded in raw pork or eggs in contaminated food [71]. The brain lesion of larva migrans in a young Japanese female was surgically removed. A cysticercus body with scolex formation was microscopically lined by eosinophilic tegument and underlying subcuticular cells. The patient's serum was weakly reactive with the tegument (**Figure 44**) [21, 23].

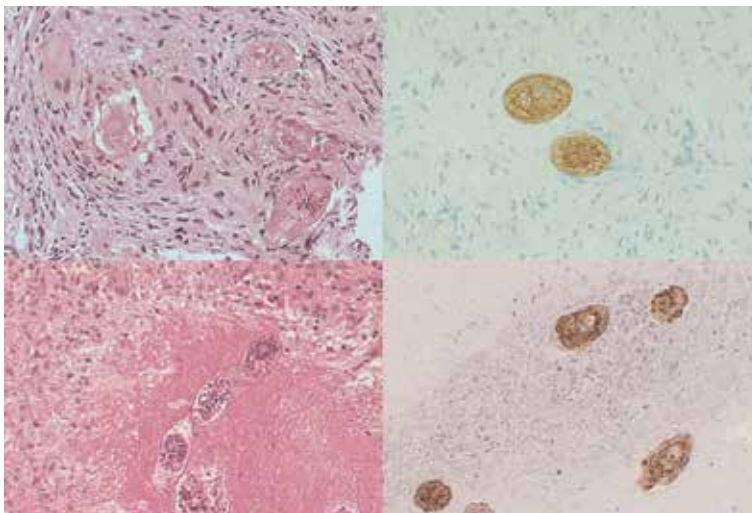


Figure 42. Bilharziasis (upper panels, egg tubercle in the sigmoid colon; lower panels, surgical material of brain lesion; left, H&E; right, reactivity with patient's own serum). Two young Japanese male patients with a history of staying in African continent complained of hematuria and presented ectopic egg tubercles in the sigmoid colon and in the brain, respectively. The multinucleated (miracidial) content of the egg of *Schistosoma haematobium* is strongly reactive with the patient's own serum in the respective lesions.

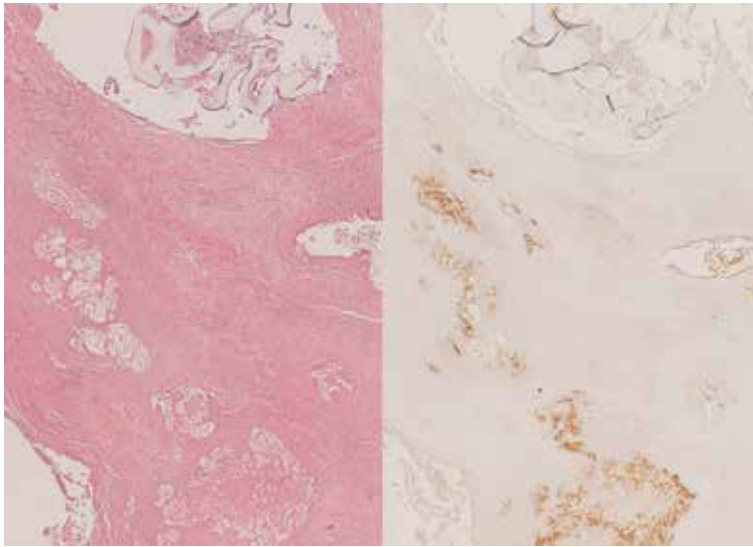


Figure 43. Multilocular echinococcosis (left, H&E; right, reactivity with patient's own serum). The liver infested by *Echinococcus multilocularis* was surgically removed from a female patient living in Hokkaido. The multilocular hydatid cyst wall has been collapsed and embedded in the fibrous tissue. The patient's serum is reactive with the collapsed cyst wall component, while the intact hydatid cyst wall reveals negativity.

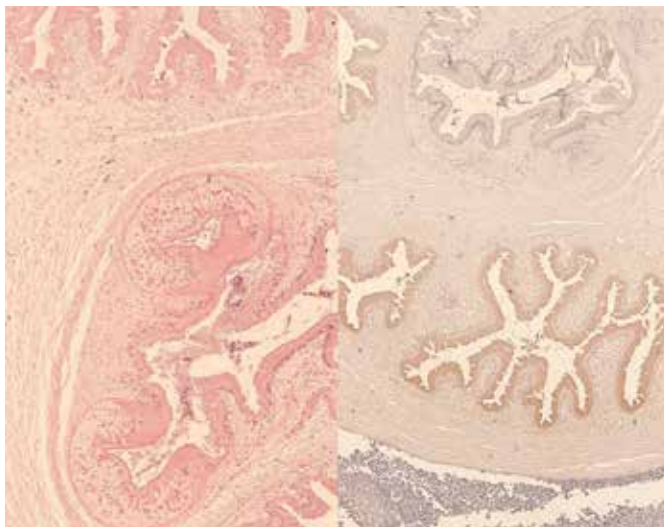


Figure 44. Neurocysticercosis (left, H&E; right, reactivity with patient's own serum). The brain lesion of larva migrans in a Japanese female was surgically removed. A cysticercus body with scolex formation is microscopically lined by eosinophilic tegument and underlying subcuticular cells. The patient's serum is weakly reactive with the tegument.

5.3 Immunostaining using the serum of patients without fixed diagnosis

When the diagnosis is unsettled, the specificity of the patient's serum remains unknown. If the positive signals reactive with the patient's serum are seen within the inflammatory lesion, it is reasonable for us to regard that the target microbes are visualized. The size and shape of the stained targets suggested certain causative pathogens within the lesion [20–23]. The final diagnosis can be made by combining

clinical information and histopathological appearance with the morphology of the pathogen. Of no doubt, this gives us the most powerful and useful situation in applying immunostaining using the patient serum.

5.3.1 *Propionibacterium acnes* folliculitis

Invasive opportunistic infection of *Propionibacterium acnes*, a commensal in the hair follicle, has been described [72]. An aged afebrile Japanese male complained of a skin nodule on the chest. Biopsy revealed hair follicle-centered inflammation, and macrophages clustered around the hair follicle contained numerous granular-looking microbes. Microscopically, the possibility of yeast-form mycosis, rickettsiosis, and protozoan infection was suspected. Grocott positivity was faint. Immunostaining using *B. cereus* antiserum revealed positivity (see **Figure 22**), while antisera to BCG, *T. pallidum*, and *E. coli* did not. The patient's own serum diluted at 1:500 clearly demonstrated the pathogen not only in macrophages but also in commensal bacterial colonies in the hair follicle [23]. Finally, PAC3 antigen specific to *P. acnes* was positive (through the courtesy of Prof. Yoshinobu Eguchi, Department of Pathology, Tokyo Medical and Dental University, Tokyo) [73], and the diagnosis of *P. acnes*-induced folliculitis was thus confirmed (**Figure 45**).

5.3.2 Ectopic liver infestation of *Ascaris lumbricoides*

Ectopic infestation of *Ascaris lumbricoides* in the hepatobiliary tract has been reported [74]. A farmer housewife aged 40's complained of abdominal pain. Liver abscess was indicated by diagnostic imaging, and partial hepatectomy specimen revealed multiple yellow-colored xanthogranulomatous nodules at the liver hilus. Microscopically, a small number of dead and calcified ova were distributed in necrotic substance, while the parasite body had been absorbed [75]. The content of the ova was immunoreactive with the diluted patient's serum [7, 20, 21, 23, 75]. Ouchterlony's diffusion-in-gel test using the extract of varied helminths identified a

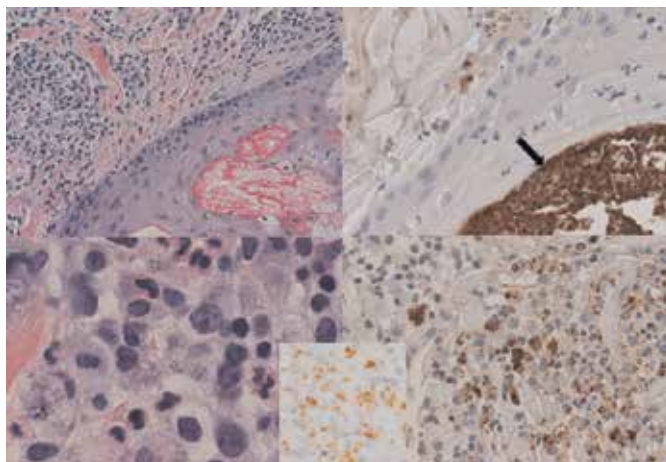


Figure 45. *Propionibacterium acnes* folliculitis (upper panels, dilated hair follicle with histiocytic reaction in the perifollicular dermis; lower panels, higher powered view of the infiltrating macrophages; left, H&E; right, reactivity with patient's own serum; inset, immunostaining for PAC3 antigen specific to *P. acnes*). Macrophages clustered around the dilated hair follicle contain numerous granular-looking microbes. The patient's own serum clearly demonstrates the pathogen not only in macrophages but also in commensal bacterial colonies in the hair follicle (arrow). Immunostaining for PAC3 antigen confirms the diagnosis of *P. acnes*-induced folliculitis.

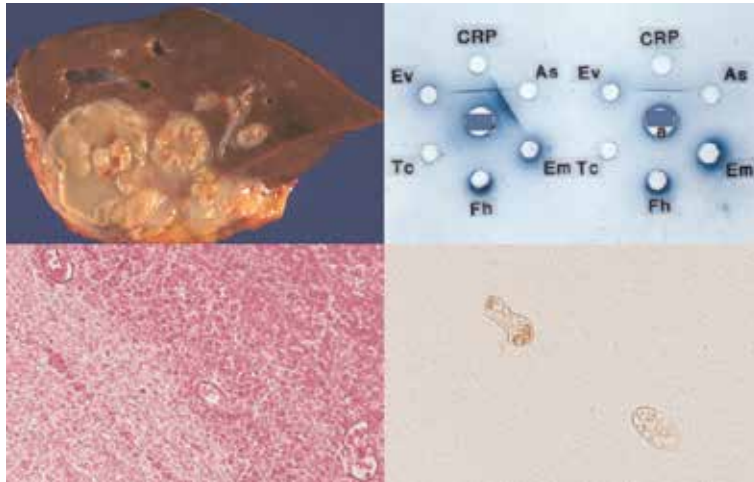


Figure 46. Hepatic ascariasis (left upper, cut surface of the resected liver; right upper, Ouchterlony's diffusion-in-gel test using the extract of varied helminths; left lower, H&E; right lower, reactivity with patient's own serum). Yellow-colored xanthogranulomatous nodules are seen at the liver hilus. Microscopically, a small number of dead and calcified ova are distributed in necrotic substance. The content of the ova is immunoreactive with the patient's serum. In Ouchterlony's test, a precipitation line against *Ascaris lumbricoides* (As) has been absorbed by the *Ascaris* extract, as shown on the right hand (Em, *Echinococcus multilocularis*; Fh, *Fasciola hepatica*; Tc, *Toxocara canis*; EV, *Enterobius vermicularis*; CRP, C-reactive protein).

clear precipitation line against *A. lumbricoides* (Figure 46). The precipitation line was abolished by preabsorbing the serum with the roundworm extract [75]. The final diagnosis was ectopic ascariasis, caused by infestation of a young (immature) female worm. The serum was unreactive with ova of *Schistosoma japonicum* and *Paragonimus miyazakii* seen in paraffin sections. The inner surface of the cell wall of *A. simplex* larva was weakly stained with the serum [21].

Figure 47 demonstrates a splenic lesion with ectopic migration of *A. lumbricoides*. Necrotizing granulomas were formed beneath the splenic capsule, and dead parasite body fragments were seen in the necrotic area. It was impossible to determine the species of nematode under microscopy. The abovementioned serum

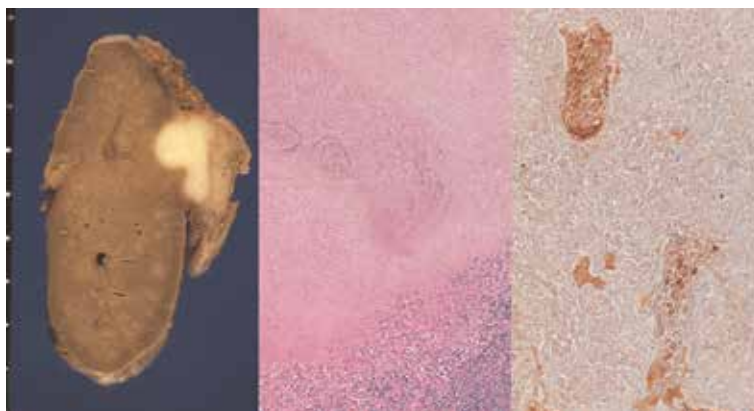


Figure 47. Splenic ascariasis (left, cut surface of the formalin-fixed spleen; center, H&E; right, reactivity with the serum of patient with hepatic ascariasis). Ectopic migration of *A. lumbricoides* has provoked necrotizing granulomas beneath the splenic capsule. Dead parasite body fragments are seen in the necrotic area. The abovementioned serum of patient with hepatic ascariasis reacts with the dead worm body, confirming the diagnosis of ectopic splenic ascariasis.

of patient with hepatic ascariasis reacted with the dead worm body, confirming the diagnosis of ectopic splenic ascariasis. The serum functioned as an immunohistochemical probe specific to *A. lumbricoides* [21].

5.3.3 Visceral leishmaniasis

Visceral leishmaniasis, sandfly-mediated systemic infection of *Leishmania donovani*, kills more than 20,000 persons in 2015 but has been classified by the World Health Organization as a neglected tropical disease [76]. A Japanese businessman aged 30's stayed in a sequential order in Australia, Thailand, Singapore, and finally India [77]. During his stay in India, he manifested headache, high fever, thrombocytopenia, and liver dysfunction. The patient was hospitalized in Japan, but his general condition was poor. In order to confirm the diagnosis, liver biopsy was performed. Small epithelioid granulomas were identified, and the possibility of Q fever in Australia, melioidosis in Thailand, brucellosis, miliary tuberculosis, and non-tuberculous mycobacteriosis was considered histopathologically. No positive findings were obtained in immunohistochemical analysis using a panel of antibodies. The patient's own serum diluted at 1:500 demonstrated red cell-sized positive signals in the cytoplasm of epithelioid cells (**Figure 48**) [7, 8, 21, 23, 77]. The size and shape of the pathogen strongly suggested visceral leishmaniasis (kala azar) endemic in India. High serum immunofluorescence titer against *L. donovani* was serologically confirmed thereafter. Administration of pentavalent antimony compound saved his life. This is the real case, in which immunostaining using the patient's own serum was practical maximally.

5.3.4 Free-living amoebic meningoencephalitis

Free-living amoeba widely seen in soil and water may cause lethal meningoencephalitis as an opportunistic or non-opportunistic infection [78]. A Japanese male

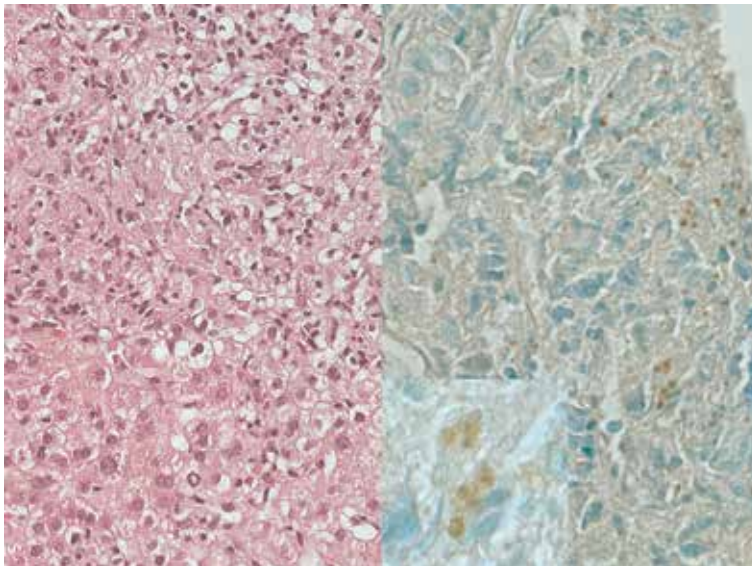


Figure 48. Visceral leishmaniasis (left, H&E; right, reactivity with patient's own serum; inset, high-powered view). During the stay in India, a Japanese businessman manifested headache, high fever, thrombocytopenia, and liver dysfunction. Liver biopsy shows small epithelioid granulomas. A panel of immunohistochemical analysis has failed to identify the causal agent. The patient's own serum demonstrates red cell-sized positive signals in the cytoplasm of epithelioid cells, strongly suggesting visceral leishmaniasis (kala azar) endemic in India. The final diagnosis was made by the serological study and successful treatment.

aged 60's suffering from alcoholic liver cirrhosis manifested left hemiparesis [79]. Computed tomography disclosed multifocal low densities in his right hemisphere. Herpetic encephalitis was clinically suspected. HIV antibody was negative. Progressive intracranial edema necessitated decompressive craniotomy with brain biopsy. The brain tissue microscopically showed perivascular chronic active inflammation, with ameba-like cells somewhat resembling macrophages being scattered. The 1:500 diluted patient's serum clearly reacted with the protozoan bodies, and mouse antiserum to *Acanthamoeba culbertsoni* (a gift from Prof. Yuji Tachibana, Department of Infectious Diseases, Tokai University School of Medicine, Isehara) also gave positivity (**Figure 49**) [7, 8, 21, 23, 77]. No reactivities for *A. polyphaga* and *A. castellanii* were noted. High immunofluorescence titer against *A. culbertsoni* was serologically confirmed in the patient's serum. Detailed microscopic observation of H&E-stained preparations disclosed the presence of acanthamebic trophozoites and cysts in the brain tissue. The final diagnosis was opportunistic acanthamebic meningoencephalitis associated with liver cirrhosis.

Balamuthia mandrillaris may cause amebic meningoencephalitis in both immunocompromised and immunocompetent individuals [80]. An amoeba-induced skin nodule may be formed before the onset of meningoencephalitis [81]. A healthy Japanese farmer housewife aged 50's suddenly complained of progressive consciousness disturbance and seizure. She daily grew vegetables. Two weeks after onset, the patient expired. At autopsy, the basal side of the brain grossly revealed hemorrhagic meningoencephalitis. Microscopically, large-sized, basophilic amebic trophozoites were clustered mainly in Virchow-Robin's spaces. Smaller-sized cysts were focally observed. PCR analysis disclosed infection of *B. mandrillaris*. Immunostaining using both the patient's own serum and the patient's serum of the abovementioned acanthamebic meningoencephalitis gave distinct positivity (**Figure 50**) [23]. *Balamuthia*-infected skin nodule seen in another patient gave clear positivity of the microbe using these two patients' sera. Cross-reactivity of the acanthamebic antigens to *Balamuthia* species was thus confirmed, but the serum

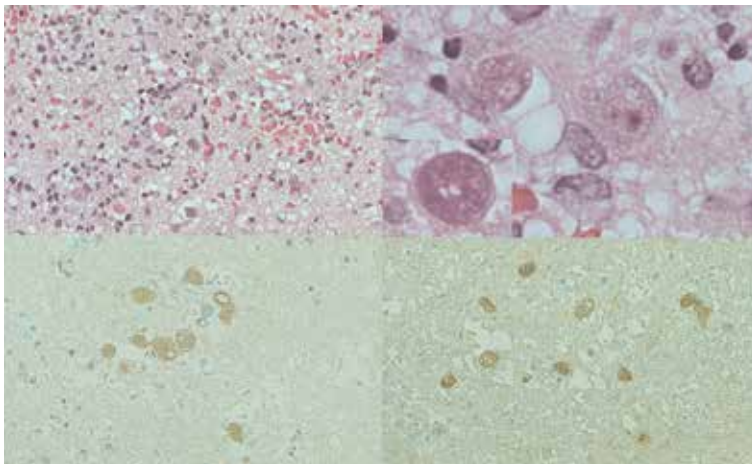


Figure 49. Acanthamebic meningoencephalitis (left upper, low-powered H&E; right upper, high-powered H&E; inset, an amebic cyst; left lower, reactivity with patient's own serum; right lower, reactivity with mouse antiserum to *Acanthamoeba culbertsoni*). An HIV-negative Japanese male suffering from alcoholic liver cirrhosis manifested left hemiparesis. Progressive intracranial edema necessitated decompressive craniotomy with brain biopsy. The brain tissue microscopically shows perivascular chronic active inflammation, and amebic trophozoites and cysts (inset) are scattered. The diluted patient's serum clearly reacts with the amebic bodies. *A. culbertsoni* infection has been confirmed by using a panel of mouse antisera against different *Acanthamoeba* subspecies.

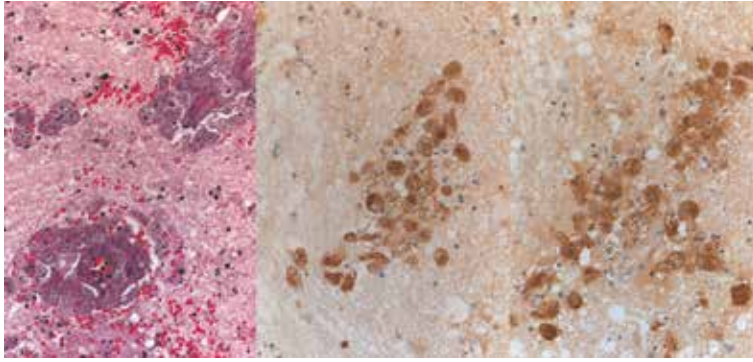


Figure 50. *Balamuthia meningoencephalitis* (left, H&E; center, reactivity with patient's own serum; right, reactivity with the serum of patient of acanthamebic meningoencephalitis). A healthy Japanese farmer housewife complained of progressive consciousness disturbance and seizure. At autopsy, hemorrhagic meningoencephalitis was observed. Large-sized, basophilic amebic trophozoites are microscopically clustered in Virchow-Robin's spaces. PCR analysis has disclosed infection of *B. mandrillaris*. Immunostaining using both the patient's own serum and the patient's serum of the abovementioned acanthamebic meningoencephalitis gives distinct positivity. Of note is that heat-induced antigen retrieval is needed for visualizing *B. mandrillaris* antigens.

was not cross-reactive to *Naegleria fowleri* (brain-eating amoeba) seen in the autopsied brain of another patient. Regarding acanthamebic keratitis, see **Figure 33**.

Of note is an exception that *Balamuthia* antigens were detectable by the diluted patient's serum only after heating pretreatment of deparaffinized sections in 10 mM citrate buffer, pH 6. Without heat-induced antigen retrieval, signals were not observed at all. Therefore, the author strongly recommends employing the heating pretreatment for immunostaining using patients' sera in order to avoid unexpected false negativity. Silane-coated glass slides should thus be used for preventing section detachment.

6. Concluding remarks

Undoubtedly, the detection of causative pathogens in the inflammatory lesion is the key step directing to the correct histopathological diagnosis of infectious diseases. Even if the specificity of the serum is unknown, the final diagnosis can be reached, based on the morphology and distribution of the positive signals, when combined with tissue reactions, laboratory data and clinical features. In the present article, the author introduced two different approaches using low-specificity antisera. The targets were formalin-fixed and paraffin-embedded sections. One approach is the use of commercially available rabbit antisera showing wide cross-reactivity to a variety of bacteria, and another is the use of diluted patients' sera.

Immunostaining using plural antimicrobial antisera commonly yielded clear positivity with low background, because of poor cross-reactivity of bacterial antigens to human cells and tissues. The approach described here was aimed at visualizing the causative bacteria within infectious lesions in routinely prepared paraffin sections through a wide cross-reactivity shown by low-specificity rabbit antisera against four kinds of bacteria.

Immunostaining using patients' sera is also quite useful in making the histopathological diagnosis. Occasionally, IgG in the patients' sera showed cross-reactivity to related pathogens wider than expected. In bacterial and fungal infection, the sera served as pan-bacterial and pan-fungal probes, respectively. Despite such broad/low specificity, this convenient procedure is excellent in selectively identifying the pathogen within the lesion in question. In viral, protozoal, and

helminthic infection, the specificity was much narrower with limited cross-reactivities, and once the specificity is known, the patients' sera turn to become specific primary antibodies for identifying pathogens in the following new cases.

In the latter approach, what one should do is, instead of ordering an expensive antibody of unknown quality, to make a brief phone call to clinicians or laboratory technicians to ask to save a small aliquot of patients' sera, soon after microscopic confirmation of the host response in histopathology specimens. This is particularly true when specific antibodies are not listed in the commercial catalog. Of note is that informed consent is unnecessary when the patient's serum is utilized primarily for making a diagnosis of the patient's own. When the serum is applied to immunostaining for another case as the primary antibody, the author strongly recommends linking the preserved serum non-anonymously.

The author sincerely hopes that the approaches shown here will be applied to the histopathological diagnosis of infectious diseases in the readers' laboratories.

Acknowledgements

The author deeply thanks many colleagues of technicians who supported the authors' idea and kindly immunostained specimens. The author has no granting for the present study.

Conflict of interest

The author has no conflict of interest in the present study.

Author details

Yutaka Tsutsumi
Pathos Tsutsumi, Toyoake, Aichi, Japan

*Address all correspondence to: pathos223@kind.ocn.ne.jp

IntechOpen

© 2019 The Author(s). Licensee IntechOpen. This chapter is distributed under the terms of the Creative Commons Attribution License (<http://creativecommons.org/licenses/by/3.0>), which permits unrestricted use, distribution, and reproduction in any medium, provided the original work is properly cited. 

References

- [1] World Health Organization. Global Health Observatory (GHO) data. Top 10 causes of death. 2016. Available from: https://www.who.int/gho/mortality_burden_disease/causes_death/top_10/en/
- [2] Tsutsumi Y. Atlas of Infectious Disease Pathology. Bunkodo: Tokyo; 2000. 349 p (in Japanese). Available from: <http://pathos223.com/atlas/index.htm>
- [3] Tsutsumi Y. Pathology of Infectious Diseases. 2003. Available from: <https://pathos223.com/en/>
- [4] Tsutsumi Y. Application of the immunoperoxidase method for histopathologic diagnosis of infectious diseases. *Acta Histochemica et Cytochemica*. 1994;27:547-560
- [5] Azumi N. Immunohistochemistry and *in situ* hybridization techniques in the detection of infectious organisms. In: Connor DH, Chandler FW, Schwartz DA, et al., editors. *Pathology of Infectious Diseases*. Vol. I. Stamford, CT: Appleton & Lange; 1997. pp. 35-44
- [6] Chandler FW. Morphology to molecular biology: Approaches to the pathologic diagnosis of infectious diseases. In: Horsburgh CR, Nelson AM, editors. *Pathology of Emerging Infections*. Washington DC: ASM Press; 1997. pp. 7-19
- [7] Tsutsumi Y. Detection of infectious pathogens in pathology specimens. *Byori-to-Rinsho*. 2003;21:74-91 (in Japanese)
- [8] Tsutsumi Y. Infectious diseases: Bacterial, fungal and protozoan infections. *Byori-to-Rinsho*. 2014;32 (Extra issue: Immunohistochemistry): 306-319 (in Japanese)
- [9] Tsutsumi Y. *Pathology of Skin Infections*. NY, USA: Nova Biomedical; 2013. 378 p. Available from: http://pathos223.com/bookintroduction/pathology_of_skin_infectious.html
- [10] Tsutsumi Y. Infectious diseases. In: Fukayama M, Oda Y, Sakamoto M, et al, editors. *Atlas of Histopathology*, Ver. 6. Tokyo: Bunkodo; 2015. pp. 497-523 (in Japanese)
- [11] Ramos-Vara JA, Miller MA. When tissue antigens and antibodies get along: Revisiting the technical aspects of immunohistochemistry—The red, brown, and blue technique. *Veterinary Pathology*. 2014;51:42-87
- [12] Kabiraj A, Gupta J, Khaitan T, Bhattacharya PT. Principle and techniques of immunohistochemistry: A review. *International Journal of Biological and Medical Research*. 2015;6: 5204-5210
- [13] Tsutsumi Y. Immunohistochemistry. Points of attention for specimen preparation and immunostaining. *I-to-Cho*. 2017;52:973-987 (in Japanese)
- [14] Keasey SL, Schmid KE, Lee MS, et al. Extensive antibody cross-reactivity among infectious Gram-negative bacteria revealed by proteome microarray analysis. *Molecular & Cellular Proteomics*. 2009;8:924-935
- [15] Murray PR, Baron EJ, Pfaller MA, et al., editors. *Manual of Clinical Microbiology*. 7th ed. Washington, DC: ASM Press; 1999
- [16] Fujii M, Mizutani Y, Sakuma T, et al. *Corynebacterium kroppenstedtii* in granulomatous mastitis: Analysis of formalin-fixed, paraffin-embedded biopsy specimens by immunostaining using low-specificity bacterial antisera and real-time polymerase chain reaction. *Pathology International*. 2018; 68:409-418

- [17] Kamoshida S, Satoh Y, Kamiya S, Tsutsumi Y. Heat shock protein 60 (HSP60) immunoreactivity in gastric epithelium associated with *Helicobacter pylori* infection: A pitfall in immunohistochemically interpreting HSP60-mediated autoimmune responses. *Pathology International*. 1999;**49**:88-90
- [18] Gonzalez-Escobedo G, La Perle KMD, Gunn JS. Histopathological analysis of *Salmonella* chronic carriage in the mouse hepatopancreatobiliary system. *PLoS One*. 2013;**8**(12):e84058. DOI: 10.1371/journal.pone.0084058
- [19] Tsutsumi Y. Immunostaining placing more emphasis on sensitivity than specificity. *Kagakuryoho-no-Ryoiki*. 2018;**34**:4-20 (in Japanese)
- [20] Tsutsumi Y, Kawai K, Nagakura K. Use of patients' sera for immunoperoxidase demonstration of infectious agents in paraffin sections. *Acta Pathologica Japonica*. 1991;**41**: 673-679
- [21] Tsutsumi Y. Histopathological diagnosis of infectious diseases using patients' sera. *Seminars in Diagnostic Pathology*. 2007;**24**:243-252
- [22] Tsutsumi Y. Histopathological diagnosis of protozoan infection using patients' sera. In: Ishikura H, editor. *Host Response to International Parasitic Zoonoses*. Tokyo: Springer-Verlag; 1998. pp. 69-81
- [23] Tsutsumi Y. Detection of pathogens using patients' sera. *Kagakuryoho-no-Ryoiki*. 2018;**34**:182-199 (in Japanese)
- [24] Kawai K, Tsutsumi Y. Immunoperoxidase visualization of acid-fast bacilli. A comparison with conventional acid-fast staining. *Byori-to-Rinsho*. 1984;**2**:862-867 (in Japanese)
- [25] Wiley EL, Mulhollan TJ, Beck B, et al. Polyclonal antibodies raised against *Bacillus Calmette-Guérin*, *Mycobacterium duvalii*, and *Mycobacterium paratuberculosis* used to detect mycobacteria in tissue with the use of immunohistochemical techniques. *American Journal of Clinical Pathology*. 1990;**94**:307-312
- [26] Tsutsumi Y. Demonstration of pathogens in archival pathology sections. *Iyaku Journal*. 2018;**54**:939-949 (in Japanese)
- [27] Miller JM, Hair JG, Hebert M, et al. Fulminating bacteremia and pneumonia due to *Bacillus cereus*. *Journal of Clinical Microbiology*. 1997;**35**:504-507
- [28] Tsutsumi Y. Malacoplakia and cystitis. *Byori-to-Rinsho*. 2010;**28**(Extra issue: Pathology Key Words):228-229
- [29] Hori S, Tsutsumi Y. Histologic differentiation between chlamydial and bacterial epididymitis: Non-destructive and proliferative versus destructive and abscess-forming. Immunohistochemical and clinicopathologic findings. *Human Pathology*. 1995;**26**:402-407
- [30] Mori M, Watanabe M, Sakuma M, Tsutsumi Y. Infectious etiology of xanthogranulomatous cholecystitis: Immunohistochemical identification of bacterial antigens in the xanthogranulomatous lesions. *Pathology International*. 1999;**49**:849-852
- [31] Tsutsumi Y. Pathology of respiratory tract infections. *Saishin Igaku Suppl: ABC of Diagnosis and Treatment 129 "Infection of the Respiratory Tract"*. 2017. pp. 29-56 (in Japanese)
- [32] Villanueva SYAM, Saito M, Tsutsumi Y, et al. High virulence in hamsters of four dominant *Leptospira* serovars isolated from rats in Philippines. *Microbiology*. 2014;**160**:418-428
- [33] Mahlen SD. *Serratia* infections: From military experiments to current

- practice. *Clinical Microbiology Reviews*. 2011;**24**:755-791
- [34] Takahashi J, Daa T, Gamachi A, et al. Human intestinal spirochetosis in Japan; its incidence, clinicopathologic features, and genotypic identification. *Modern Pathology*. 2008;**21**:76-84
- [35] Tanaka Y, Matsumoto Y, Shimada N, et al. Identification and characterization of *Brachyspira aalborgi* and *Brachyspira pilosicoli* isolated from humans. *Nihon Rinsho Biseibutugaku Zasshi*. 2016;**26**:30-40 (in Japanese with English abstract)
- [36] Horseman MA, Surani S. A comprehensive review of *Vibrio vulnificus*: An important cause of severe sepsis and skin and soft-tissue infection. *International Journal of Infectious Diseases*. 2011;**15**:e157-e166
- [37] Snyder J, Fisher D. Pertussis in childhood. *Pediatrics in Review*. 2012; **33**:412-420
- [38] Stelter K. Tonsillitis and sore throat in children. *GMS Current Topics in Otorhinolaryngology—Head and Neck Surgery*. 2014;**13**:Doc07. DOI: 10.3205/cto000110
- [39] Sezer B, Akdeniz BG, Günbaya S, et al. Actinomycosis osteomyelitis of the jaws: Report of four cases and a review of the literature. *Journal of Dental Sciences*. 2017;**12**:301-307
- [40] Shariff M, Gunasekaran J. Pulmonary nocardiosis: Review of cases and an update. *Canadian Respiratory Journal*. 2016;**2016**:7494202. DOI: 10.1155/2016/7494202
- [41] Oshima Y, Fujii M, Shiogama K, et al. *Bartonella henselae* infection caused by cat flea bite. *Pathology International*. 2016;**66**:177-179
- [42] Nakamura M, Kurimoto M, Kato T, Kunieda T. Cat-scratch disease presenting as a solitary splenic abscess in an elderly man. *BML Case Reports*. 2015 Mar 24; 2015. DOI: 10.1136/bcr-2015-209597
- [43] Zhou F, Yu L-X, Ma Z-B, et al. Granulomatous lobular mastitis. *Chronic Diseases and Translational Medicine*. 2016;**2**:17-21
- [44] Ahmed ARH, El-Badawy ZH, Mohamed IR, Abdelhameed WAM. Rhinoscleroma: A detailed histopathological diagnostic insight. *International Journal of Clinical and Experimental Pathology*. 2015;**8**:8438-8445
- [45] Yuasa H, Ogiyama H, Fujita Y, et al. A case of rhinoscleroma in nasal cavity. *Shindan Byori*. 2018;**35**:206-209 (in Japanese with English abstract)
- [46] Luce-Fedrow A, Lehman ML, Kelly DJ, et al. A review of scrub typhus (*Orientia tsutsugamushi* and related organisms): Then, now, and tomorrow. *Tropical Medicine and Infectious Diseases*. 2018;**3**(1):8. DOI: 10.3390/tropicalmed3010008
- [47] Tsutsumi Y. Electron microscopic study using formalin-fixed, paraffin-embedded material, with special reference to observation of microbial organisms and endocrine granules. *Acta Histochemica et Cytochemica*. 2018;**51**: 63-71
- [48] de Lima Barros MB, de Almeida Paes R, Schubach AO. *Sporothrix schenckii* and sporotrichosis. *Clinical Microbiology Reviews*. 2011;**24**:633-654
- [49] Prindaville B, Belazarian L, Levin NA, Wiss K. Pityrosporum folliculitis: A retrospective review of 110 cases. *Journal of the American Academy of Dermatology*. 2018;**78**:511-514
- [50] Ono M, Nishigori C, Tanaka C, et al. Cutaneous alternans in an immunocompetent patient: Analysis of

- the internal transcribed spacer region of rDNA and Brm2 of isolated *Alternaria alternata*. The British Journal of Dermatology. 2004;**150**:773-775
- [51] Dimino-Emme L, Gurevitch AW. Cutaneous manifestations of disseminated cryptococcosis. Journal of the American Academy of Dermatology. 1995;**32**:844-850
- [52] Suwabe H, Yabe H, Tsutsumi Y. Relapsing hemorrhagic varicella. Pathology International. 1996;**46**: 605-609
- [53] Arvin AM, Kinney-Thomas E, Shriver K, et al. Immunity to varicella-zoster viral glycoproteins, gp I (gp 90/58) and gp III (gp 118), and to a nonglycosylated protein, p 170. Journal of Immunology. 1986;**137**:1346-1351
- [54] Paz C, Samake S, Anderson JM, et al. *Leishmania major*, the predominant *Leishmania* species responsible for cutaneous leishmaniasis in Mali. The American Journal of Tropical Medicine and Hygiene. 2013; **88**:583-585
- [55] Kumar R, Bumb RA, Ansari NA, et al. Cutaneous leishmaniasis caused by *Leishmania tropica* in Bikaner, India: Parasite identification and characterization using molecular and immunologic tools. The American Journal of Tropical Medicine and Hygiene. 2007;**76**:896-901
- [56] Lorenzo-Morales J, Khan NA, Walochnik J. An update on *Acanthamoeba* keratitis: Diagnosis, pathogenesis and treatment. Parasite. 2015;**22**:10. DOI: 10.1051/parasite/2015010
- [57] Takashima Y, Kimura M, Watanabe K, et al. A case of *Acanthamoeba* keratitis with histological detection of trophozoites and cysts. Shindan Byori. 2018;**35**:54-58 (in Japanese with English abstract)
- [58] Mackey-Lawrence NM, Petri WA Jr. Amoebic dysentery. Clinical Evidence. 2011;**01**:918. PMID: 21477391
- [59] Saadatnia G, Golkar M. A review on human toxoplasmosis. Scandinavian Journal of Infectious Diseases. 2012;**44**: 805-814
- [60] Rossle NF, Latif B. Cryptosporidiosis as threatening health problem: A review. Asian Pacific Journal of Tropical Biomedicine. 2013;**3**:916-924
- [61] Post L, Garnaud C, Maubon D, et al. Uncommon and fatal case of cystoisosporiasis in a non HIV-immunosuppressed patient from a non-endemic country. Parasitology International. 2018;**67**:1-3
- [62] Agholi M, Aliabadi E, Hatam GR. Cystoisosporiasis-related human acalculous cholecystitis: The need for increased awareness. Polish Journal of Pathology. 2016;**67**:270-276
- [63] Babb RR, Wagener S. *Blastocystis hominis*: A potential intestinal pathogen. The Western Journal of Medicine. 1989; **151**:518-519
- [64] Kaneda Y, Horiki N, Cheng X-J, et al. Serologic response to *Blastocystis hominis* infection in asymptomatic individuals. The Tokai Journal of Experimental and Clinical Medicine. 2000;**25**:51-56
- [65] Ligon BL. Gnathostomiasis: A review of a previously localized zoonosis now crossing numerous geographical boundaries. Seminars in Pediatric Infectious Diseases. 2005;**16**:137-143
- [66] Sakanari JA, McKerrow JH. Anisakiasis. Clinical Microbiology Reviews. 1989;**2**:278-284
- [67] Ishii A, Tsuji M, Tada I. History of Katayama disease: Schistosomiasis japonica in Katayama district,

Hiroshima, Japan. Parasitology International. 2003;52:313-319

[68] Zhou Y-B, Zheng H-M, Jiang Q-W. A diagnostic challenge for schistosomiasis japonica in China: Consequences on praziquantel-based morbidity control. Parasites Vectors. 2011;4:194. DOI: doi.org/10.1186/1756-3305-4-194

[69] Gray DJ, Ross AG, Li Y-S, McManus DP. Diagnosis and management of schistosomiasis. British Medical Journal. 2011;342:d2651. DOI: 10.1136/bmj.d2651

[70] Takahashi K, Uruguchi K, Kudo S. The epidemiological status of *Echinococcus multilocularis* in animals in Hokkaido, Japan. Mammal Study. 2005; 30:S101-S105

[71] Gripper LB, Welburn SC. Neurocysticercosis infection and disease. A review. Acta Tropica. 2017; 166:218-224

[72] Achermann Y, Goldstein EJC, Coenye T, Shirliff ME. *Propionibacterium acnes*: From commensal to opportunistic biofilm-associated implant pathogen. Clinical Microbiology Reviews. 2014;27:419-440

[73] Eishi Y. Propionibacterium Acnes as a Cause of Sarcoidosis. InTechOpen (Open Access Peer-reviewed Chapter), London, U.K; 2013. DOI: 10.5772/55073

[74] Das AK. Hepatic and biliary ascariasis. Journal of Global Infectious Diseases. 2014;6:65-72

[75] Nagakura K, Tsutsumi Y, Moriya H, et al. Serologic findings in hepatic ascariasis: A case report. The Tohoku Journal of Experimental Medicine. 1992; 167:121-126

[76] Bi K, Chen Y, Zhao S, et al. Current visceral leishmaniasis research: A research review to inspire future study.

BioMed Research International. 2018, Article ID 9872095. DOI: 10.1155/2018/9872095

[77] Nagata H, Kato G, Kimura M, Okabe H. A case of kala azar. Shindan Byori. 2001;18:388-391 (in Japanese)

[78] Trabelsi H, Dendana F, Sellami A, et al. Pathogenic free-living amoebae: Epidemiology and clinical review. Pathologie-biologie. 2012;60:399-405

[79] Tsutsumi Y, Tachibana H, Azuma S, et al. Acanthoamebic meningoencephalitis associated with alcoholic liver cirrhosis. Pathology Case Reviews. 2002;7:273-277

[80] Jung S, Schelper RL, Visvesvara GS, Chang HT. *Balamuthia mandrillaris* meningoencephalitis in an immunocompetent patient. Archives of Pathology & Laboratory Medicine. 2004;128:466-468

[81] Siddiqui R, Khan NA. *Balamuthia mandrillaris*: Morphology, biology, and virulence. Tropical Parasitology. 2015;5: 15-22

In Situ Identification of Ectoenzymes Involved in the Hydrolysis of Extracellular Nucleotides

Mireia Martín-Satué, Aitor Rodríguez-Martínez and Carla Trapero

Abstract

Adenosine triphosphate (ATP) and other nucleotides and nucleosides, such as adenosine, are signaling molecules involved in many physiological and pathophysiological processes. The group of cell and tissue responses mediated by these molecules is known as purinergic signaling. Ecto-nucleotidases are ectoenzymes expressed at the cell membrane that act sequentially to efficiently hydrolyze extracellular ATP into adenosine, and they are key elements of this signaling. There is growing interest in studying these enzymes in relation to various pathologies, especially those with an inflammatory component such as cancer. This review summarizes the main protocols for the study of the expression and in situ activity of ectoenzymes in tissue slices and cultured cells.

Keywords: nucleotidase, in situ histochemistry, CD39, CD73, lead staining

1. Introduction

In this chapter, we intend to detail basic protocols for the in situ detection of ecto-nucleotidases as an introduction to the technique for those who have never made these experimental approaches. This chapter does not aim to be a review on ecto-nucleotidases because there are already excellent highly recommended reviews [1–4].

Ecto-nucleotidases are broadly expressed enzymes active in almost all tissues of all organisms, both animals and plants. What varies among the cell (and tissue) types are the subtype(s) of enzyme(s) and the combination of them, expressed in a particular cell type. In general, these enzymes convert adenosine triphosphate (ATP), as well as diphosphate (ADP) and monophosphate (AMP), into adenosine. In situ detection of these enzymes confers functional sense on immunodetection studies. It is also a convenient tool for the validation of new inhibitors of these enzymes, which can be studied in the cell context of the tissue where they are found. The study of ecto-nucleotidases and their inhibitors (many of them antibodies) is at the center of oncological research to therapeutically target the adenosinergic pathway, a fact reflected in the increased number of high impact publications in the field.

The technique is feasible because ecto-nucleotidases maintain their activity of hydrolyzing nucleotides in formalin-fixed frozen tissues (and cells). Inorganic phosphorous (Pi) generated upon their activity combines with a lead salt added to the reaction mixture, forming brown precipitates in the places where the enzymes are active, which can be visualized under light microscope. The protocol, with slight modifications, can also be used for electron microscopy.

There are four families of membrane-bound ecto-nucleotidases. Other nucleotidases act intracellularly but are not studied here. The main features of ecto-nucleotidases are included in **Figure 1** and summarized below.

1.1 Ecto-nucleoside triphosphate diphosphohydrolases (E-NTPDases)

The E-NTPDase family is composed of eight members, four of which are cell surface-located: NTPDase1, also known as CD39; NTPDase2 or CD39L1; NTPDase3 or CD39L3; and NTPDase8. They perform the ATP (and ADP) hydrolysis to AMP with different ADP production abilities. These differences between enzymes reflect different consequences in cells depending on the ATP receptors expressed [5]. The four members display similar structural properties, with two transmembrane domains, close to the N and C terminus, and a catalytic extracellular domain [3]. They require millimolar concentrations of Mg^{2+} and Ca^{2+} ions in order to perform ATP hydrolysis, and the absence of these ions results in no enzymatic activity. All of them hydrolyze nucleoside triphosphates (NTP), but they differ in substrate specificity. NTPDase1 hydrolyzes ATP and ADP equally, while NTPDase3 and NTPDase8 hydrolyze ATP or uridine triphosphate (UTP) more efficiently than ADP or uridine diphosphate (UDP). Finally, the NTPDase2 is the most ATP-specific NTPDase, and for this reason it is also named the ecto-ATPase [2].

Most of the available NTPDase inhibitors are ATP analogues such as ARL-67156 and PSB-6426, a potent NTPDase2 inhibitor. Non-nucleotide-based inhibitors also described in literature are compounds related to dyes bearing sulfonate groups such

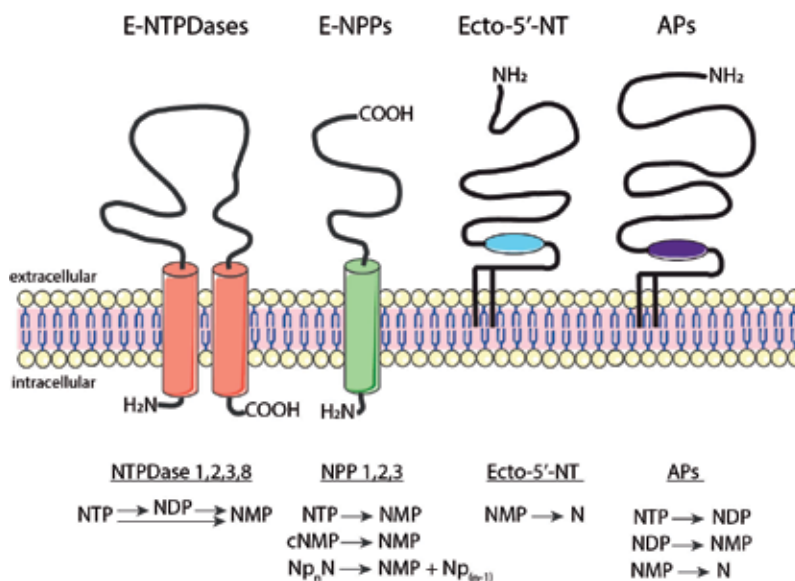


Figure 1. Schematic representation of the four families of membrane-bound ecto-nucleotidases and their substrate specificities. E-NTPDases, ecto-nucleoside triphosphate diphosphohydrolases; E-NPPs, ecto-nucleotide pyrophosphatase/phosphodiesterases; ecto-5'-NT, ecto-5'-nucleotidase; APs, alkaline phosphatases; NTP, nucleoside triphosphate; NDP, nucleoside diphosphate; NMP, nucleoside monophosphate; cNMP, cyclic nucleoside monophosphate; N, nucleoside.

as suramin, a nonselective inhibitor, and the pyridoxal phosphate-6-azophenyl-2',4'-disulfonic acid (PPADS). Other inhibitors are the polyoxometalates, such as POM 1 [6]. Inhibitory antibodies, mainly against CD39, are being developed for use in cancer therapy [7].

1.2 Ecto-nucleotide pyrophosphatases/phosphodiesterases (E-NPPs)

The E-NPP family represents a versatile group of seven structurally related enzymes with pyrophosphatase and phosphodiesterase activities having a wide range of hydrolysable substrates. The membrane-bound ectoenzymes NPP1 and NPP3 and the secreted NPP2 are the most studied members. Catalytic activity of E-NPPs is composed of a two-step hydrolysis consisting of a first attack on the phosphate of the incoming substrate by a threonine/serine metal-activated catalytic site and a second attack on the intermediate substrate by a metal-activated site, thus releasing a nucleoside 5'-monophosphate. In general, NPP1–3 are typed as alkaline ecto-nucleotide pyrophosphatases that hydrolyze a number of phosphodiester bonds (e.g., from oligonucleotides, lysophosphatidylcholine, sphingomyelin, and glycerophosphorylcholine or from artificial substrates like the p-nitrophenyl 5'-thymidine monophosphate (p-Nph-5'-TMP)) and pyrophosphate bonds (e.g., from (d)NTPs, (d)NDPs, NAD, FAD, and UDP sugars or from artificial substrates like the thiamine pyrophosphate (TPP)) to generate nucleoside 5'-monophosphates. TPP is the “false” substrate mainly used for NPP identification in *in situ* activity assays. Like most of the enzymes, E-NPPs can be inhibited *in vitro* by the substrates and products of the NPP reaction, as well as by heparin and heparan sulfate glycosaminoglycans, and by other substances such as imidazole, 2-mercaptoethanol, and metal ion-chelating agents [8]. Anti-NPP3 inhibitory antibody represents a promising therapeutic tool for the treatment of renal cell carcinoma [9].

1.3 Ecto-5'-nucleotidase (ecto-5'-NT, eN)/CD73

Extracellular AMP resulting from the hydrolysis of ATP and ADP by most of the ecto-nucleotidases can in turn be efficiently hydrolyzed into adenosine by eN, a glycosylphosphatidylinositol-linked membrane-bound glycoprotein also known as CD73 [10], which hydrolyses nucleotide-5'-monophosphates (NMP) [3]. It is broadly expressed as an alpha dimer bound with disulfide bridges and shows different functions depending on the cell type. Although eN activity is ion-independent in physiological conditions, *in vitro* the presence of Mg^{2+} ions can considerably increase its ability to hydrolyze AMP. In addition to its AMPase activity, eN hydrolyzes 2-deoxyribose compounds but much less effectively than AMP. Unlike other ectoenzymes such as NPPs, eN is not inhibited by Pi. Alpha,beta-methylene-ADP and some of its derivatives and analogues are efficient inhibitors [11]. Inhibitory anti-CD73 antibodies are used in clinical trials [7].

1.4 Alkaline phosphatases (APs)

Phosphatases are a superfamily of proteins that mediate the phosphate removal of proteins and other substrates [12]. Depending on their substrate specificity, they are divided into two major groups: the protein phosphatases, which mediate the hydrolysis of phosphate groups from protein residues (e.g., serine/threonine phosphatases), and the membrane-bound phosphatases, which mediate the hydrolysis of phosphate groups from nonprotein substrates (e.g., acid and alkaline phosphatases). In this chapter, we are focusing on the membrane-bound phosphatases, in particular the AP family [12, 13].

APs are zinc-containing dimeric membrane-bound glycoproteins that require magnesium ion for the hydrolysis of a wide range of phosphomonoesters. Although optimum activity occurs at alkaline pH (9.3–10.3), they are also active at a physiological pH, and they are primarily responsible for the P₁i phosphohydrolysis in neutral and alkaline environments. APs are classified by their tissue expression and distribution [14]; in humans there are four types of APs in two main groups: the tissue nonspecific alkaline phosphatase (TNAP), with only one member, and the tissue-specific APs, which include the placental-like alkaline phosphatase (PLAP), the germ cell alkaline phosphatase (GCAP), and the intestinal alkaline phosphatase (IAP). Despite the fact that TNAP expression is not tissue-specific, it is mainly found in the liver, bone, and kidneys [15].

APs catalyze the hydrolysis of monoesters of phosphoric acids and have extensive substrate specificity *in vitro*. For example, TNAP is able to hydrolyze ATP, ADP, AMP, P₁i, glucose-1-phosphate, glucose-6-phosphate, fructose-6-phosphate, and β -glycerophosphate; however, only a few compounds have been considered as natural *in vivo* AP substrates, like P₁i, pyridoxal-5'-phosphate (PLP or vitamin B₅), and phosphoethanolamine (PEA). APs by themselves are extremely efficient ATPase enzymes, but an autoregulatory mechanism has been described in order to modify the substrate specificity depending on the environmental concentrations of free inorganic phosphates or cell and tissue demands. Pi itself is known to inhibit the hydrolytic activity through a competitive mechanism, and therefore Pi levels will impact the ability of AP to hydrolyze P₁i [15, 16]. Levamisole is an inhibitor of the APs. Because of the ability to cleave all forms of adenosine phosphates, APs significantly influence purinergic signaling [17].

2. In situ nucleotidase activity experiments

The protocol detailed here for the detection of E-NTPDases, E-NPPs, and eN is based on the Wachstein-Meisel lead phosphate method [18], and the protocol for AP identification is based on the Gossrau method [19], with some modifications.

2.1 Wachstein-Meisel lead phosphate-based method

2.1.1 In tissue samples

Tissue pieces are fixed with 4% paraformaldehyde for a time period varying from a few hours to 2 days depending on the size (**Figure 2**). Following fixation, tissue pieces are cryopreserved by embedding them in 30% sucrose (in Milli-Q H₂O) O/N or until tissue sinks. Tissues are then embedded in optimum cutting temperature (OCT) compound and cut with a cryostat into 15 μ m-thick sections that are put on slides. It is recommended that pretreated slides be used, either homemade polylysine-treated or the commercial ones, to eliminate tissue loss during the procedure. Sections are stored at -20°C until use.

Tissue slides are rinsed with phosphate buffered saline (PBS) to remove OCT compound and washed twice with 50 mM Tris-maleate buffer pH 7.4 at RT. Slides are then incubated for 30 min at RT with preincubation buffer (50 mM Tris-maleate buffer pH 7.4 containing 2 mM MgCl₂ and 250 mM sucrose) and then for 1 h at 37°C with the enzyme reaction buffer (50 mM Tris-maleate buffer pH 7.4 supplemented with 250 mM sucrose, 2 mM MgCl₂, 5 mM MnCl₂, 2 mM Pb(NO₃)₂, and 2 mM

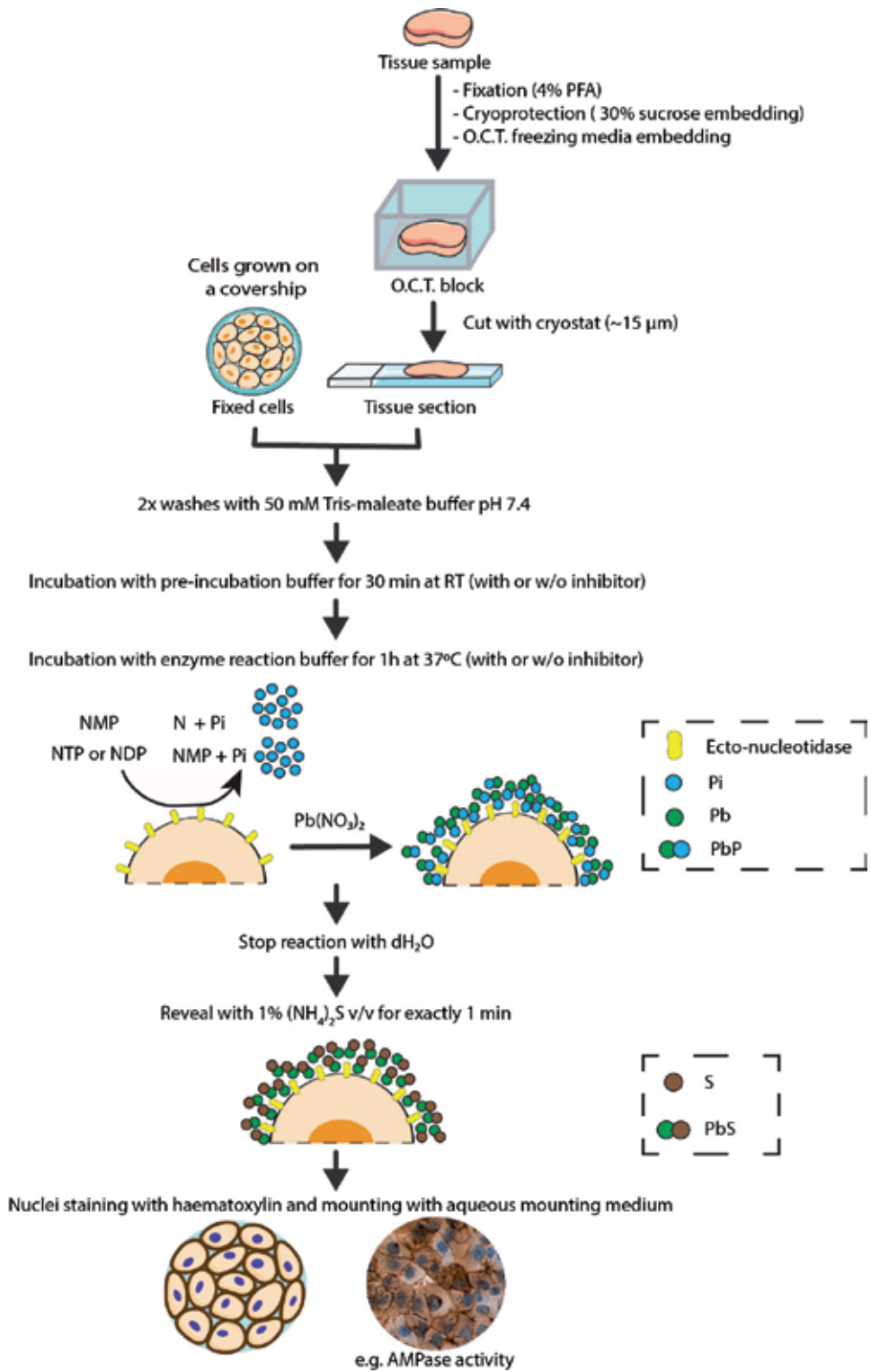


Figure 2. Scheme including the main steps of the lead phosphate-based method for ecto-nucleotidase activity detection.

CaCl₂ and stabilized with 3% Dextran T-250) in the presence or absence of nucleotide as substrate (e.g., ATP). The incubation time and the substrate concentration may vary depending on the experiment, but 1 h at 1 mM is generally suitable. To avoid interference with AP activity, experiments are performed in the presence of the inhibitor levamisole (2.5 mM). Note that the optimum pH for APs is 9, but they are also active at a pH of 7.4. The reaction is stopped with dH₂O and revealed by incubating with 1% (NH₄)₂S v/v for exactly 1 min. A control slide in the absence of nucleotide, in which no reaction is expected, is included in the experiment. Nuclei are counterstained with hematoxylin. Samples are then mounted with aqueous mounting medium (e.g., Fluoromount™, Sigma-Aldrich); dehydration is not recommended because of the eventual loss of lead precipitates. Finally, samples are observed and photographed under light microscope; enzyme-active sites are brownish black. An adapted protocol with slight modifications, including the replacement of ammonium sulfide by glutaraldehyde, can be applied for electron microscopy [20]. **Table 1** includes buffer formulations.

PRE-INCUBATION BUFFER			
Reagent	Stock Solution	Final Concentration	Volume (iV=1mL)
Tris-maleate	200 mM	50 mM	250 µL
Sucrose	1 M	0.25 M	250 µL
MgCl ₂	1 M	2 mM	2 µL
Milli-Q H ₂ O	/	/	498 µL

ENZYME REACTION BUFFER			
Reagent	Stock Solution	Final Concentration	Volume (iV=1mL)
Tris-maleate	200 mM	50 mM	250 µL
Sucrose	1 M	0.25 M	250 µL
Dextran	10 %	3 %	300 µL
MnCl ₂	1 M	5 mM	5 µL
MgCl ₂	1 M	2 mM	2 µL
CaCl ₂	1 M	2 mM	2 µL
Levamisole	250 mM	2.5 mM	10 µL
Pb(NO ₃) ₂	1 M	2 mM	2 µL
Substrate	10 mM	1 mM	100 µL
Milli- Q H ₂ O	/	/	79 µL

Table 1. Formulation of buffers used for the lead phosphate-based method. The most right column includes the reagent amounts calculated to prepare a 1 mL final volume (FV) solution. Different nucleotides can be used as substrate. Inhibitors can also be added to both preincubation and reaction buffers; H₂O to adjust the volume must then be modified accordingly.

Besides levamisole, enzyme inhibitors might be included in both preincubation and incubation buffers. For example, 1 mM α,β-methylene-ADP efficiently inhibits CD73, and POM 1 inhibits NTPDases (**Figure 3**).

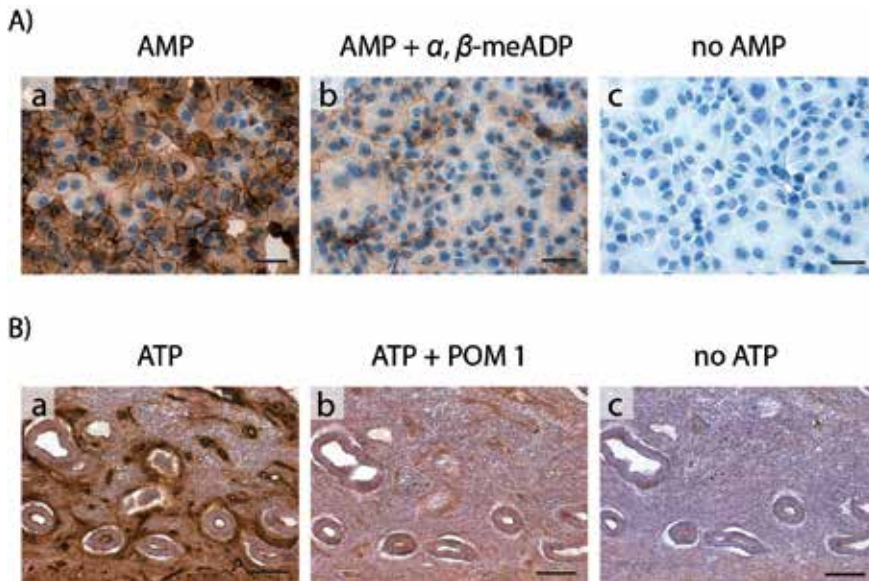


Figure 3.
(A) *In situ* AMPase activity in the endometrial carcinoma human HEC-1B cell line in the presence of 1 mM AMP (a). Note that most of the activity is located at the cell membrane, where CD73 is expressed. Incubation in the presence of the inhibitor α,β -methylene-ADP (α,β -meADP) drastically diminished the activity (b). No AMPase activity is detected when AMP is omitted in the reaction (c). (B) *In situ* enzyme ATPase activity in human endometrium in the presence of 1 mM ATP (a). Activity is strongly inhibited with the NTPDase inhibitor POM 1 (b). No ATP activity is detected when ATP is omitted (c). Scale bars are 50 μm (a) and 200 μm (B).

2.1.2 In cell cultures

Cells are seeded onto coverslips and allowed to grow with their regular medium until the desired confluence is achieved. The medium is then removed, and the cells are washed twice with PBS before fixation with 4% paraformaldehyde for 5–10 min at RT. Cells are washed three times with PBS to wash out the fixative and kept at 4°C with PBS until use. To proceed with the protocol, coverslips are washed twice for 5 min with gentle rocking with 50 mM Tris-maleate buffer pH 7.4 at RT and then incubated for 30 min at RT with the preincubation buffer. The following steps are as reported for the tissue slices.

2.2 Gossrau-based method for APs

In situ localization of APs can be addressed by using the Gossrau method that utilizes nitroblue tetrazolium (NBT) and 5-bromo-4-chloro-3-indolyl phosphate (BCIP) as artificial substrates for the APs. Briefly, tissue slices or fixed cells grown on coverslips are washed twice in 0.1 M Tris-HCl buffer pH 7.4 containing 5 mM MgCl_2 and then preincubated with the same buffer at pH 9.4 for 15 min at RT. Enzymatic reaction starts by adding the revealing reagent BCIP/NBT (Sigma-Aldrich) for 7 min (up to 15 min) at RT and stopped with 0.1 M Tris-HCl buffer pH 7.4. In AP inhibition experiments, 5 mM levamisole can be added to both preincubation and enzyme reaction buffers. In control experiments, the revealing reagent is omitted. Since the reaction generates blue precipitates, nuclei staining with hematoxylin should be avoided. Alternatively nuclei can be counterstained with methyl green dye. Samples are then mounted with aqueous mounting medium (e.g., Fluoromount™, Sigma-Aldrich) and observed and photographed under light microscope.

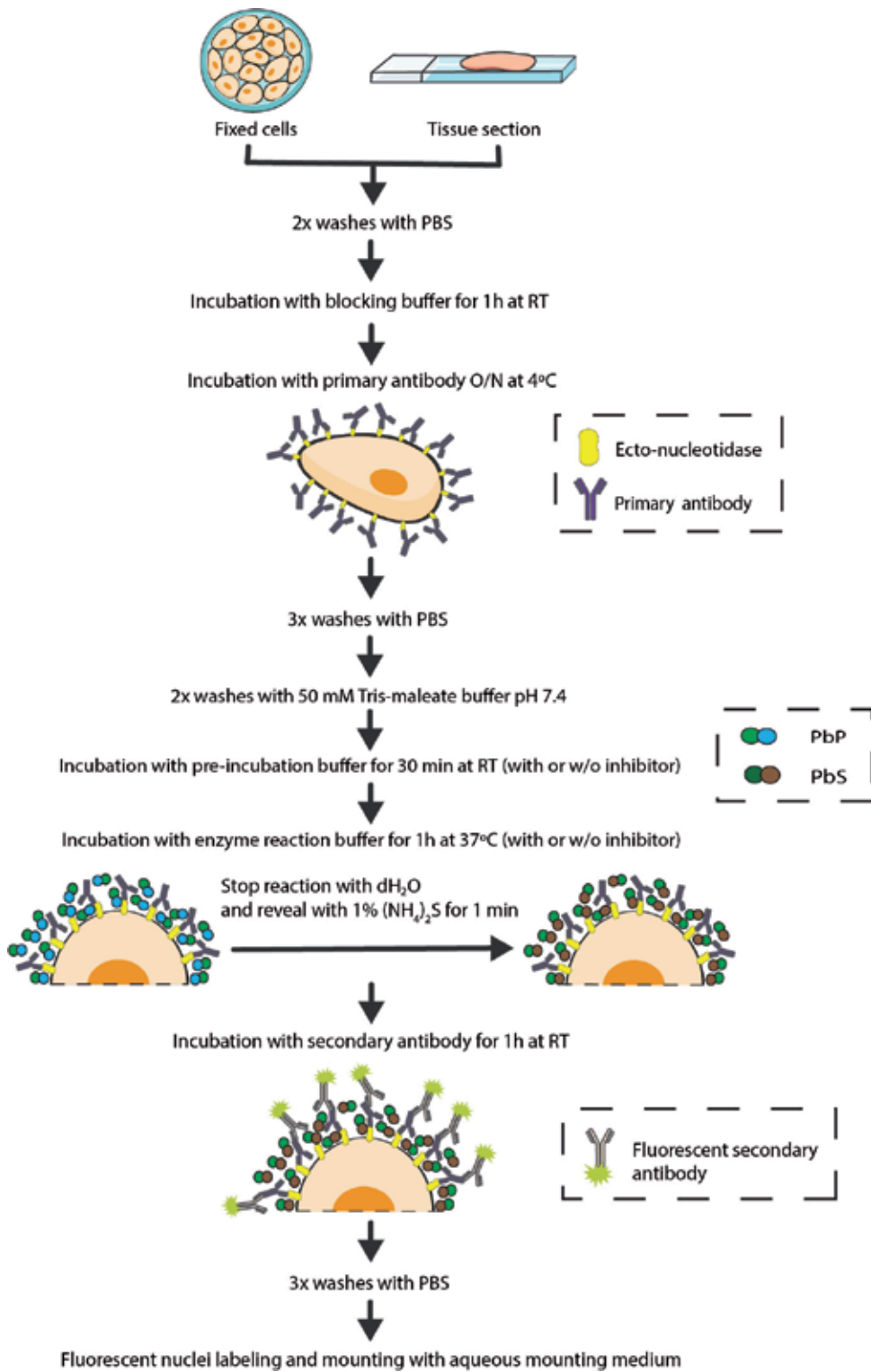


Figure 4. Scheme including the main steps of the method combining immunofluorescence and in situ ecto-nucleotidase activity detection protocols.

2.3 Combined immunolabeling and in situ nucleotidase activity experiments

The technique uses the same tissue slide (or the same coverslip of cells) to identify both the activity, with in situ histochemistry (or cytochemistry), and the protein, with immunofluorescence (**Figure 4**) [21, 22]. Tissue sample sections or fixed cells grown on coverslips are washed twice with PBS and incubated with a blocking solution containing 20% normal goat serum and 0.2% gelatin in PBS at RT for 1 h and then incubated O/N at 4°C with the appropriate primary antibody. The samples are washed three times with PBS and twice with 50 mM Tris-maleate buffer. In situ nucleotidase activity experiment is performed as detailed previously, adding the appropriate nucleotide as substrate. Subsequently, the tissues are washed three times in PBS before incubating with the appropriate fluorescent-labeled secondary antibody. After three final washes with PBS, nuclei are labeled, and the samples mounted with aqueous mounting medium; a mounting medium containing DAPI can be used for this purpose (e.g., ProLong Gold antifade reagent with DAPI mounting medium from Thermo Fisher Scientific). The sections are observed and photographed under a Nikon Eclipse E800 Microscope. Pictures of bright field (for activity) and fluorescence (for protein immunolocalization and nuclei visualization) are taken sequentially from the same field.

We recommend that histochemistry be performed between primary and secondary antibody incubations, but other protocols are also feasible. This is of interest when using inhibitory antibodies. In these cases the in situ histochemistry should be performed at the beginning of the procedure. It also has to be taken into account that it might be necessary to test different nucleotide concentrations and incubation times in order to optimize the results for a particular tissue in order to minimize hampering of fluorescence capture by the dark brown lead deposits.

Figures 5 and 6 are examples of this combined technique in tissue and cell culture, respectively. **Figure 5** shows immunofluorescence to localize NTPDase1, and in situ histochemistry for the ADPase activity in human fallopian tubes. The

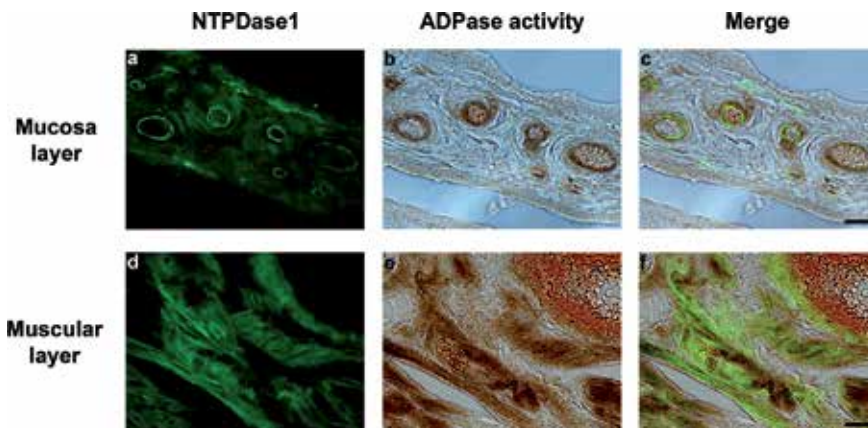


Figure 5. Immunolocalization of NTPDase1 (a, d) and in situ ADPase histochemistry (b, e) in cryosections of human oviducts. NTPDase1 was detected with immunofluorescence in endothelial cells of lamina propria (a) and in smooth muscle cells (d). Microphotographs b and e show dark brown deposits corresponding to in situ ADPase activity. Merge images (c, f) confirmed that NTPDase1 is active in the same structures where it immunolocalizes. Reddish structure at top right of image is the blood inside the vessel. Scale bar is 25 μm . Reprinted by permission of Springer Nature Histochemistry and Cell Biology, Characterization of Ecto-nucleotidases in Human Oviducts with an Improved Approach Simultaneously Identifying Protein Expression and In Situ Enzyme Activity, Villamonte et al. [21].

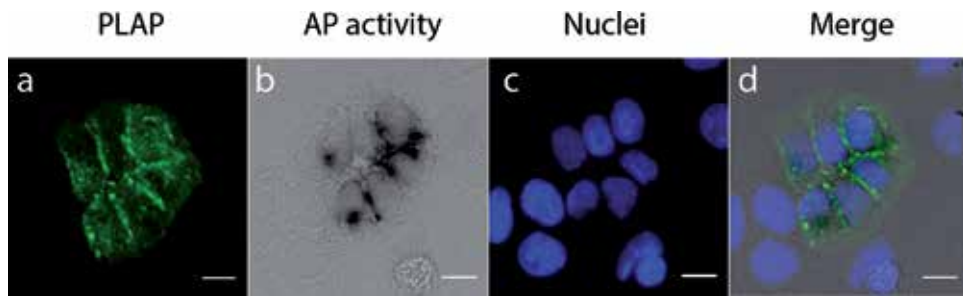


Figure 6. Placental-like alkaline phosphatase (PLAP) immunofluorescence (a) and *in situ* enzyme AP activity (b) in the Ishikawa endometrial carcinoma cell line. Nuclei are labeled with DAPI (c). Merge image (d) shows that precipitates are formed in cells expressing PLAP. Note that activity microphotograph (b) was obtained in gray scale, and in consequence blue deposits are visualized in black. Scale bar is 25 μm .

antibodies used were mouse antihuman NTPDase1 primary antibody (clone BU-61, Ancell) and Alexa Fluor 488 goat anti-mouse secondary antibody (Thermo Fisher Scientific). Label is seen together with the lead precipitate in endothelium of blood vessels, especially abundant in the lamina propria of the mucosa layer, and in muscle cells, predominant in the muscular layer [21]. In **Figure 6**, the antibody against human placental-like alkaline phosphatase (PLAP; clone 8B6, Sigma-Aldrich) was used in Ishikawa cells to localize the protein by immunofluorescence, together with the activity obtained with the BCIP/NBT reagent.

3. Conclusions

In conclusion, *in situ* histochemistry for ecto-nucleotidases is an easy-to-perform, reproducible technique suitable for tissues and cells. The combined technique allows identification of the protein that has a precise enzyme activity. The technique is suitable for testing enzyme inhibitors.

Acknowledgements

This study was supported by a grant from the Instituto de Salud Carlos III (FIS PI15/00036), co-funded by FEDER funds/European Regional Development Fund (ERDF)—“a Way to Build Europe”—/FONDOS FEDER “una manera de hacer Europa”, and a grant from the Fundaci3n Merck Salud (Ayuda Merck de Investigaci3n 2016-Fertilidad). ARM was awarded a fellowship from the Asociaci3n Espa3ola Contra el C3ncer (AECC). We thank CERCA Programme (Generalitat de Catalunya) for the institutional support. We are grateful to Serveis Científics I Tecnol3gics (Campus Bellvitge, Universitat de Barcelona) for the technical support. The authors thank Tom Yohannan for language editing.

Figure 5 is reprinted by permission of Springer Nature Histochemistry and Cell Biology, Characterization of ecto-nucleotidases in human oviducts with an improved approach simultaneously identifying protein expression and *in situ* enzyme activity, Villamonte et al. [21]. License number: 4487101229606.

Conflict of interest

The authors declare that there is no conflict of interest regarding the publication of this book chapter.

Author details

Mireia Martín-Satué*, Aitor Rodríguez-Martínez and Carla Trapero
Unit of Histology, Department of Pathology and Experimental Therapeutics,
Faculty of Medicine and Health Sciences, University of Barcelona; Bellvitge
Biomedical Research Institute (IDIBELL)—CIBERONC, Barcelona, Spain

*Address all correspondence to: martinsatue@ub.edu

IntechOpen

© 2019 The Author(s). Licensee IntechOpen. This chapter is distributed under the terms of the Creative Commons Attribution License (<http://creativecommons.org/licenses/by/3.0>), which permits unrestricted use, distribution, and reproduction in any medium, provided the original work is properly cited. 

References

- [1] Yegutkin GG. Nucleotide- and nucleoside-converting ectoenzymes: Important modulators of purinergic signalling cascade. *Biochimica et Biophysica Acta*. 2008;**1783**(5):673-694
- [2] Yegutkin GG. Enzymes involved in metabolism of extracellular nucleotides and nucleosides: Functional implications and measurement of activities. *Critical Reviews in Biochemistry and Molecular Biology*. 2014;**49**(6):473-497
- [3] Zimmermann H, Zebisch M, Strater N. Cellular function and molecular structure of ecto-nucleotidases. *Purinergic Signalling*. 2012;**8**(3):437-502
- [4] Al-Rashida M et al. Ectonucleotidase inhibitors: A patent review (2011-2016). *Expert Opinion on Therapeutic Patents*. 2017;**27**(12):1291-1304
- [5] Robson SC, Sévigny J, Zimmermann H. The E-NTPDase family of ectonucleotidases: Structure function relationships and pathophysiological significance. *Purinergic Signal*. 2006;**2**(2):409-430
- [6] Baqi Y. Ecto-nucleotidase inhibitors: Recent developments in drug discovery. *Mini Reviews in Medicinal Chemistry*. 2015;**15**(1):21-33
- [7] Vijayan D et al. Targeting immunosuppressive adenosine in cancer. *Nature Reviews. Cancer*. 2017;**17**(12):709-724
- [8] Hosoda N et al. Inhibition of phosphodiesterase/pyrophosphatase activity of PC-1 by its association with glycosaminoglycans. *European Journal of Biochemistry*. 1999;**265**(2):763-770
- [9] Doñate F et al. AGS16F is a novel antibody drug conjugate directed against ENPP3 for the treatment of renal cell carcinoma. *Clinical Cancer Research*. 2016;**22**(8):1989-1999
- [10] Colgan SP et al. Physiological roles for ecto-5'-nucleotidase (CD73). *Purinergic Signalling*. 2006;**2**(2):351-360
- [11] Bhattarai S et al. Alpha, beta-methylene-ADP (AOPCP) derivatives and analogues: Development of potent and selective ecto-5'-nucleotidase (CD73) inhibitors. *Journal of Medicinal Chemistry*. 2015;**58**(15):6248-6263
- [12] Fahs S, Lujan P, Kohn M. Approaches to study phosphatases. *ACS Chemical Biology*. 2016;**11**(11):2944-2961
- [13] Millán JL. The role of phosphatases in the initiation of skeletal mineralization. *Calcified Tissue International*. 2013;**93**(4):299-306
- [14] Lowe D, John S. *Alkaline Phosphatase*. Treasure Island (FL): StatPearls; 2018
- [15] Buchet R, Millán JL, Magne D. Multisystemic functions of alkaline phosphatases. *Methods in Molecular Biology*. 2013;**1053**:27-51
- [16] Simko V. Alkaline phosphatases in biology and medicine. *Digestive Diseases*. 1991;**9**(4):189-209
- [17] Sebastián-Serrano Á et al. Tissue-nonspecific alkaline phosphatase regulates purinergic transmission in the central nervous system during development and disease. *Computational and Structural Biotechnology Journal*. 2015;**13**:95-100
- [18] Wachstein M, Meisel E. Histochemistry of hepatic phosphatases of a physiologic pH; with special reference to the demonstration of bile canaliculi. *American Journal of Clinical Pathology*. 1957;**27**(1):13-23
- [19] Gossrau R. Azoindoxyl methods for the investigation of hydrolases. IV.

Suitability of various diazonium salts
(author's transl). *Histochemistry*.
1978;57(4):323-342

[20] Kirino M et al. Evolutionary origins of taste buds: Phylogenetic analysis of purinergic neurotransmission in epithelial chemosensors. *Open Biology*. 2013;3(3):130015

[21] Villamonte ML et al. Characterization of ecto-nucleotidases in human oviducts with an improved approach simultaneously identifying protein expression and in situ enzyme activity. *Histochemistry and Cell Biology*. 2018;149(3):269-276

[22] Langer D et al. The ectonucleotidases alkaline phosphatase and nucleoside triphosphate diphosphohydrolase 2 are associated with subsets of progenitor cell populations in the mouse embryonic, postnatal and adult neurogenic zones. *Neuroscience*. 2007;150(4):863-879

Edited by Charles F. Streckfus

Immunohistochemistry - The Ageless Biotechnology is a book that is ideal for undergraduate and graduate biomedical researchers, and medical and dental health professionals. It is a detailed text, which emphasizes the laboratory and clinical implications of immunohistochemistry. The text covers the advances of immunohistochemistry from its humble origins in the 1930s up to the new decade of 2020. The book also offers a review of the immunohistochemistry detection systems with emphasis on their principles, history, and their advantages. It also stipulates the limitations and delineates the factors that need to be considered for choosing an appropriate detection system for IHC applications. The book describes current laboratory techniques and new applications for the technology. As the reader will observe, the book provides new and useful information concerning the rapidly advancing field of immunohistochemistry.

Published in London, UK

© 2020 IntechOpen
© unoL / iStock

IntechOpen

